FOG

Freiberg Online Geology

FOG is an electronic journal registered under **ISSN 1434-7512**

2006, VOL 17

Horst, Axel

Use of Stable and Radioactive Isotopes and Gaseous Tracers for Estimating Groundwater Recharge, Time of Residence, Mixing of the Different Types of Groundwater and Origin in the Silao Romita Aquifer, Guanajuato, Central Mexico

119 pages, 47 figures, 6 tables, 104 references

List of Contents

ABSTRACT

Multitracer studies are an effective tool to determine flow conditions and mean residence times of groundwater. Stable and radioactive isotopes and gaseous tracers together with water chemistry are used to estimate mean residence time, origin and mixing of groundwaters and recharge regions in the aquifer of Silao-Romita.

To determine residence times, different methods were applied (tritium, ^{14}C, CFC-11, CFC-12 and CFC-113). Tritium yielded mean residence times of almost zero to more than 50 years for piston flow and 73 to more than 300 years for the exponential model. Comparing tritium and CFC "ages", large differences became apparent which may be due to enrichment of CFCs caused by pumping or possible irrigation return flow. Nonetheless CFCs provided plausible information to determine the groundwater flow model. The exponential model (EM) appeared to be most appropriate. The determination of mean residence times by radiocarbon was very problematic due to huge uncertainties in estimating $\delta^{13}C$ of soil air and carbonates. A qualitative estimation revealed in some cases the existence of fossil waters with mean residence times of several thousand years.

The interpretation of chemical analyses and strontium showed a grouping of the majority of the samples into two types of groundwater. One is primarily present at the margins of the study area and the other in the centre of the basin. A detection of mixtures by strontium isotope ratios was problematic due to the high strontium content of the carbonates in the sediments which masks possible differences in $^{87}Sr/^{86}Sr$ signatures of different groundwaters.

Using ^{2}H and ^{18}O revealed evaporative effects in the extracted groundwater which possibly contains larger proportions on paleowaters. A comparison with data of a former report shows increasingly enriched values which are attributed to irrigation return flow.

Chloride Mass Balance (CMB) was applied to identify recharge regions which are at the margins of the study area. The *Sierra de Guanajuato* and the hills in the east and south showed the highest recharge values. Due to poor precipitation data of chloride these values were not reliable and interpretation was done qualitatively

Resumen

Los estudios de la aplicación de trazadores múltiples son una herramienta efectiva para determinar los condiciones del flujo y el tiempo de residencia del agua subterránea. Se utilizaron isótopos estables y radioactivos así como trazadores gaseosos y la hidroquímica para determinar el tiempo de residencia media, el origen y la mezcla de las aguas subterráneas así como las zonas de recarga en el acuífero de Silao-Romita.

Se aplicaron diferentes métodos (tritio, ^{14}C , CFC-11, CFC-12 and CFC-113) para determinar el tiempo de residencia. Con el tritio se obtuvieron tiempos de residencia de casi cero hasta más que 50 años para el modelo de flujo piston y 73 hasta más que 300 años para el modelo exponencial. Comparando las “edades” del tritio con las de los CFCs se ven diferencias grandes que se pueden atribuir al enriquecimiento de los CFCs evocado por el fuerte bombeo en los pozos o posiblemente por el flujo de retorno de riego. Sin embargo, los CFCs proporcionaron información plausible que permitió determinar el modelo del flujo del agua subterranea. El modelo tipo exponencial pareció el más adecuado. La determinacón del tiempo de residencia con radiocarbono es muy problemática, lo cual es atribuido a la incertidumbre en la estimación de $\delta^{13}C$ del aire, del suelo y de los carbonatos. Una estimación cualitativa indicó que en algunos pozos hay evidencias de agua fósil con tiempos de residencia que superan varios miles de años.

La interpretación de los análisis químicos y del isótopo de estroncio arrojó la agrupación de la mayoría de las muestras en dos tipos de agua subterránea. Un tipo es presente principalmente en las regiones marginales del área de investigación y el otro se encuentra en el centro de la cuenca. La identificación de las mezclas por medio de las proporciones de los isótopos de estroncio se demostró difícil debido a las concentraciónes altas de estroncio de los carbonatos en los sedimentos que enmascaran posibles diferencias en las signaturas de $^{87}Sr/^{86}Sr$ de las diferentes aguas.

Utilizando ^{2}H y ^{18}O se reconocen efectos evaporativos en las aguas extraídas que posiblemente contienen partes mayores de agua fósil. Comparando los resultados con un informe previo se identifica un enriquecimiento con valores crecientes de deuterio y ^{18}O que se puede atribuir al flujo de retorno de riego.

El método del balance de masa de cloruro se aplicó para identificar las regiónes del recarga que se encuentran a los márgenes del area de investigación. La Sierra de Guanajuato y los lomeríos y cerros al este y sur tienen valores de recarga más altos. Debido a los datos muy pobres de cloruro en la precipitación, los valores de recarga no son confiables y se hizo solamente una interpretación cualitativa.

Auszug

Sogenannte Multi-Tracer-Studien sind eine effektive Methode um die Fließbedingungen von Grundwässern zu bestimmen. Stabile und radioaktive Isotope sowie gasförmige Spurenstoffe wurden zusammen mit wasserchemischen Untersuchungen angewandt, um die mittlere Verweilzeit, Herkunft, Mischungstypen von Grundwässern sowie die Regionen der Grundwasserneubildung abzuschätzen.
Verschiedene Methoden wurden zur Grundwasserdatierung verwendet (Tritium, ^{14}C, FCKW-11, FCKW-12 und FCKW-113). Tritium lieferte Verweilzeiten von fast null bis größer 50 Jahre für „Piston Flow“ und 73 bis größer 300 Jahre für das Exponentialmodell. Der Vergleich zwischen ^{3}H und FCKW offenbarte große Abweichungen der berechneten „Grundwasseralter“. Die Diskrepanz könnte mit der Anreicherung der FCKWs durch Pumpen oder dem Bewässerungsrückfluss begründet werden. Trotzdem konnten die FCKWs zur Abschätzung des Grundwasserfließmodells herangezogen werden, wobei das Exponentialmodell die Fließbedingungen im Untersuchungsgebiet am besten beschreibt. Die Abschätzung der mittleren Verweilzeiten mit Hilfe von Radiokohlenstoff erwies sich aufgrund großer Unsicherheiten in der Abschätzung der $\delta^{13}C$-Werte für Bodenluft und Karbonate als sehr problematisch. Eine qualitative Betrachtung der ^{14}C- Konzentrationen lässt allerdings in einigen Fällen die Existenz von fossilen Wässern mit Verweilzeiten von mehreren tausend Jahren erkennen.
Die Interpretation der chemischen Analysen und des Strontiums offenbart die Gruppierung der Mehrheit der Proben in zwei Grundwassertypen. Ein Typ ist überwiegend in den Randbereichen des Untersuchungsgebietes zu finden während der zweite Wassertyp im Zentrum des Beckens verteilt ist. Grundwassermischungstypen mit Hilfe von Strontiumisotopenverhältnissen zu erkennen erwies sich als schwierig, da die hohen Strontiumkonzentrationen in den Karbonaten der Sedimente die Unterschiede der $^{87}Sr/^{86}Sr$- Signaturen verschiedener Grundwässer überdeckten.
Deuterium und ^{18}O zeigten Verdunstungseffekte im Grundwasser auf, das möglicherweise größere Anteile an Paläowasser hat. Der Vergleich mit Daten eines früheren Berichtes lässt eine zunehmende Anreicherung von ^{2}H and ^{18}O erkennen was mit dem Rückfluss von Bewässerungswasser begründet wird.
Die Chloridmassenbilanzmethode wurde eingesetzt, um die Regionen der Grundwasserneubildung zu erkennen, die in den Randbereichen des Untersuchungsgebietes zu finden sind. Die höchsten Neubildungswerte zeigten dabei die *Sierra de Guanajuato* und die Erhebungen im Osten und Süden. Weil zur Berechnung nur unzureichende Chloridmessungen im Niederschlag zur Verfügung standen, konnten die Ergebnisse lediglich qualitativ bewertet werden.

1 INTRODUCTION

1.1 SITUATION

Water shortage is an important problem in numerous regions around the world. Not only in the arid and semiarid zones in South and Central America, Asia and Africa, but also in regions receiving more precipitation like Bangladesh but due to very poor quality potable water is short. In many countries the exploitation of fossil waters is common practice.

Mexico also faces problems concerning water shortage resulting from overexploitation of groundwater resources and contamination by trace elements like arsenic (WHO, web) or remains of agricultural activity like pesticides (Sparks, 1988).

The investigation area is situated in the state of Guanajuato, Central Mexico between the cities of León, Irapuato and Guanajuato. Agriculture and some industries (e.g. General Motors) are present in the area. Since the fifties of the last century the water demand has increased due to the growing, improved agricultural techniques and a change of plant species. In addition, water of the Silao-Romita aquifer is taken for the drinking water supply of the city of Leon in the vicinity of the area, and is as well used for instance by the local car manufacturer (General Motors). Altogether, there are 1984 extraction points from which 6 are connected to springs, 281 are boreholes without pumps and 1697 are pumping wells. The extracted water is used primarily for agriculture (87 %). 11 % are pumped for drinking water and 1% for industry and cattle respectively. The extraction by pumping amounts to 408 Million m^3/a. The recharge rate is lower than the abstraction rate, therefore the water table decreases annually by 2-5 meters on average because of a deficit of approximately 33 Million m^3/a (CEAG, 2003).

Socio-economic conflicts have occurred due to increasing competition for subsurface water and the resulting decrease of the water tables (e.g. Mahlknecht et al, 2004). For several years efforts to ease the situation have been made. Some geological and geophysical investigations were accomplished to describe the subsurface situation (e.g. CEASG, 1998; CEASG, 1999; CEAG 2003; COREMI et al., 2004). Up to now groundwater dynamics is not yet fully understood. With the help of isotopic techniques this MSc thesis will provide a better understanding of the groundwater flow of the subsystem of Silao- Romita.

1.2 OBJECTIVES

The investigations are part of the project: “Estudios isotopicos para el desarrollo de un modelo conceptual del funcionamiento hidrodinamico del subsistema Silao-Romita, Estado de Guanajuato” (Isotopic studies for the development of a conceptual model of the hydrodynamic function of the subsystem of Silao-Romita, State of Guanajuato). The project is financed within the scope of the treaty 04-12-A-044 (Fondo Mixto Guanajuato) between Consejo de Ciencia y Technología de Guanajuato (CONCyTEG) and Instituto Tecnológico de Estudios Superiores de Monterrey (ITESM) Campus Monterrey. On the basis of isotopic analyses and the use of environmental tracers the project is intended to facilitate the understanding of recharge, mean residence time and mixing of groundwaters of the aquifer of Silao-Romita. In a second part of the project, which is not part of this thesis as well as the third part, a model concerning the vulnerability of the aquifer will be developed. At the end the results of both reports will be used to estimate the susceptibility of the aquifer and to give recommendations regarding the sustainable usage of groundwater in the investigation area.

There are numerous isotopes for estimating groundwater flow and origin. In this thesis stable (^{13}C, ^{18}O, ^{2}H, ^{87}Sr) and radioactive isotopes (^{14}C, ^{3}H) as well as the gaseous tracers CFC-11, CFC-12 and CFC-113 are applied. Some of them (^{87}Sr, ^{14}C and CFC’s) are used for the first time in that area.

Deuterium and ^{18}O are stable isotopes used to determine the origin of groundwater. They are applied, for example, to differentiate meteoric from thermal waters. Another type of stable isotopes for the determination of the origin of water is ^{87}Sr, being an indicator for water-rock-interaction. Different rocks have different $^{87}Sr/^{86}Sr$ ratios and water interacting with these rocks may adopt this ratio in its dissolved Sr^{2+}-content, thus reflecting the flow path. ^{13}C acts as a tracer for carbon sources and reactions between organic and inorganic species. It is also used to correct the ^{14}C ages. Radiocarbon (^{14}C) incorporated in CO_2 in the atmosphere reaches the groundwater via plants or directly dissolved in rain- or soilwater. With its half-life of 5730±40 years (Godwin, 1962) it is appropriate for determining waters of longer residence times. “Younger” waters will be identified by the analysis of tritium having a relatively short half-life of 4500 ± 8 days which corresponds to 12.32 years (Lucas and Unterweger, 2000). CFC’s also serve for groundwater “age dating” and are used to determine unambiguously tritium recharge dates (Clark and Fritz, 1997).

2 DESCRIPTION OF THE INVESTIGATION AREA

2.1 GENERAL DESCRIPTION

The aquifer of Silao-Romita is a subarea of the subbasin of the River Guanajuato that is situated in the eastern centre of the state of Guanajuato between the northern latitudes 20°42' and 21°9' and the western longitudes 101°10' and 101°44' containing the urban areas of Guanajuato, Silao, Romita and Irapuato. The maximum extension in SW – NE direction is approximately 67 km and in NW – SE direction 48 km. The city of León, having approximately 1,134,000 inhabitants (INEGI, web), is located in the northwest of the aquifer. The investigation area covers about 1,950 km^2. It is limited in northeast by the *Sierra de Guanajuato* (Highland of Guanajuato), in northwest by the *Valle de León* (Valley of León), in the south by the *Sierra de Penjamo* and the *Cerro el Veinte* and *Cerro Arandas* and in the west by uprisings of volcanic origin. The border of the study area is equal to the superficial watershed. The aquifer has a different catchment area.

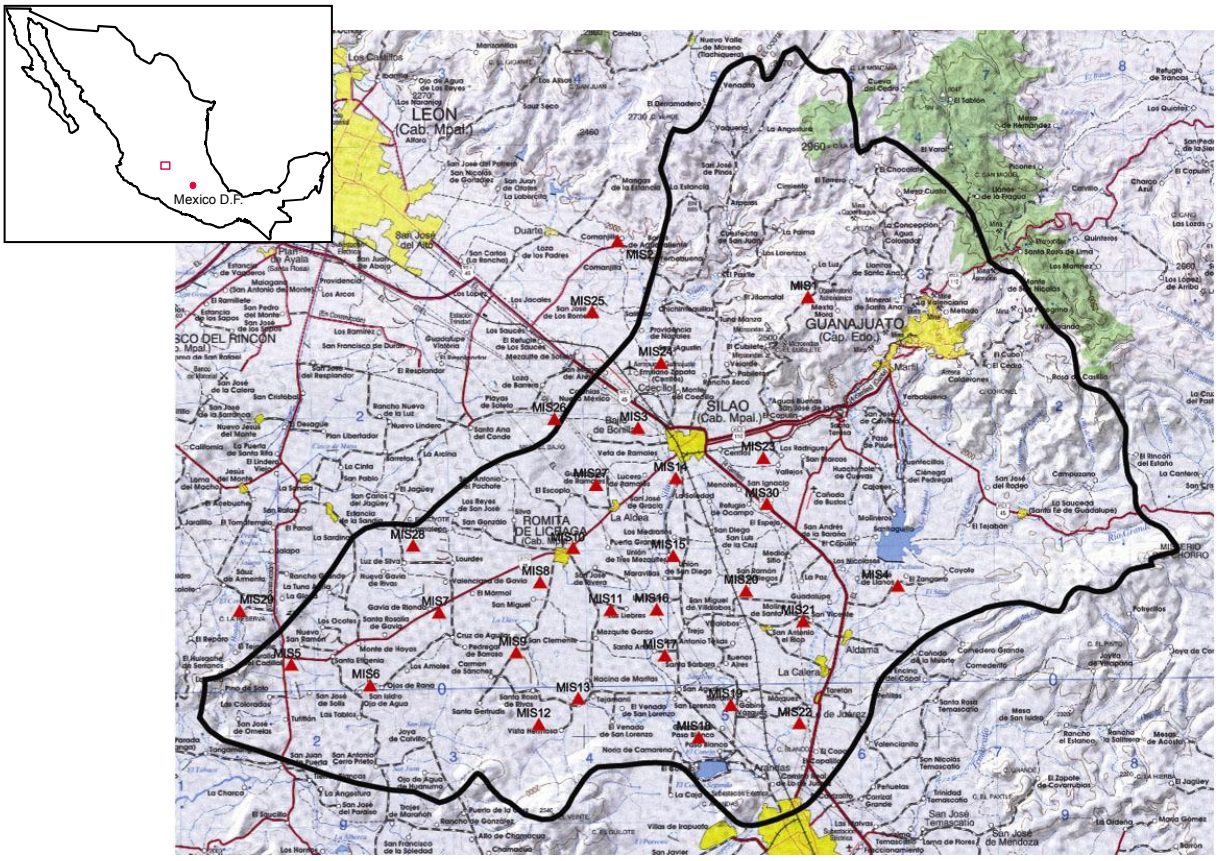

Figure 1: Topographic map of the investigation area (with sampling points) taken from INEGI maps Guanajuato F14-7 and Queretaro F14-10.

2.2 CLIMATES

The three predominant climates of the region are classified as ACw, Cw and BS1h (CEAG, 2003; referring to Köppen). ACw is semihumid semihot climate with the principal precipitation in summer. This type predominates in the investigation area and is present primarily in the lower parts with agricultural activity. Cw indicates semihumid warm climate where summer precipitations are the most important of the year. This type is developed in the elevated regions of the investigation area. The Bs1h- type is only present in the extreme northwest in direction to León. It indicates semiarid semihot climate where winter precipitation occupies less than 5 % of the annual amount (CEAG, 2003).

The annual average air temperature amounts to 18.5 °C, with a minimum of 15 °C in January and maximum of 22 °C in May. Figure 2 and Appendix 2 illustrate mean monthly values of the measuring stations *Silao* and *Romita*. Temperature data from *El Conejo* and *Comanjilla* weren't obtainable. The mean of these four stations represents the annual mean of 18.5 °C for the study area (e.g. CEAG, 2003).

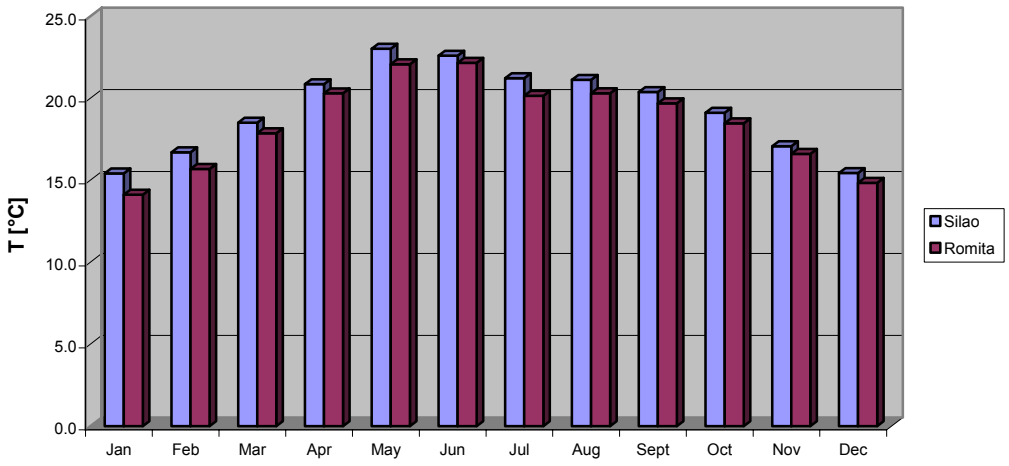

Figure 2: Mean monthly temperatures from Silao (1981-1996) and Romita (1981-1993)

COREMI et al. (2004) calculated the precipitation on the basis of the water balance of surface water. According to this the average annual precipitation amounts to 622 mm and the average annual evapotranspiration to 516 mm. Another report (Ibarra-Olivares, 2004) calculated the precipitation on the basis of data of the four stations El Conejo, Comanjilla, Silao and Romita (provided by CNA, Celaya) measured between 1978 and 1996 and obtained an average of 635 mm These data can also be seen in Appendix 1. Precipitation variates between 0 mm in winter months to 426 mm in Juli 1991 measured at the station *Romita*. The dispersion of precipitation throughout the year is shown by Figure 3.

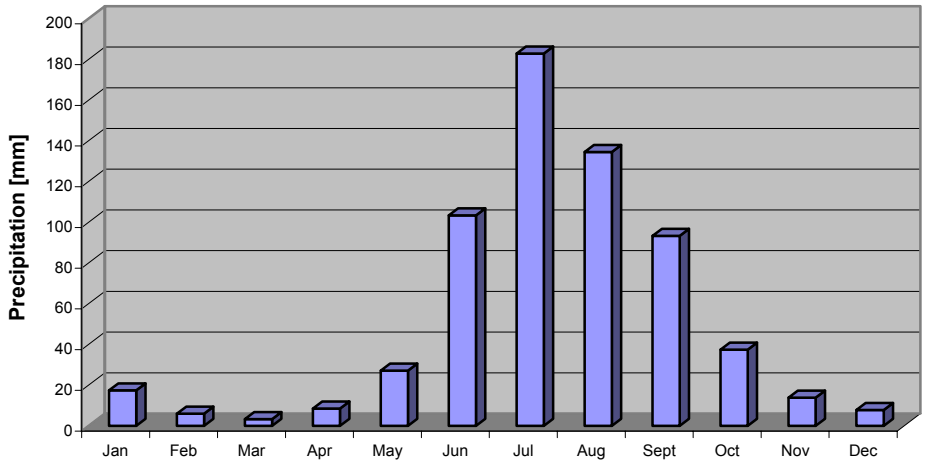

Figure 3: Mean monthly precipitation data of El Conejo, Comanjilla, Silao and Romita.

CEASG (1999) calculated the real evapotranspiration between 450 and 590 mm using the method of TURC. Calculations of evapotranspiration don't regard the irrigation which increases the amount of evapotranspiration considerably. Mean annual potential evapotranspiration, determined (unknown method) at the four above mentioned stations, is 1923 mm. Monthly and annual means illustrates Appendix 3.

Due to semihumid conditions also some streams and rivers exist. The investigation area is drained primarily from north to south. The two most important rivers are *Guanajuato* and *Silao* flowing together in the vicinity of Irapuato into the reservoir *Presa El Conejo*. After CEAG (2003) the river *Guanajuato* has a mean discharge of 115 million m^3 per year. For the river Silao no data were obtainable.

2.3 VEGETATION, SOIL AND LANDUSE

As seen above, the climate is classified as semihumid in the area of investigation. In the basin irrigating agriculture prevails. Landscapes not being irrigated show a steppe-/savanne-like vegetation where brush and cacti prevail. In the *Sierra de Guanajuato* partially primary vegetation can be found consisting of forests with deciduous trees (e.g. oak) and partially coniferous trees (e.g. pine) formerly prevailing in the whole *Sierra*.

In the investigation area seven different types of soil, referring to the FAO-classification are present. Primarily in the north-eastern part of the investigation area, represented by the *Sierra de Guanajuato*, furthermore around the towns of Silao and Romita and along the assumed border of the aquifer in the east Phaeozems can be found. The second type covering the south-western and southern part of the valley is Vertisol. These two soil groups cover more than 80 % of the investigation area. Phaeozems are typical soils of steppes having an upper soil horizon rich in

humus but are depleted in limestone in the upper layers. Vertisols also can be found in steppes and are characterised by an upper horizon rich in clay which swells and shrinks due to water content. This leads to kneading of the soil and consecutively to stirring.

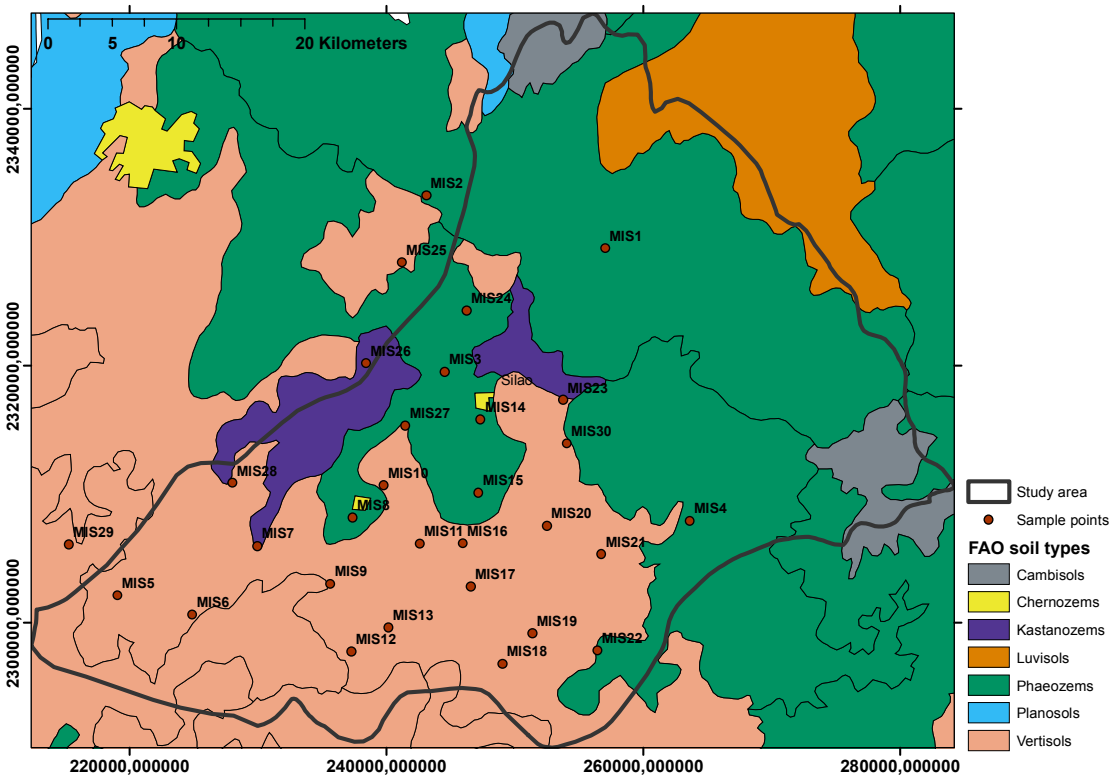

Figure 4: Soil types in the study area (after INEGI soil map)

Sporadically other types of soil appear. In the north of Silao and the northwest of Romita Kastanozems can be found, being soils of the steppe too, but less precipitation leads to less leaching of nutrients and carbonates. The upper soil horizon is less rich in humus and of smaller thickness. In the extreme north and the west Cambisols are present. This type belongs to the hardly or moderately developed soils showing leaching of carbonates and formation of sesquihydroxides as result of weathering. The texture is sandy or finer and in the upper layer lacks the original rock because of alteration. Luvisols are only in the bordering regions in the northeast of the investigation area and represent soils having an eluviated and an illuviated horizon due to water influence and develop primarily under forest cover. Just in very small proportions the types of Planosols and Chernosems are present. The first, in the extreme north, represents soils having an eluvial horizon due to stagnic properties of the underlying horizon. The second is only developed in the urban areas of Silao and Romita. Just as Kastanozems and Phaeosems the Chernosems belong to the soils of the steppe and have a larger humous horizon due to reduced water supply and higher content of carbonates.

The basin of Silao is used intensively through agriculture. Mais, cereals and sorghum are the most seen crops. Additionally fodder plants like Alfalfa are cultivated. In minor quantities a great variety of fruit and vegetables are growed, for instance agave, apple, strawberry, limone, mango, peach, tomato, chilli, onion, potato or jícama. The steppes, deforested slopes of the *Sierra de Guanajuato* and harvested farmlands are used as pasture land for goat and sheep (INEGI, map of landuse).

Large parts of the study area are irrigated, especially the *Valle de Silao*. In the districts of Silao and Romita approximately one third of the farmland is irrigated (see Figure 5). In the district of Guanajuato its only 7 % but in Irapuato almost the whole agricultural used area needs irrigation (CEAG, 2003 and references therein). Same authors realised a supervised thematic classification of Landsat 7 images from October. Sorghum (13100 ha), maize (10772 ha), alfalfa (3511 ha), potato (202 ha), onion (89 ha), carrots (48 ha), asparagus (42 ha), strawberry (24 ha) and 216 hectares of different vegetables were classified. Furthermore 5691 hectares of cereals through non-supervised classification were found.

The use of irrigation water is not very effective. CEAG (2003) investigated 469 wells and in 82 % primarily ineffective methods like ditch irrigation are applied. Therefore a lot of water is lost by evaporation or seepage. Irrigation probably leads to a return flow. CEASG (1999) estimated this return flow to approximately 15 % of overall recharge by means of stable isotope techniques.

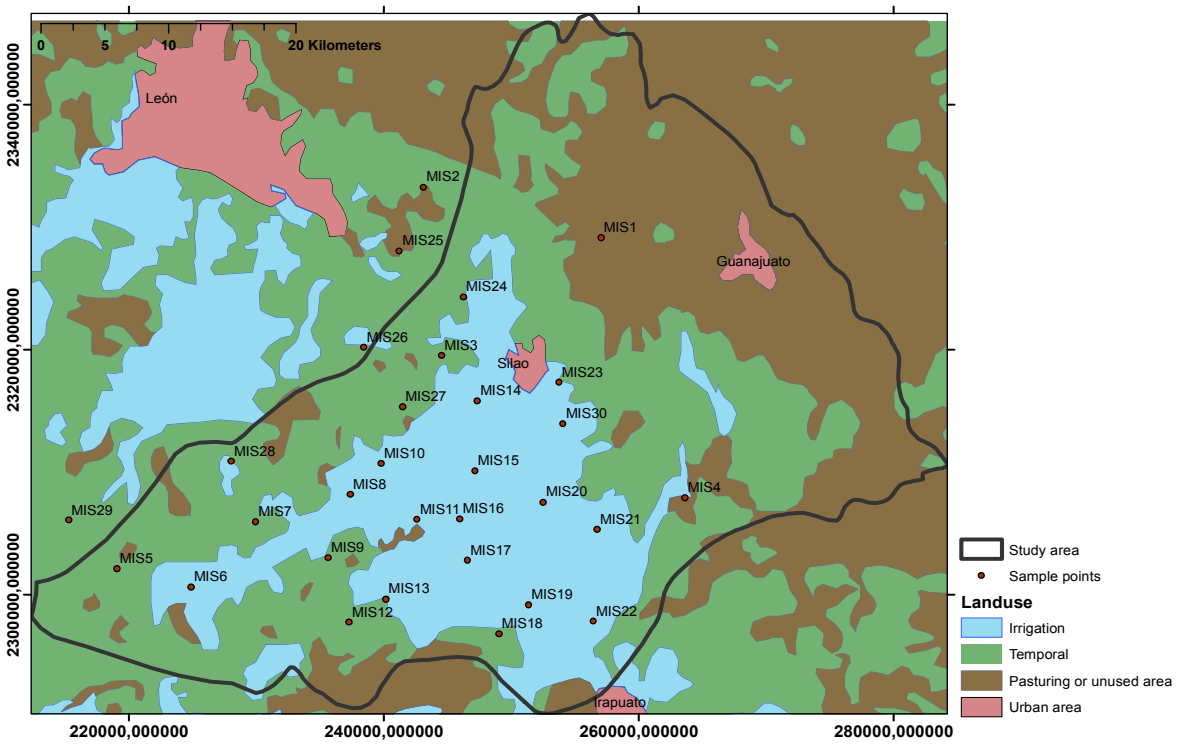

Figure 5: Agricultural landuse (changed after INEGI, web)

2.4 GEOLOGY

2.4.1 Physiography

The study area is dominated by highlands of different altitudes. Between these landscapes are plains with smooth and steeper hills, partially isolated. These plaines are primarily used for agriculture. The highlands are oriented northwest-southeast as for example the “Sierra Guanajuato” as well as hills of volcanic origin within the valley forming small groups.

The investigation area is part of two large physiographic units: The *Cinturón Volcánico Mexicano* (Mexican Neovolcanic Belt) and the *Mesa Central* (Central Highland). The former covers the southern and larger part of the study area, the second forms the *Sierra de Guanajuato.* The province of the *Mesa Central* is affected by volcanism of the *Sierra Madre Occidental* which is presented through ample plains interrupted by hills. In-between lays the *Sierra de Guanajuato* consisting of rocks of diverse lithology and displaying abrupt topography. The *Cinturón Vólcanico Mexicano* is a tectonic arc which developed during the Pliocene and the subduction of the *Cocos Plate* under the *North-American Plate.* It is represented by solidified lava-streams and diverse cones.

The major elevations within the area reach altitudes of about 2500 m above sea level and are primarily situated in the *Sierra de Guanajuato*. In the north the *El Ocote* (2500 m) limits the basin. In the sierra for example the *Cerro El Timbal* (2730 m), *Mesa El Zacate* (2780 m), *Mesa Cuatralba* (2840 m), *Cerro Verde* (2730 m) and *Mesa del Obispo* (2450 m) forming the northeastern watershed.

In the west the area is bordered by the “*Cerro Bola*” and in the south by the *Sierra Penjamo* with its highest elevation *Cerro el Veinte* (2330 m) and *Cerro Arandas* (2026 m). *Cerro el Veinte* is a volcanic formation representing the southern watershed of the investigation area and also between the subbasins of the rivers *Turbio* and *Guanajuato*. In the northeast of Irapuato the *Cerro la Mina* y *Cerro El Chorro* form the border of the basin. The plains between the elevations have altitudes of 1740-1780 m in the valley of Silao-Romita and are primarily used for agriculture (COREMI et. al, 2004).

The following figure illustrates the morphology of the study area: For construction the SRTM3-DEM was used which is obtainable on the website of the NASA:

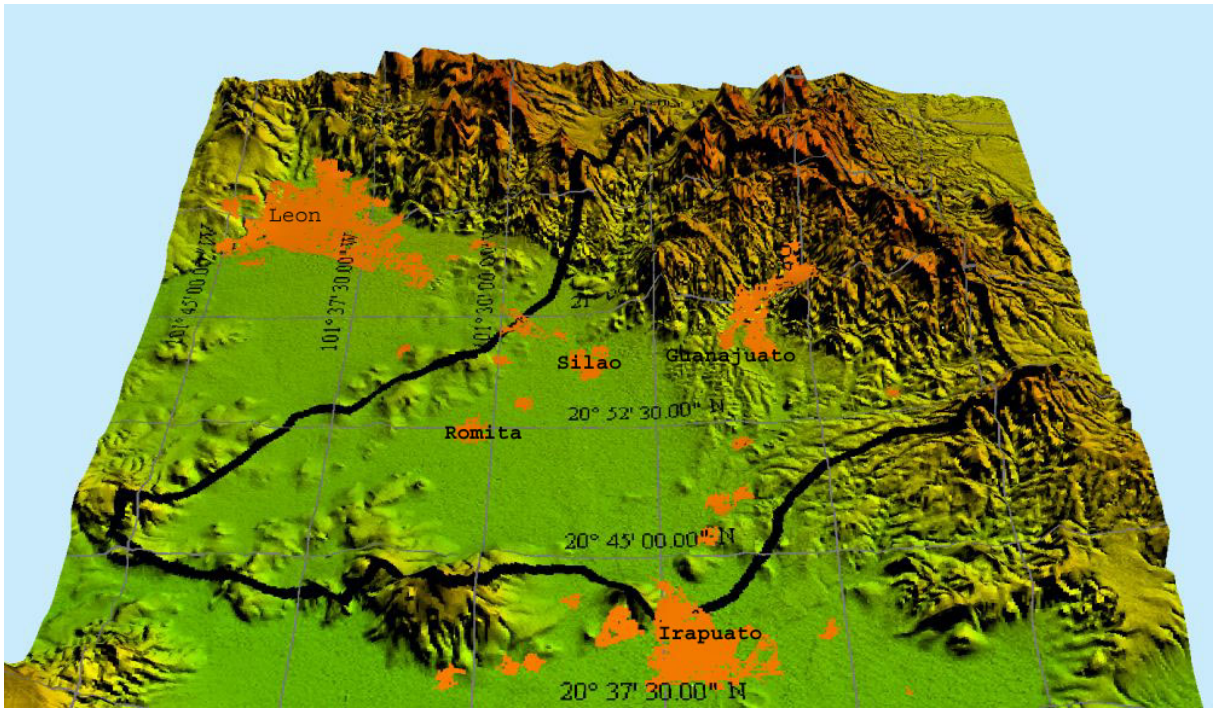

Figure 6: Digital Elevation Model (DEM) of the study area based on SRTM3 data of the NASA (web). Illustrated elevations are 20-fold inflated.

2.4.2 Geomorphology

The investigation area can be classified in two larger groups. First there are mountains of different altitudes as well as hills representing the older geological history of the area. Second there are juvenile forms represented by sedimentary basins, alluvial fans and hills of volcanic origin being still active and showing little erosion.

The first group is represented primarily by the *Sierra de Guanajuat*o in the north-eastern region of the investigation area. It corresponds to the older mesozoic and tertiary geologic units containing sedimentary, volcanoclastic and intrusive rocks, as well as minor quantities of consolidated conglomerates. The mountains coincide with folds having the same NW-SE – orientation like for example the *Falla El Bajio*, but are also intersected by faults following the NE-SW- orientation (*Falla Aldana*) representing the general orientation of the majority of the faults in the area (Ibarra-Olivares, 2004).

The drainage pattern in the area appears to be dendritic and denser than in the juvenile landscapes. The rocks of the mountains are also superposed by basalts and acid rocks of the upper tertiary and quaternary origin whose morphology contrasts the subordinated units. In the lower tertiary rocks frequently canyons and terraces occur, reflecting the tectonic activity in this era as well as solidified lava streams in front of volcanoes.

The second group represents the rest of the area by juvenile forms associated to volcanic material of the middle tertiary and quaternary origin, as well as alluvial deposits. In the east of the investigation area there are relatively young mountains of volcanic origin showing little erosion. These elevations have an abrupt, steep and angular appearance. Tables of pyroclastic material are dissected by the fractures and faults. In the central part tertiary and quaternary sediments and alluvial deposits prevail, forming the relatively plain valley of Silao-Romita.

Within the juvenile appearances volcanic highlands, hills and mountains acidic, intermediate and basic rocks of tertiary and quaternary origin cover sedimentary and metamorphic rocks.

2.5 STRATIGRAPHY

The rocks appearing in the investigated watershed can be classified into two (lithological) groups. The first, forming the *Sierra de Guanajuato*, consists of a mesozoic, plutonic, volcano-sedimentaric complex affected by metamorphism of a low stadium and intrusions (tertiary plutones). This geological unit corresponds to a mesozoic intraoceanic arc formed during the early Cretaceous.

The second lithological unit covers the main part of the investigation area. It consists of volcanic and continental sedimentary rocks as well as ashes and tertiary and quaternary granular alluvial and lacustrine deposits. This unit corresponds to geological events associated to the formation of the *Sierra Madre Occidental* and the *Mexican Neovolcanic Belt.* In the subbasin of Silao-Romita outcrops of middle and upper tertiary volcanic rhyolithic rocks are predominating. Some basalts and andesites also occur. Quaternary alluvial and lacustrine sediments are also present with some outcrops of lava and basaltic ashes of the same era.

Subsequently the different stratigraphical units appearing in the investigation area will be described from the oldest to the youngest (see also Figure 7). The description corresponds to COREMI et al. (2004) that refers to the geological map (scale 1:250000) of COREMI.

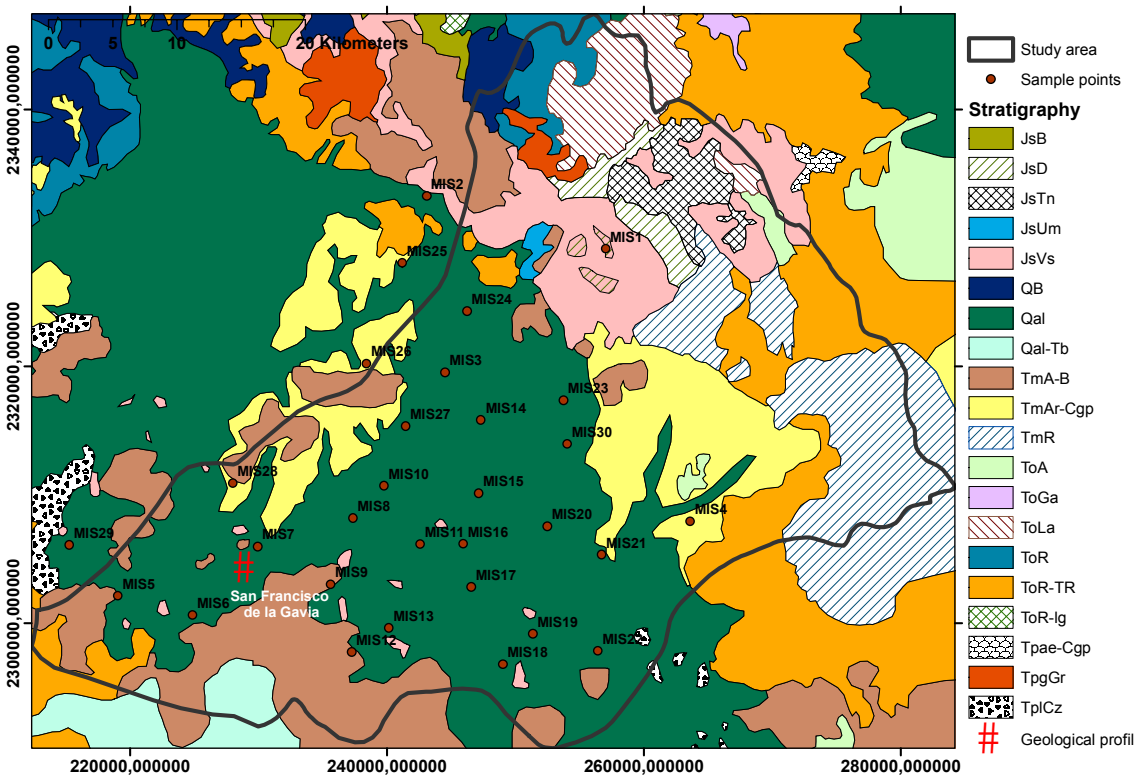

Figure 7: Geology (changed after COREMI et al. 2004)

Ultramafic unit *San Juan de Otates* (JsUm)

This unit is considered to be the base of the plutonic-volcanosedimentary complex of the *Sierra de Guanajuato*. It consists of serpentinites, peridotites, serpentinised clinopyroxenites and gabbros showing texture of accumulation. The age is estimated to be of the upper Jurassic.

This unit appears primarily in the *Sierra the Guanajuato*. It presents a dark greyish bluish colour with brown shades and is intensively fractured, even though most discontinuities are closed. The massive and consolidated rocks exhibit features of weathering in the surface up to a thickness of 5 to 10 meters. Geochemically the *San Juan de Otates*-formation corresponds to tholeiitic magmatism with depletion of TiO_2, K_2O and rare earth elements.

Diorite *Tuna Mansa* (JsD)

This formation designates different crystalline facies of dioritic composition, especially granitic and gabbroitic, being an indication for tectonic activity. This unit is crossed by doleritic basaltic dykes forming together a swarm complex of veins.

This unit appears at diverse locations, primarily in the *Sierra de Guanajuato* northwest of the city of Guanajuato, superposing a volcano-sedimentary and another basaltic unit. The age is radiometrically estimated to be of the upper Jurassic.

The rock is massive and crystalline with light and dark shades, ranging from yellow ochre and greyish white to green and dark blue. The intensive fractured rock appears to be weathered in a high to moderate degree. The discontinuities are closed or in an opening stadium filled with clays. Mineralogically the rock consists of plagioclase, hornblende, clinopyroxene and quartz.

Tonalite *Cerro Pelon* (JsTn)

The *Cerro Pelon* – Tonalite is represented by massive rocks in terms of tectonic scales. This unit shows a great number of acidic kaolinised and oxidised dykes. It appears massive and crystalline with phanerite texture with quartz, plagioclase, chlorite and epidote.

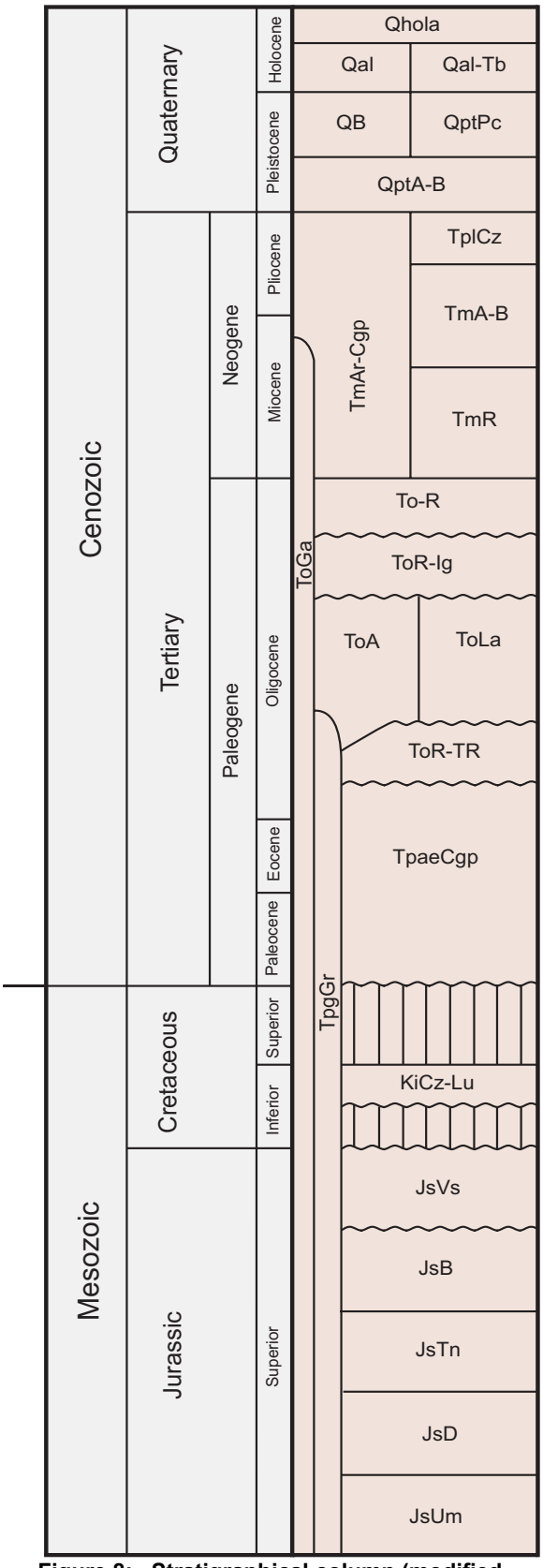

Figure 8: Stratigraphical column (modified from COREMI et al., 2004)

The outcrops are fractured and weathered and are located in the south-eastern part of the *Sierra de Guanajuato* typically at the *Cerro el Pelón*. The formation possesses high secondary porosity due to the high degree of weathering in the surficial region. At greater depths the rocks are less weathered and the primary porosity is close to zero. The age is radiometrically estimated to 157 Ma.

Basalt *La Luz* (JsB)

Basalt of the *La Luz* type is recognised by a succession of outflows of basaltic lava and andesitic basalt with a massive or pillow structure and a thickness of about 1000 m. This unit contains lavas and breccias of dark green to yellowish green color. The pillow lava is occasionally cementated with calcareous material. The breccias consist of angular fragments in an aphanite (finegrained) or light crystalline matrix. Frequently inclusions of limestone and epidote are existent in the lavas and the breccias. The unit shows high alteration expressed in chloritisation, oxidation and propylitisation and is affected by regional metamorphism of low degree of the greenschist facies. The discontinuities appear as fissures and fractures either closed or filled with altered minerals. The primary porosity is very low. The detected radiometric age is about 108 Ma. This age normally would correspond to the lower Cretaceous but in COREMI et al. (2004) it was classified as upper Jurassic. Geochemically it belongs to the tholeiites of the insular arc representing the first magmatic manifestations of an insular arc over an oceanic crust. The main outcrops of this type appear in the vicinity of *La Luz* about 10 km in north-western direction of Guanajuato.

Volcano-sedimentary unit (JsVs)

This unit consists of argillaceous limestone and sandstone, black flintstone and limestone with lamination of siltstone and occasional bancs of conglomerates. The formation includes basaltic and andesitic lavas and breccias of massive or pillowish structure. The whole unit is affected by regional metamorphism of low degree and hydrothermal alteration and has a predominant clayish character. The age of the formation is not clearly defined but estimated to be of lower or upper Jurassic, as well as the thickness seems to be more than 500 m.

This formation is widespread in the *Sierra the Guanajuato*. Outcrops appear for example in the *Sierra de Comanja* at the *Cerro del Cubilete* and in the mining district of Guanajuato. Within the sub-basin exist several small outcrops of mesozoic limestone and siltstone layers of low thicknesses (5 cm) and are not registered in the map. Outside the investigation area are extended outcrops of this unit superposing the volcanic-sedimentary formation. This unit is determined to be of upper Jurassic – lower Cretaceous and represents marine conditions of deposition in shallow water.

Formation Gunajuato (TpaeCgp)

The formation Guanajuato consists of polymictic conglomerates being badly arranged and composed of fragments of igneous, sedimentary and metamorphic rocks with pieces of quartz, limestone, granite and andesite, cementated in a clayish matrix. The thickness is estimated to be 1500 m. The matrix, being primarily sandy, shows brownish-redish colour, whereas in greater depths through hydrothermal alteration the rock appears light green.

The main outcrops are situated in the proximity of the city of *Guanajuato*, particularly in the south and in the west. Outcrops of similar rocks having the same lithology and chronology appear at the border of the investigation area in the east of the city of *Leon*. The formation represents the basis of the tertiary in the area, superposing irregularly the volcano-sedimentary sequence of the arc of *Guanajuato* and is superposed by volcanic rocks of the middle and upper tertiary itself. The rocks of this formation are hardly porous and its sandy matrix is well cemented by ferrous oxide, showing generally a low degree of alteration.

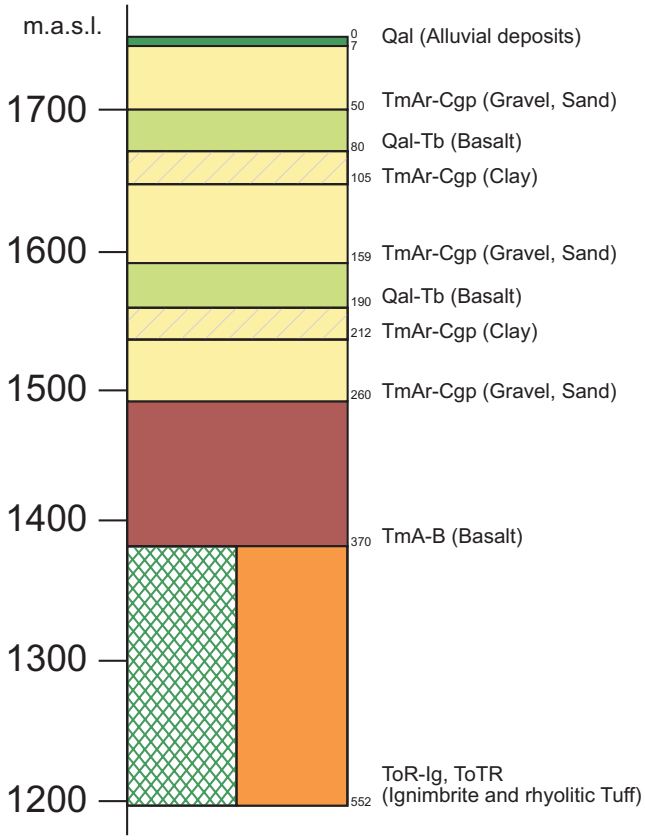

Figure 9: Geological profile of the well San Francisco de la Gavia (modified from CEASG, 1998)

Volcanic rocks of the Oligocene (ToR-Ig, ToTR, ToR-TR, ToA, ToR, ToLa)

Some series of volcanic acidic oligocenic rocks, appearing in the *Sierra de Guanajuato*, are described by the nomenclature ToR-Ig (rhyolithe-ignimbrite), ToTR (tuff-rhyolithe) and ToR-TR (tuff-rhyolithe rhyolithic). Within these rock series 3 formations exist: *Losero*, *La Bufa* and *Ignimbrita Cuatralba.*

The first is formed of thin layers of 5-20 cm thick light shaded lithic tuff of greenish grey colour. The rock of this formation presents a low degree of alteration and low or intermediate porosity. This unit is formed by effluents and rhyolithic tuffs of phaneritic and porphyritic texture and has a thickness of 350 m. The age is estimated to be about 37 Ma (middle Oligocene). The formation appears massive with discontinuities forming columnar rocks and domes.

The ignimbrite *Cuatralba* outcrops for example in the central north of the *Sierra de Guanajuato* and consists of rhyolithic tuff stratified in layers of 10 to 40 cm thickness. It shows colours of light pink to yellow – ochre with red shades. The texture is holocrystaline, porphyritic and fluidal forming columnar structures. Furthermore it presents phenocrystals of quartz and feldspar in vitreous ashes showing flow structures. The observed thicknesses of this formation don't exceed 200 m, but is possibly larger. The altered and moderate fractured rock with low porosity is assumed to have an age of approximately 25 Ma.

The unit ToLa (tertiary oligocenic latite outcrops primarily 15 km northeast of the city of Guanajuato and is presented by effluents of lava and domes. It displays a colour of café with shades of pink and grey. The texture appears to be porphyritic with some phenocrystals of feldspar and quartz in an afanitic matrix. The rocks are moderate to intensively fractured and weathered. The fractures are semi-closed or open occasionally filled with clay and altered material. The fracturing leads to intermediate secondary porosity. The maximum thickness of this unit is about 350 m and the estimated age 31 Ma

The andesitic unit ToA, including the formations *Calderones* and *Cedros*, outcrop in the west, southeast and northeast of the city of Guanajuato. The Calderon formation contains tuff lapilli and volcanoclastic horizons with blockish, sandy and silty material. The rocks are moderately arranged with colours of grey and greenish café, due to chloritisation. The thickness varies between 200 and 250 m. The *Cedros* formation is represented by andesitic and basaltic effluents with porphyritic texture and a colour of grey or dark café and a thickness of 250 m. The degree of fracturing and alteration is moderate, the secondary porosity reaches from moderate to low. The age is not radiometrically determined but stratigraphically estimated to be of middle Oligocene.

The Rhyolite *Chichindaro* is described with the nomenclature ToR. This unit outcrops in the north of the investigation area and north-east of Guanajuato. The structure is columnar with variable porphyritic fluidal and vitreous texture with folds. Within the vitreous matrix often crystals of quartz and feldspar appear. The rock shows a light grey colour and moderate fracturing and alteration.

Two other igneous sequences are prevalent in the investigation area generated by volcanic activity. The first contains dacite, trachyte, andesite and ignimbrite. The second consist of rhyolithic rocks superposed by basaltic andesites.

Volcanic rocks of the Miocene (TmR, TmA-B)

The following units originate from volcanic activity with emissions of andesitic and rhyolithic lava 11 – 16 Ma before present.

The unit TmR is located in the east of the investigation area. It appears massive, showing light brown-red colour with white shades and has a thickness of 250 to more than 400 m. The afanitic and vitreous matrix contains crystals of quartz and feldspar. The weathering and fracturing of the rocks is generally low.

The unit TmA-B includes andesits and basalts of the age tertiary superior. The major outcrops are in the hills bordering the southern and north-western part of the valley of Silao- Romita. The unit forms also isolated hills in the southwest of the city of Guanajuato.

The basalts show colours of dark to light grey with shades of café, ochre and red from oxidation. Generally very fractured the rocks have discontinuities, partially filled products of erosion and weathering, with sand and clay.

Sedimentary units of the Miocene and Pliocene (TmAr-Cgp, TplCz)

During the upper tertiary the filling of the *Depresión de Bajío* with sediments like sands, conglomerates and deposits of lacustrine and clastic origin took place, as well as the deposition of outflows of some lava and ashes.

The polymictic sandstone-conglomerate (TmAr-Cgp) consists of a sequence of horizons of sand and conglomerates, frequently with a clayish-silty or tuff-like matrix in the form of fine ashes. The clasts consist of rounded volcanic rocks and of the other prevailing rocks in the southern region of the subbasin of Guanajuato. The size of the fragments varies from sands to pebbles (10-15 cm). The deposits show light grey colour with shades of light ochre café.

The deposits form large alluvial fans extending from the city of Guanajuato in southern or south-eastern direction or forming hills between the cities of Silao and Irapuato. The deposits possess high porosity although containing variable amounts of clay. The thickness of these sediments is approximately 50 m, visible in insections of roads or in wells. Frequently horizons of clastic sediments of about 10 m are observed.

In the west of the investigation area and in the north of Irapuato are outcrops of lacustrine limestone with the signature TplCz. The limestone contains clay and appears in white colour with shades of yellowish ochre and light café. The unit shows moderate fracturing with frequent discontinuities, filled with silt and clay. The thickness amounts to 0.2 to 1 m.

Sedimentary recent deposits (Qal, Qal-Tb)

The alluvial deposits of the unit Qal cover the major part of the valley of Silao-Romita and contain sediments being deposited during the quaternary: sand, silt clay and gravel having a maximum thickness of 100 m. The deposits constitute the superficial filling of the valley, occasionally embeddings of lacustrine sediments, ashes or volcanic outflows occur. The cover of organic soils is also included to the unit. The sediments show generally light, white, café, ochre or grey colours. The particle size is variable ranging from conglomerates to clays. As well the porosity varies from high to low.

In the vicinity of Irapuato, beyond the border of the investigation area but very close, volcanic apparatuses, belonging to the Neovolcanic Belt, can be found (Qal-Tb). The volcanic activity created extensive deposits of volcanic basaltic ashes and sandstone, as well as the lapilli- type between the alluvial sediments. The ashes of light and dark grey colour with shades of red, green and reddish café show grain-sizes between fine and coarse sand. Forming single horizontal layers of 10 to 50 cm, the material appears compacted or lightly consolidated. The complete layer adds up to several tenths of meters. These materials present a low degree of alteration and high porosity.

Tertiary intrusive rocks (TpgGr, ToGa)

The *Granito Comanja* is an intrusive body outcropping in different zones of the investigation area, especially in the *Sierra the Guanajuato*. The age was estimated to be 55 million years and is added to the era of Paleocene- Eocene. The brown and light green rocks form hills of convex profile. The altered cover of this unit normally has thicknesses of some tenths of meters. Beneath rock is massive crystalline and compacted with a lot of fractures.

Another type of intrusive outcrops of gabbroic composition is known as *Gabbro Arperos* (ToGa), appearing in the extreme north of the area in the vicinity of the village with the same name. The colour is dark to black café containing visible crystals of olivine plagioclase and pyroxene.

2.6 HYDROGEOLOGY

Hydrogeology and geology of distinct areas always correspond with each other depending on grain size of sediments or number of fractures in massive rocks determining the permeability of the subsystem regarding to water.

The rocks of the investigation area can be classified in two larger groups. There are massive igneous and metamorphic rocks of the mountains (*Sierra de Guanajuato*) having low primary porosity and generally lower permeability. The water flows primarily in faults, fissures and fractures. The second group contains the sediments of the *Valle de Silao-Romita* (valley or basin of Silao-Romita), having primary porosity and altogether higher permeability. These sediments contain the aquifer which may be connected to adjacent aquifers in northwest (León) and south (Irapuato) of the study area.

The aquifer of Silao-Romita consists of several horizons. Some sources (CEASG, 1998; CEASG, 1999) mention 3 connected zones: a shallow, an intermediate and a deep horizon. The shallow and intermediate layers were overexploited in the last years and are exhausted. The principal source of water is the profound aquifer. Recent sources (e.g. COREMI et al., 2004) prefer the classification into two zones: An unconfined aquifer close to the surface (“aquífero superior”) with a maximum thickness of 30 m. Beneath follows the so called regional aquifer with widely differing extension and thickness. The border between these two layers is constituted by numerous lenses of clay (COREMI et al., 2004). Having a thickness of up to 1000 m and more, the aquifer appears unconfined and partially semiconfined.

In COREMI et al. (2004) six hydrogeological units are recommended, depending on the permeability and composition of the material. Figure 10 gives a rough overview to the dispersion of these units in the study area. The hydrogeological sections 1 to 4 are inserted at the end of this chapter. Unfortunately no groundwater levels were provided for these wells in COREMI et al. (2004) and couldn’t be inserted into the sections. The sections were digitised from existing maps (COREMI et al., 2004) of poor quality. The vertical scale is not uniform in all cross- sections.

Unit I: Granular unit of high permeability.

The quaternary sediments, sometimes with interlayers of tuff, pyroclastical deposits and small shares on consolidated conglomerates belong to this unit. These rocks are the important ones for the recharge from meteoric waters and furthermore for the return-flow of irrigation waters.

Unit II: Granular unit of medium permeability:

The major part of all wells penetrates the tertiary sands and conglomerates of this unit as well as the major part of the subterranean water circulate in this medium. The grain size varies from fine gravel to clayish. The clay forms lenses and locally provokes semi-confined conditions.

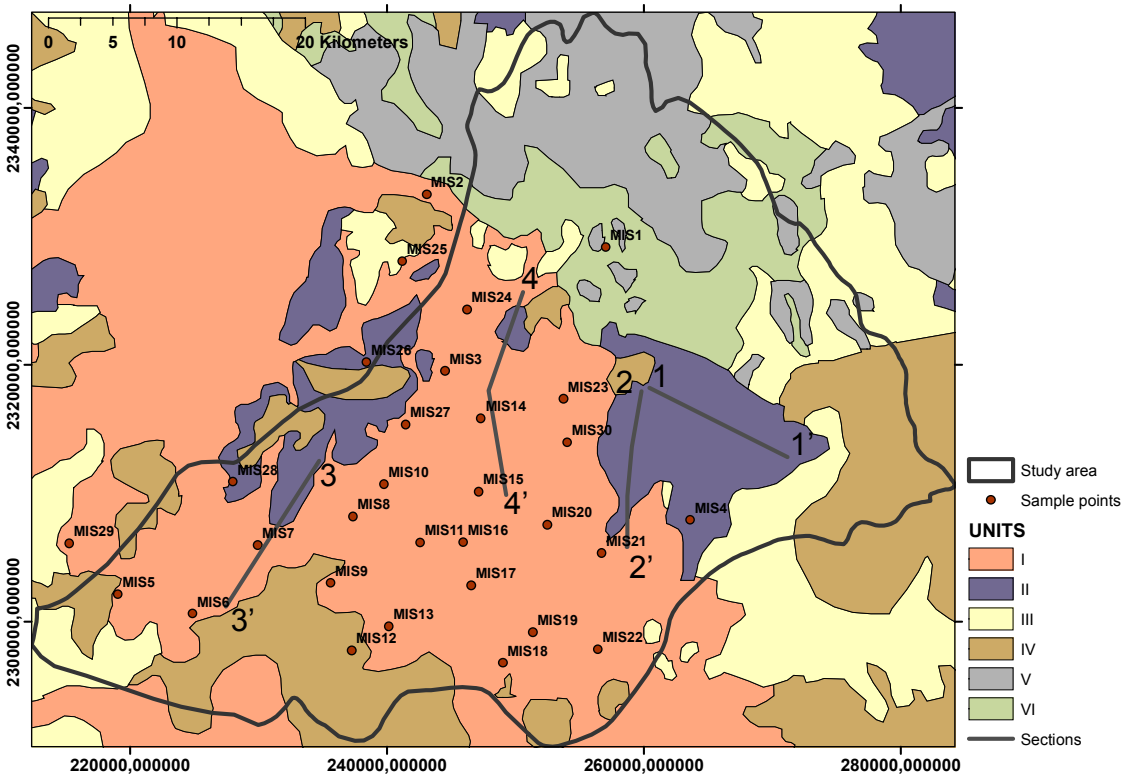

Figure 10: Dispersion of hydrogeological units I-VI (changed after COREMI et al., 2004).

Unit III: Fractured unit of high permeability:

This unit contains superficially highly fractured tertiary rocks like basalt, limestone and rhyolithic tuff. The fracturing is declining with depth.

Unit IV: Fractured unit with medium permeability

These tertiary rhyolithes and basaltic andesits are medium fractured and act as conductive layer or agent of discharge over less permeable rocks. Between rocks of higher permeability larger blocks of this unit tend to act like barriers.

Unit V: Fractured unit with low permeability.

Diorite and ultramafic rocks of the upper Jurassic and tertiary andesits, gabbros and granits while fractured are considered to have low permeability. These rocks conduct minor quantities of water in its fractures and folds.

Unit VI: Fractured unit with very low permeability

This unit describes the tertiary conglomerate of Guanajuato and the metasedimentary sequence (upper Jurassic). These rocks constitute the hydrogeological basement of the aquifer.

The recharge of the groundwater originates from various natural and artificial sources. First there exists the infiltration of meteoric waters through the rocks of different permeability. Second the horizontal recharge from the *Sierra de Guanajuato* and the other uprisings are sources of water, if porosity or fracturing allow recharge. There are three principal zones of horizontal inflow: The mountains around Guanajuato and in the east of Irapuato. The third zone is situated in the west of the reservoir *Presa el Conejo*. Other minor sources of recharge are the rivers, lakes and reservoirs. The third main source of infiltrating water may originate from the agricultural activities (e.g. irrigation).

The discharge of water occurs primarily by wells and evapotranspiration. The volumes of natural discharge (springs) are comparatively small and their number has diminished during the last decades. This also has been observed in neighbour basins (Mahlknecht et al., 2004) .

The traditional U-shape model proposes three types of subterranean fluxes (Toth, 1963): Local flow, intermediate flow and regional flow. In the study area the local flow is considered to be induced by meteoric and infiltrating water and limited to less than 30 m. The shallow aquifer recovers practically immediately. The intermediate flow takes place in the fractured and granular materials originating from the horizontal flux of the mountains and the vertical infiltration that is not retarded by impermeable materials. Due to the geological and structural conditions and chemical characteristics the existence of regional flow is suggested, flowing primarily in fractured rocks in depths of about 800 m. The thermal activity proofed by the water temperature of some wells and springs enforce this assumption (COREMI et al., 2004).

The estimation of the hydrogeological parameters were realised by pumping tests (Guysa, 1998) in the valley of León and Silao-Romita. Permeability values of 4.6×10^{-7} m/s – 6.5×10^{-6} m/s for granular medias and 1.2×10^{-7} m/s – 3.7×10^{-5} m/s for the fractured rocks were determined.

COREMI et al. (2004) reinterpreted the values with the program “Aquitest” using the method of Neuman for unconfined aquifers. The permeability was calculated to 3.6×10^{-6} m/s - 2.1×10^{-3} m/s being higher than the values calculated by Guysa who assumed semiconfined conditions.

Calculating the original flow velocity (average interstitial velocity) of groundwater in media with permeabilities between 10^{-3} and 10^{-7} m/s, velocities of 4 km to 4 cm per year are yielded. For this calculation the superficial gradient of the basin between north-western and south-eastern border near Irapuato was assumed (corresponding to the blue line in Figure 12) which is 0.025. For porosity 0.2 was considered. Through pumping this velocity may differ substantially.

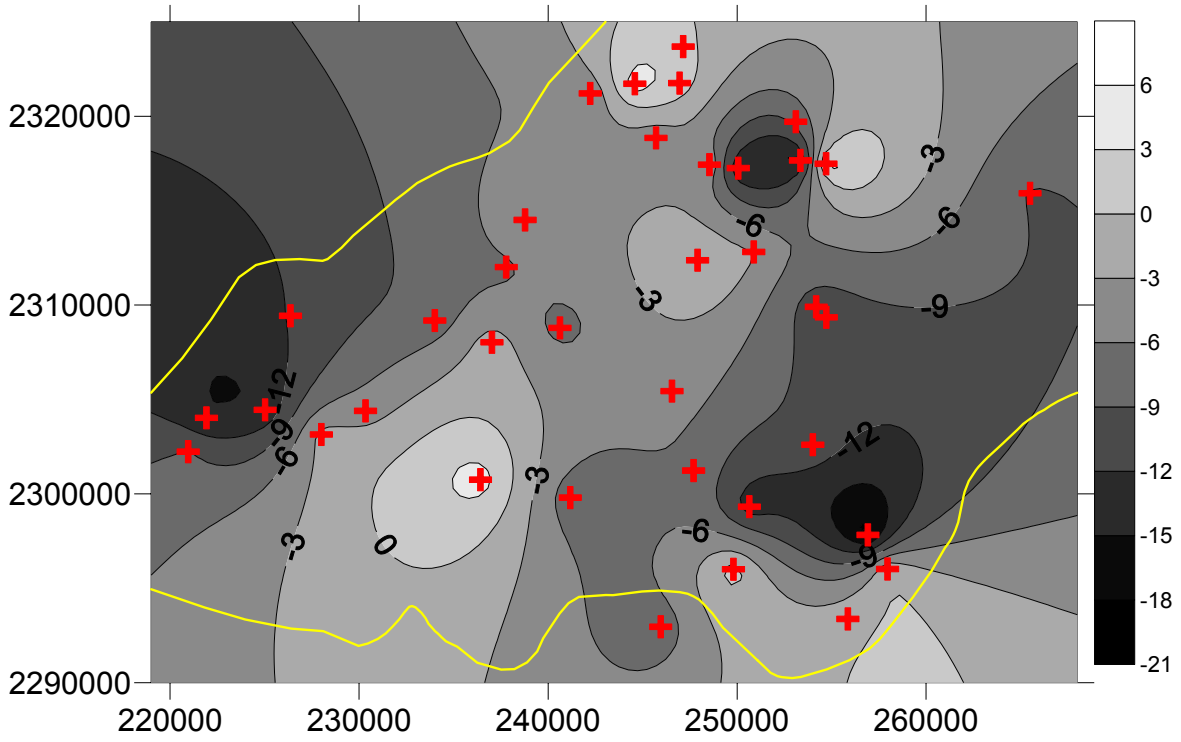

Figure 11: Development of the water level (in metres) within 6 years (1998-2004). Data were taken from COREMI et al., 2004.

In the valley of Silao Romita the water table is declining for years. Because of the threatening or already existent shortage of water since 1998 the CEASG has been realising a monitoring program for the measurement of the piezometric water levels in the aquifer. Measurements were made in dry and rain seasons respectively. The extractions induced considerable cones of depression, particularly in the south near Irapuato and in the north of Silao (see also Figure 12).

Figure 11 illustrates the development of the water table between 1998 and 2004. Measurements were done in October. Data had to be filtered because in some cases depressions of 50 metres within one year were determined which probably is attributed to erroneous measurements, e.g. during extraction of water. These values were not included. Figure 11 also shows some domes of recovery which might be due to increased precipitation (COREMI et al., 2004) in this period in comparison to the annual mean.

COREMI et al. (2004) calculated a median depression of 3.36 m/a for the period between 1998 and 2003. In the regions of recharge the drawdown amounts to 2.49 m/a anyway. Without the extensive exploitation of the aquifer the water would follow the flow direction of the rivers from north to south, accordingly to the gradient of the terrain and the geological strata. The extraction caused changes in the flow regime that now is adjusted from the zones of recharge in direction to the large cones of depression in the centre of the valley.

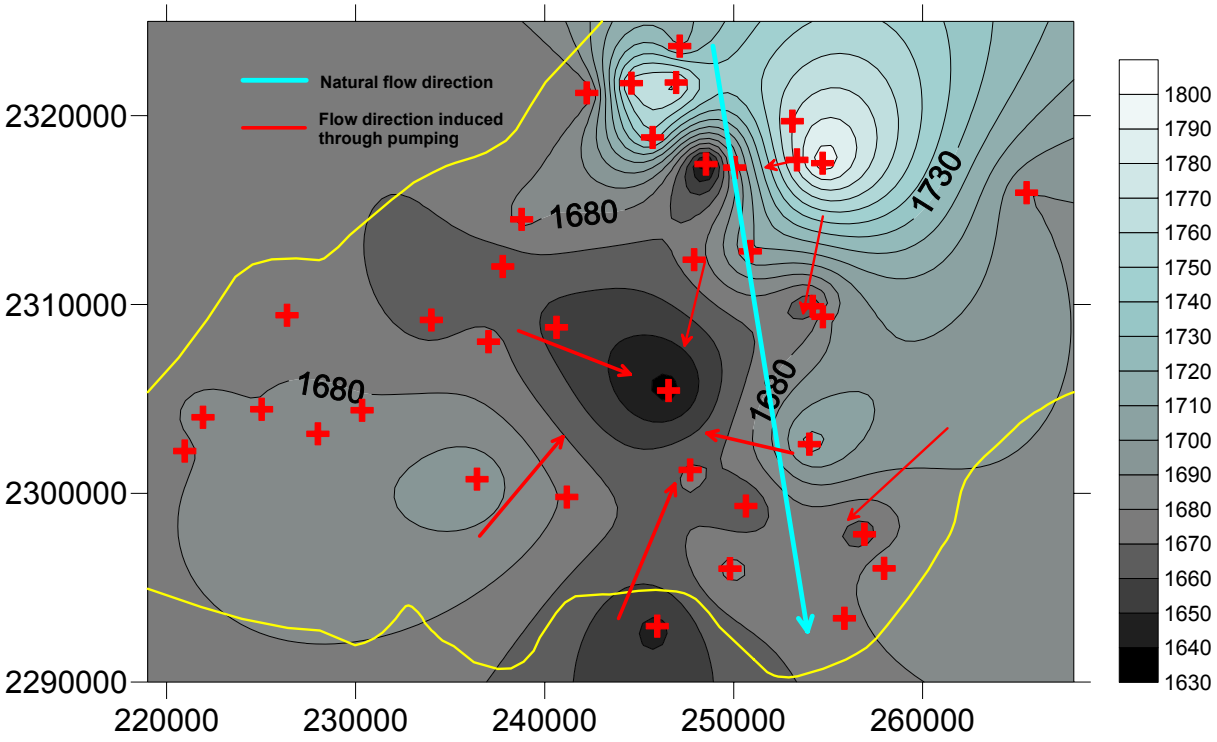

Figure 12: Groundwater table and assumed natural and apparent flow directions in 2004. Data were taken from COREMI et al. (2004).

In the northwest between the towns of Silao and León and in the southeast, near the town of Irapuato, no horizontal barrier is detectable. It is assumed that the aquifer of Silao- Romita corresponds with the adjacent aquifers (COREMI et al.; 2004).

Figure 12 illustrates the groundwater table during piezometric measurements in October 2004. The natural groundwater flow direction from north to south (blue arrow) is considerably changed through pumping. The predominant flow goes in direction to the cones of depression.

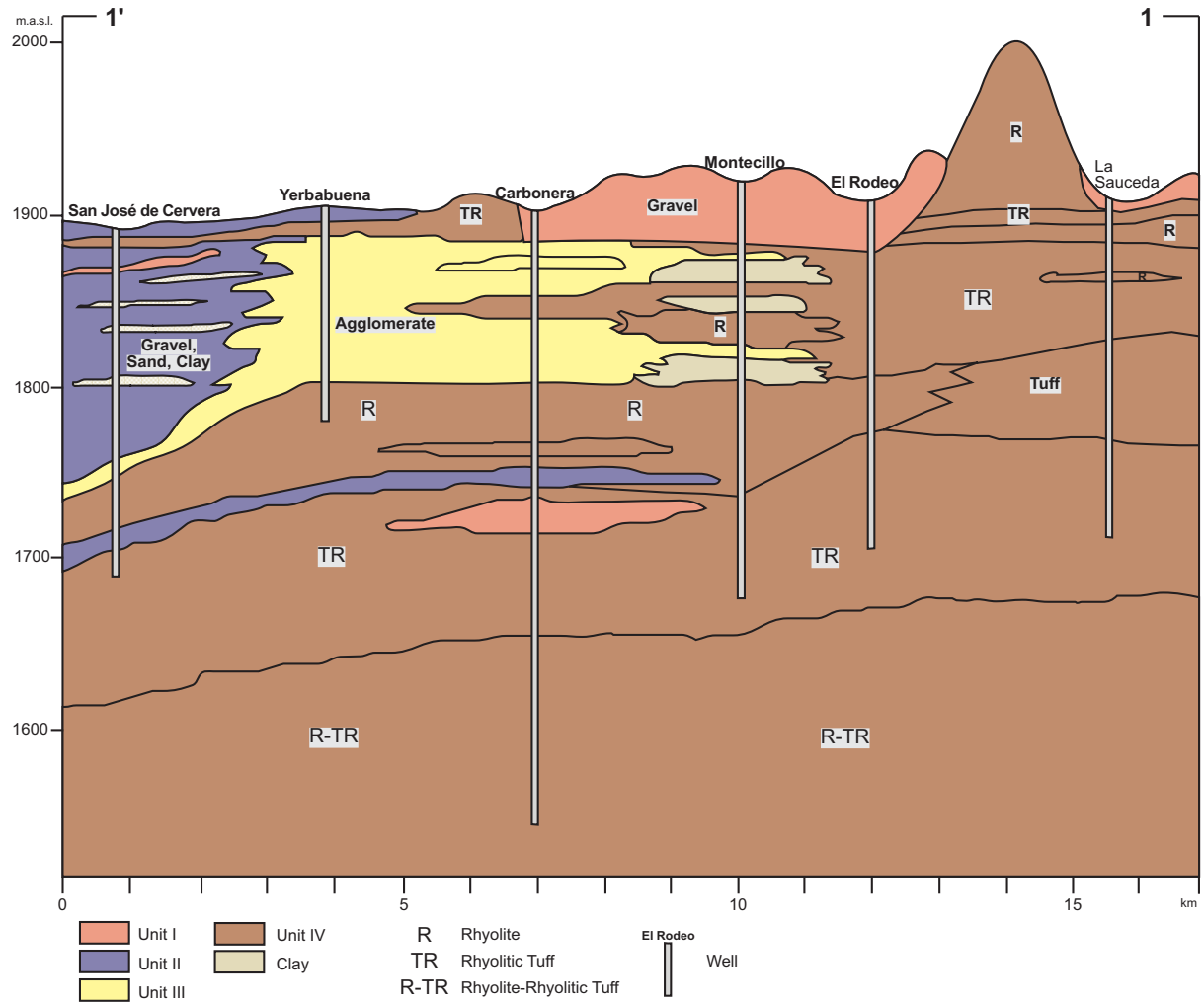

Figure 13: Hydrogeological section 1 (changed after COREMI et al., 2004).

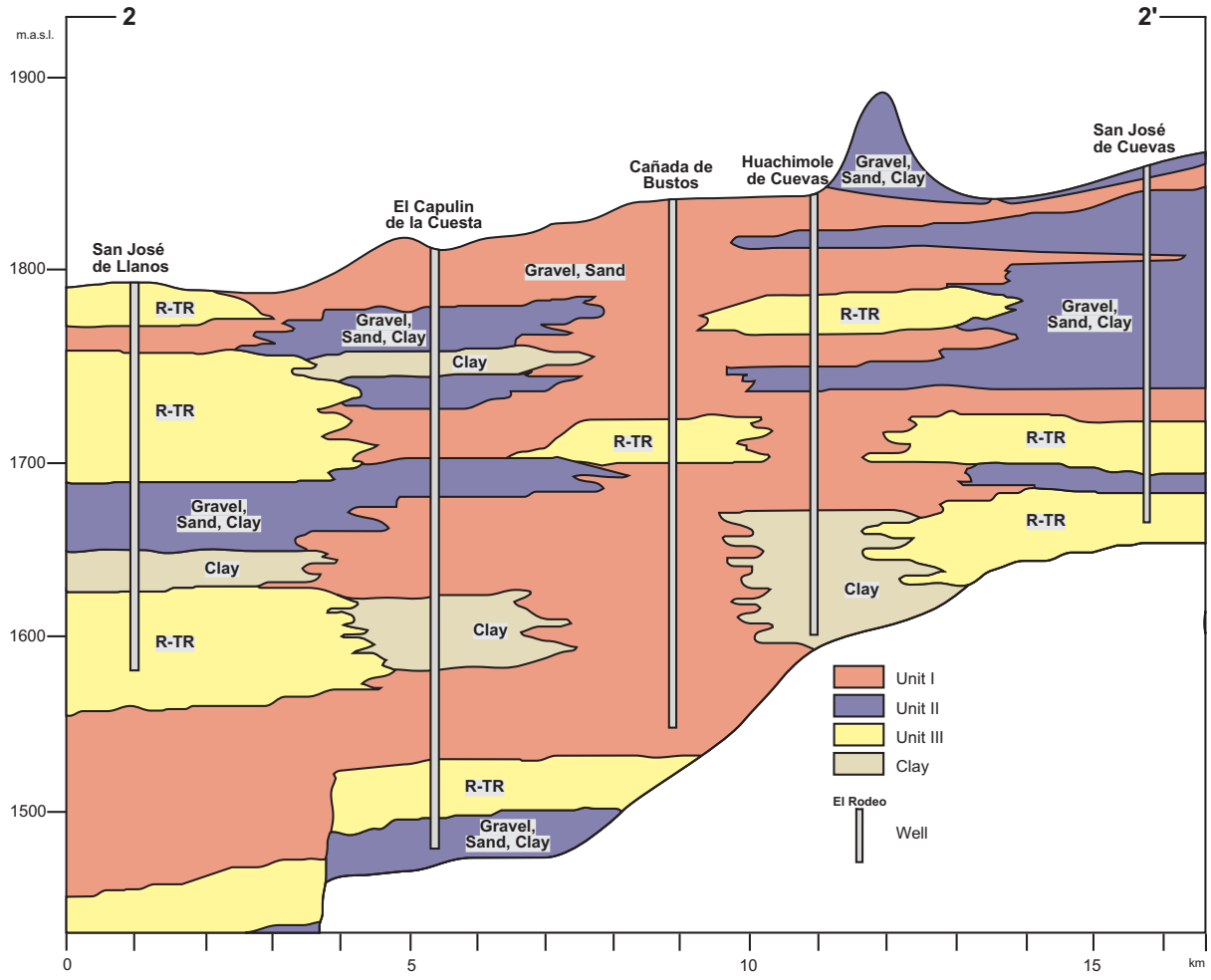

Figure 14: Hydrogeological section 2 (changed after COREMI et al., 2004).

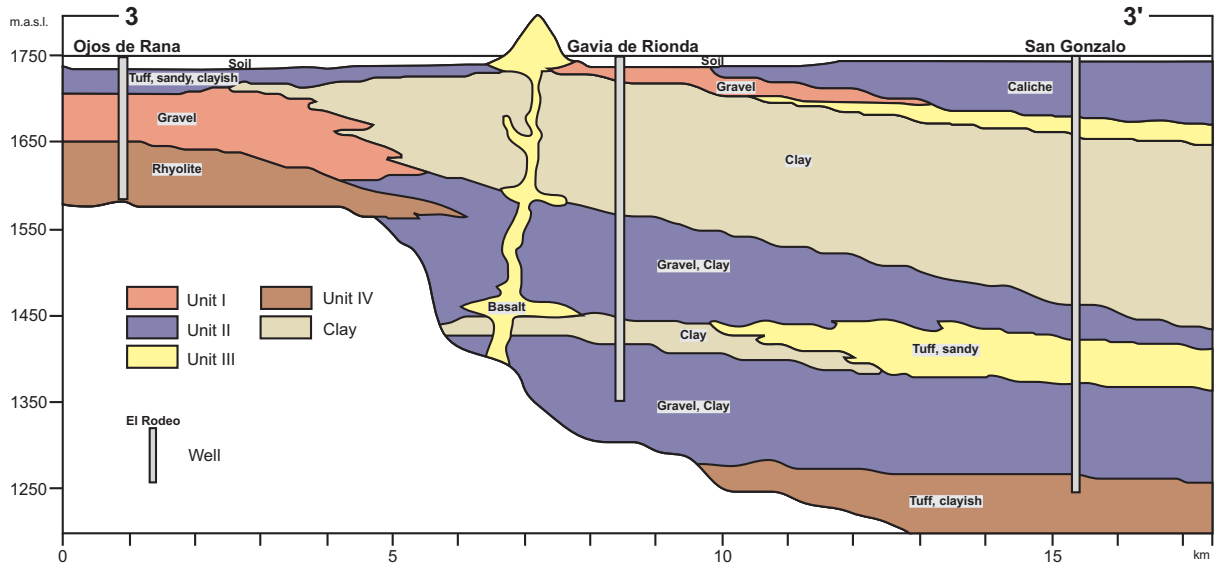

Figure 15: Hydrogeological section 3 (changed after COREMI et al., 2004).

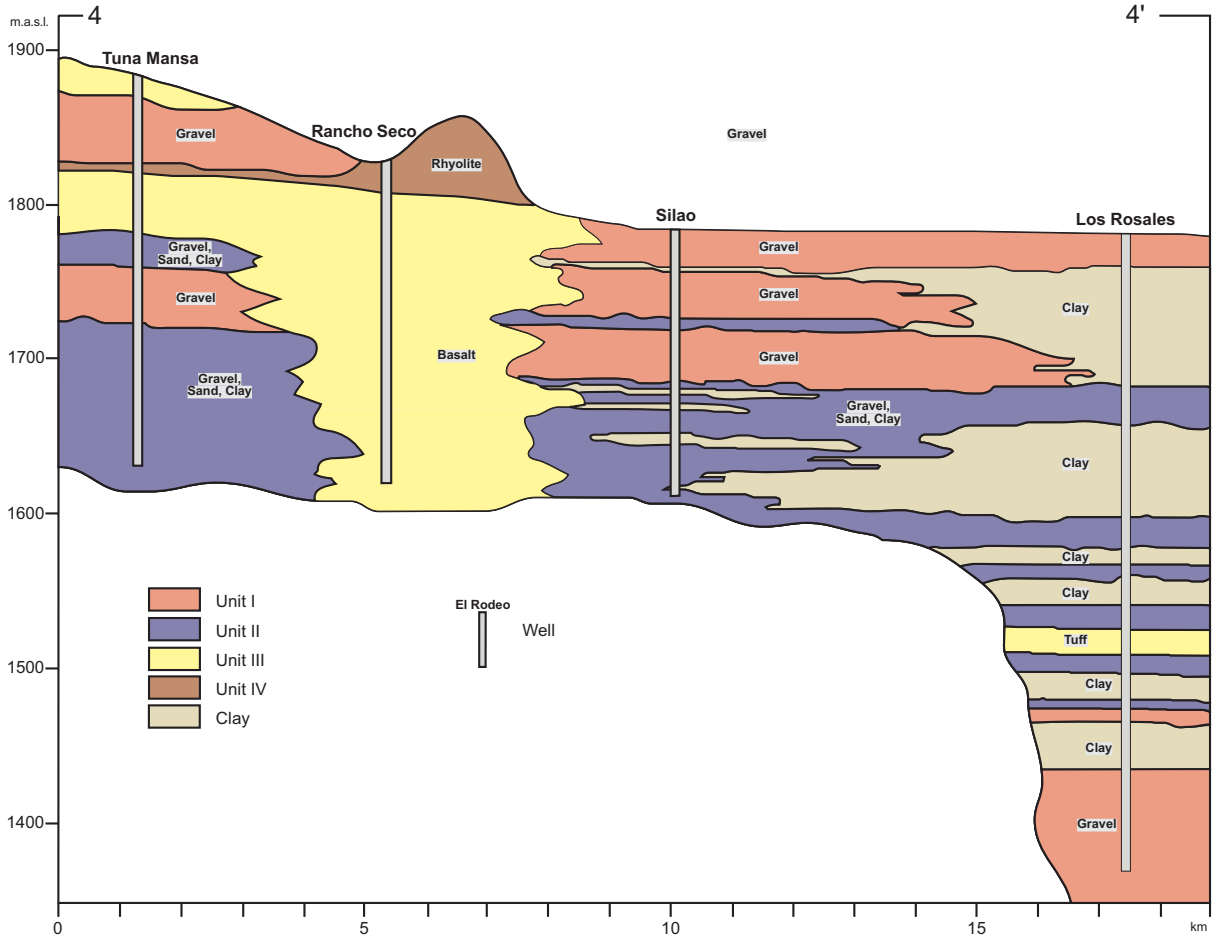

Figure 16: Hydrogeological section 4 (changed after COREMI et al., 2004).

2.7 HYDROCHEMISTRY

In a former report (COREMI et. al., 2004) the major part of the water was classified to be the sodic- bicarbonatic type with variations to Na-Ca-HCO_3, Na-Ca-Mg-HCO_3 and Na-Mg-HCO_3. A second sulphuric group corresponds to profound waters and is of the type Na-Ca-HCO_3-SO_4 and Na-HCO_3-SO_4. These sulphatic groundwaters show high values of TDS (Total Dissolved Solids).

Several wells in the valley of Silao-Romita present temperatures higher than 30 °C. They are considered to have their origin in larger depths and are circulating along faults and fractures, for example *Falla del Bajío* in the mountains of Guanajuato. Two further districts with thermal (> 30 °C) waters are situated in the north of the reservoir *Presa el Conejo* and in the southwest of the investigation area.

In former reports (COREMI et al., 2004; Cortés et al., 2001) analyses of the composition and quality of the subterranean water were made. For the investigation area partially increased values of trace metals were detected. For example elevated concentrations of Cr (up to 54 µg/l), As (> 25 µg/l) and Hg (>1 µg/l) were detected in several wells and springs.

Also slightly increased values of Nitrate (> 10 mg/l) in the valley of Silao-Romita were found, with the highest values of 30 mg/l in the vicinity of Romita. Chloride concentrations are almost always below the assumed natural background of 13 mg/l. Only in the north of Irapuato towards the reservoir *Presa El Conejo* the values of chloride are between 30 and 40 mg/l indicating anthropogenic influences (COREMI et al., 2004).

Isotope studies have been made in the investigation area but mostly only comprise deuterium/ oxygen-18 analyses. Strontium, Carbon and gaseous tracers haven't been used yet to estimate flow conditions. For instance in CEASG (1998) deuterium values ranged from -84 ‰ to -66 ‰ and ^{18}O from -9 ‰ to -10.6 ‰ VSMOW indicating effects of evaporation. This campaign was performed in the dry season. A later study (COREMI et al., 2004), made in the rain season, found Deuterium values between -81.8 ‰ and -67.3 ‰ and Oxygen- 18 values between -10.96 ‰ and -8.95 ‰ VSMOW. Contrary to 1998 these values correlate well with the LMWL which means, that these waters are not affected by fractionation processes.

Only one recent study that also comprises tritium measurements was found (CEASG, 1999). Apart from one well which had Tritium activities of 1.3 TU the five remaining groundwater samples were below the detection limit of 0.8 TU. An older study (CFE-SIB, 1979) determined activities of tritium in surface and groundwater being 23±0.7 TU and 30±8 TU respectively near the town of Salamanca which is situated in the south-east of the investigation area.

3 SCIENTIFIC BASICS

3.1 MATHEMATICAL MODELS

To interpret the results obtained from analyses, the geometry of the aquifer has to be taken into account. Particularly for estimating the time of recharge and residence time with isotopes (tritium, ^{14}C) and trace gases (CFCs) it is necessary to use mathematical models that match more or less exactly the aquifer conditions, because mixing processes alter the results considerably. Reversely with time series aquifer conditions may be determined and described.

The most common approach is the use of so-called black-box or lumped-parameter models. In such a model the state of the system is considered to be homogeneous and spatial variations are ignored (Zuber, 1986). It exist various different types of models and their mixture. Some of them can be seen in Figure 17.

The Piston Flow Model (PFM) describes confined aquifers with a small recharge area far away from the sampling points. It assumes that sampled water was recharged in the same composition without interacting with different "water parcels". The residence time represents the time span from recharge to discharge.

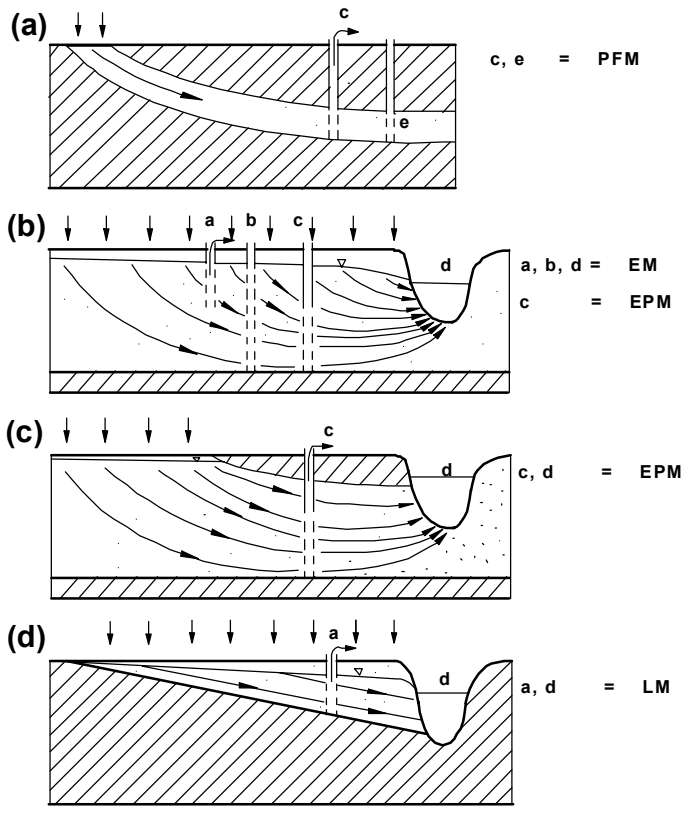

Figure 17: Boxmodels (changed after Zuber, 1986). PFM = Piston Flow Model, EM = Exponential Model, EPM = Exponential Piston Flow Model, LM = Linear Model

The Exponential Model (EM) is applicable in unconfined aquifers with fully penetrating wells and constant unsaturated zone thickness. It also describes the "age" distribution in the outflow of well mixed reservoirs. The aquifer contains a mixture of "young" to "old" water which means that they have been recharged in different times. The proportions of the components of different residence times decrease exponentially with increasing time of residence (Zuber, 1986).

The Linear Model (LM) corresponds to an unconfined aquifer of linearly enlarging depth. The mean residence time increases with the depth.

For the Dispersion Model (DM), besides, the time dispersion parameters have to be adopted additionally. This model is used, for instance, in small catchment areas with high permeabilities or in tracer tests.

Mixtures of these models are used to obtain a better adaptation to the corresponding aquifer. The example of an Exponential Pistonflow Model (EPM) is illustrated by Figure 17c. For the unconfined part of the aquifer the exponential model is valid. The second part occurs confined which requires the piston flow model.

3.2 TRITIUM

Tritium is an isotope of hydrogen, but unlike Deuterium it behaves radioactive. It disintegrates to ^{3}He emitting β^{-}particles. Its half-life amounts to 12.43 (Unterweger, 1980) years. The IAEA recommends (IAEA 2, web) the use of the recently corrected value from Lucas and Unterweger (2000) of 4500 ± 8 days (12.32 years). Tritium is produced in the stratosphere by the disintegration of ^{15}N which was formed through interaction with cosmic ray neutrons.

$$^{14}N + n \rightarrow {}^{15}N \rightarrow {}^{12}C + {}^{3}H$$

Thus formed, the tritium combines with oxygen to water.

Another natural tritium source is the disintegration of ^{6}Li, being produced by the spontaneous fission of Uranium. Although these sources can be considered to be low, they are able to change the results of groundwater investigations in for instance silicate rocks like granites.

Natural tritium levels in precipitation are low, approximately 5 TU (Mazor, 2003), and represent the equilibrium between production in the atmosphere and loss by decay or transportation to the hydrosphere. The production is dependent from the geomagnetic latitude, being greater in higher latitudes (Clark and Fritz, 1997).

With the beginning of nuclear bomb testing the contents increased considerably from about 5 TU before 1952, to a maximum in 1963 of several thousands of tritium units in the atmosphere. Since this time the concentrations are decreasing permanently, at the moment with a rate of 5.5 % per year by decay and additionally by attenuation through oceans and groundwater and have already reached the pre 1952- values.

An important feature is the annual fluctuation of tritium due to the transfer of ^{3}H from the stratosphere to the troposphere during spring in mid-latitudes. Another important feature of tritium in the atmosphere is the variation in the global distribution resulting from the latitudinal constrained

circulation of the stratosphere leading to different concentrations dependent from the latitude. The higher latitudes tend to have more ^{3}H in precipitation than the lower ones (Hebert, 1989). Similar to deuterium and ^{18}O a continental effect can be observed. Air masses charged with marine moisture, rain out over landmasses. At the same time they are charged with tritium rich moisture from higher layers of the troposphere and enrich with locally evaporating tritium rich water. This leads to higher tritium values with increasing continentallity. The effect is more distinctive in summer than in winter (Hebert, 1989 and references therein).

Besides these expanded sources there are also punctual sources for Tritium, primarily the emission of nuclear power plants or nuclear fuel reprocessing. Smaller amounts are emitted during the production of watches or use of medical equipments emitting radiation.

The concentration of tritium is expressed in tritium units (TU) which are absolute concentrations without the reference to a standard. One TU corresponds to one tritium atom in 10^{18} atoms of hydrogen. The radioactivity of 1 litre water having the activity of 1 TU is equivalent to 0.118 Bq whereas one Becquerel equals to one disintegration per second (Clark and Fritz, 1997).

Tritium as well as Deuterium is part of the water molecule and therefore the only radioactive isotope being ideal for estimating ages of groundwater. Qualitative and quantitative approaches are common for dating the age of groundwater.

The qualitative approach refers to the radioactive decay. The input must be known and the measured tritium is assumed to be only the product of decay according to the equation:

$$a_t^{\,3H} = a_0^{\,3H} \cdot e^{-\lambda t}$$

Equation 1

$a_0^{\,3H}$ …initial ^{3}H-activity

$a_t^{\,3H}$ …measured activity

The decay term λ equals to $\ln 2/t_{1/2}$. If the half-life of tritium is used, the equation results to:

$$t = -17.77 \cdot \ln \frac{a_t^{\,3H}}{a_0^{\,3H}}$$

Equation 2

Quantitative approaches are for example the identification of the velocity of the 1963 bomb-peak preserved in soil or groundwater that clearly determines the time of residence of the water. This approach is only useful in special hydrogeological systems with little mixing and thick unsaturated zones, displaying the reverse precipitation curve. This method is only in very few aquifers appli-

cable yet, because the bomb peak has passed the unsaturated zone in most cases. The typical profile is only preserved in very thick aquifers or where the infiltration rates are very low.

Another approach uses Equation 1 and the local input function. Starting from the measured Tritium values and calculating the activity of former years, the activity increases gradually and the decay curve intersects the graph of the input function. The corresponding year is the recharge date. Unfortunately the results are not unambiguous because usually there are several intersections of the decay line with the input function and therefore several recharge dates are possible. Furthermore this approach is only applicable for piston-flow conditions (see section 3.1), because it assumes, that the analysed sample reached the water table in the same composition and doesn't undergo mixing (Clark and Fritz, 1997).

In some areas a seasonality of precipitation is present. In such cases the input function has to be weighted to the infiltration rates of the single months because atmospheric tritium values fluctuate due to different radiation intensities of the sun resulting in different production rates in summer and winter (Zuber, 1986).

3.3 CFCs

CFCs are relatively stable synthetic organic compounds released solely through anthropogenic production into the atmosphere. It is assumed that there are no natural sources for CFCs (Lovelock, 1971). CFCs are still used as refrigerants, aerosol propellants, solvents, cleaning agents or blowing agents in the production of foam rubber or plastics. At the beginning of the nineties of the last century approximately 10^9 kg per year were produced (Busenberg and Plummer, 1992).

Dichlorodifluoromethane (CCl_2F_2, CFC-12) and trichlorofluoromethane (CCl_3F, CFC-11) make up 77% of the global production of CFC. Trichlorotrifluoroethane ($C_2Cl_3F_3$, CFC-113) together with dichlorotetrafluoroethane ($C_2Cl_2F_4$ or CFC-114) and chloropentafluoroethane (C_2ClF_5) make up almost all the remaining 23 % (Derra, 1990).

Although CFCs are non-toxic they contribute to the greenhouse effect (Dickinson, R. and Cicerone, R., 1986) and to the depletion of the ozone layer (Molina and Rowland, 1974). The Montreal Protocol (WMO, 1988) restricted the release of CFCs and since 1996 almost no CFCs are produced (Bauer et al., 2001).

The production has been increasing since the forties and led to a characteristical input function which is assumed to be valid for the whole northern hemisphere due to atmospheric mixing. Measurements in Colorado (USA) and Adrigole/ Macehead (Ireland) show almost equal values (Engesgaard et al., 2004). Even though the majority of CFCs have been produced and released in the northern hemisphere, the mixing ratios in the southern hemisphere only lag slightly behind.

In 1990 air sampled at Tuluila, American Samoa (14.23 °S 170.54 °W) and Cape Grim, Tasmania (40.41 °S 105.54 °W) just had 20 pptv less CFC-12 and 14 pptv less CFC-11 than air in Nivot Ridge, Colorado (Elkins et al., 1996). The atmospheric mixing ratios for the three most important CFCs can be seen in Figure 18. Cunnold (1994) assumes that CFC- concentrations globally are within a variation of 10 %.

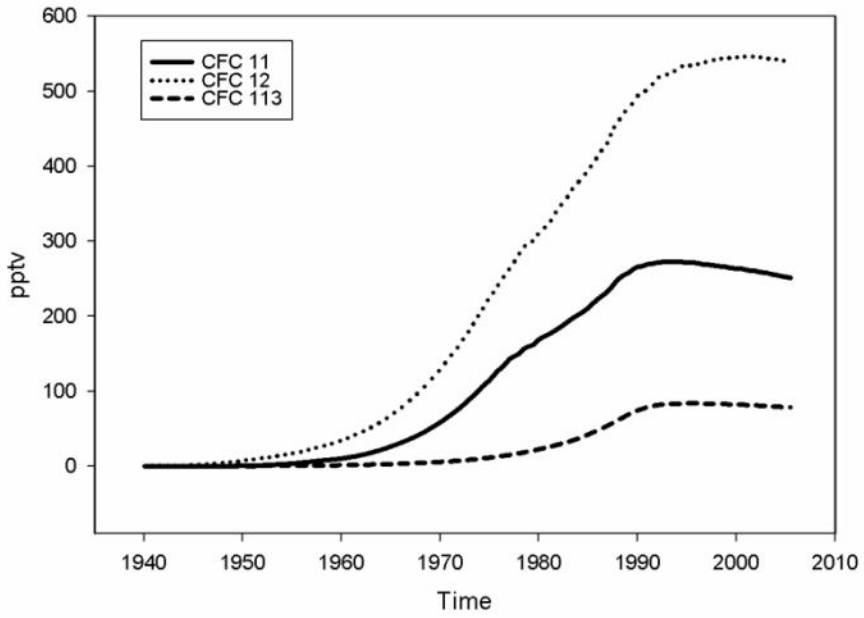

Figure 18: Atmospheric mixing ratios of CFC-11, CFC-12 and CFC-113 in North American air

Since the peak in 1993 (Plummer and Busenberg, 2000) the atmospheric contents of CFC-11 and CFC-113 are decreasing. The CFC-12 mixing ratio slowed later, and started to decrease too. Prior to the seventies no measurements of CFCs are available. Therefore an exponential function was used to reconstruct the temporal development of atmospheric concentration of CFC-113 (Bauer et al., 2001). The values of CFC-11 and CFC-12 prior to 1970 base on manufactured amounts of CFCs (Chemical Manufacturers Association, 1983), rates of release into the atmosphere and hydrosphere (McCarthy et al., 1977; Gamlen et al., 1986), the rate of photolysis in the stratosphere (Cunnold et. al., 1986; Derra, 1990) and the rate of removal by the soils, hydrosphere; biosphere (Plummer and Busenberg, 2000). The values from 1976 to present base on National Oceanic and Atmospheric Administration (NOAA) measurements from Niwot Ridge, Colorado. Data for the above curve were taken from the USGS – CFC – Lab website: http://water.usgs.gov/ lab/software/air_curve/.

Groundwater “dating” with CFCs is based on the solubility of these substances. The partial pressure of the gas in air equals to the concentration of the gas dissolved in water in equilibrium with air (Warner and Weiss; 1985).

$$p_i = x_i\left(P - p_{H_2O}\right)$$

Equation 3

p_i … partial pressure
x_i … dry air mole fraction
P … total atmospheric pressure
p_{H_2O} ... water vapour pressure

The water vapour pressure has to be subtracted from total pressure because recharge occurs in the moist unsaturated zone. Weiss and Price (1980) estimate the vapour pressure using the following equation:

$$\ln p_{H_2O} = 24.4543 - 67.4509\left(\frac{100}{T}\right) - 4.8489\ln\left(\frac{T}{100}\right) - 0.000544 \cdot S$$

Equation 4

S … salinity in parts per thousand (range 0-40 ‰)

For ideal gases air mole fraction can be replaced by air mixing ratio. Henry´s Law describes the solubility of CFCs in water:

$$C_i = k_H\, p_i$$

Equation 5

C_i …solubility
k_H …Henry´s law constant

The solubility of CFCs has been determined by Warner and Weiss (1985) for CFC-11 and CFC-12 and by Bu and Warner (1995) for CFC-113. They estimated square fitting parameters to the temperature and salinity dependency of K_H. The effects to K are given in the following equation:

$$\ln K_H = a_1 + a_2\left(\frac{100}{T}\right) + a_3\ln\left(\frac{T}{100}\right) + S\left[b_1 + b_2\left(\frac{T}{100}\right) + b_3\left(\frac{T}{100}\right)^2\right]$$

Equation 6

K_H …solubility in mol/(kg*atm)
T …temperature in degrees Kelvin (range 273 – 313 K)

The constants for calculating the solubility with Equation 6 are given in the following table:

Table 1: Constants for calculating K_H (Warner and Weiss, 1985; Bu and Warner, 1995)

	a_1	a_2	a_3	b_1	b_2	b_3
CFC-11	- 136.2685	206.1150	57.2805	- 0.148598	0.095114	- 0.0163396
CFC-12	- 124.4395	185.4299	51.6383	- 0.149779	0.094668	-0.0160043
CFC-113	-136.129	206.475	55.8957	-0.02754	0.006033	-

Actually the CFCs are not stable. The atmospheric residence times are determined by Volk et al. (1997) being 45± 7 (CFC-11), 87± 17 (CFC-12) and 100± 32 years for CFC-113, showing the potential for "age-dating" of primarily younger waters. Near urban areas Oster et al. (1996) found concentrations of trace gases being increased locally relative to background concentrations due to industrial and anthropogenic emissions. Other processes that change the residence time are temperature, excess air, sorption, recharge elevation, thickness of the unsaturated zone, microbial degradation and mixing with "younger" and "older" waters. Temperature and recharge elevation are considered in the equations above.

The widely used expression "apparent age" doesn't really represent the residence time. It is the residence time since the isolation from atmosphere through entering the groundwater in the saturated zone. It doesn't include the residence time in the unsaturated zone (Plummer and Busenberg, 2000). Cook and Solomon (1995) found that there is a significant time lag for the transport of trace gases through thick unsaturated zones. CFC concentrations at the top of the water table will be lower than the atmospheric CFC content. The MRT (mean residence time) will be overestimated. The same authors found that thicknesses of less than 10 metres cause a time lag of approximately 2 years which in most cases is negligible. In very shallow unsaturated zones barometric pumping and diffusion mix the trace gases sufficiently and soil gas concentrations correspond to tropospheric contents (Engesgaard et al., 2004). For a water table depth of 30 m in a coarse-crained aquifer the time lag ranges between 8 and 15 years. It is dependent on water content, gas solubility and gas diffusion coefficient. Cook and Solomon (1995) developed an analytical expression for the estimation of the time lag in the unsaturated zone, assuming that chlorofluorocarbons are lowly soluble and diffusion in the gas phase therefore is the dominant transport process. Advective transport only can be observed in the upper few metres. The infiltration rate doesn't seem to play an important role on CFC- time lags in semiarid or arid areas. Increasing the rate from 0 to 600 mm/a in a numerical flow model, Engesgaard et al. (2004) only found a difference of approximately half a year.

A further assumption is the exponential increase of the trace gases in the atmosphere. The concentration profile in the unsaturated zone is described by the following equation:

$$c_g(z,t) = c_0 e^{kt} \left\{ \frac{\cosh\left[(H-z)^2 k\theta^* / D^*\right]^{\frac{1}{2}}}{\cosh\left[H^2 k\theta^* / D^*\right]^{\frac{1}{2}}} - \frac{4}{\pi e^{kt}} \sum_{n=1,3,}^{\infty} \frac{(-1)^{(n-1)/2} \cdot e^{\left(-D^* n^2 \pi^2 t / 4H^2 \theta^*\right)}}{n + 4\theta^* k H^2 / \pi^2 n D^*} \cdot \cos\left[n\pi(H-z)/2H\right] \right\}$$

Equation 7

For large t the second term will become very small. The apparent time lag t_L is defined by:

$$c_g(z,t) = c_0 e^{k(t-t_L)}$$

Equation 8

This can be inserted into Equation 7 and the second term for large t neglected. This means that a certain time has elapsed since initial conditions. The time lag then is:

$$t_L = \frac{\ln\left\{\cosh\left[H\left(k\theta^* / D^*\right)^{\frac{1}{2}}\right]\right\}}{k}$$

Equation 9

c_g	concentration of species in the gas phase, mol/cm^3
c_l	concentration of species in the liquid phase, mol/g
c_s	concentration of species in the solid phase, mol/g
D_g	effective gaseous diffusion coefficient, m^2/a
D_l	liquid phase dispersion coefficient, m^2/a
D^*	lumped dispersion parameter : $D^* = D_g + D_l \rho_l K_w$, m^2/a
H	water table depth, m
k	exponential growth rate, 1/a
k_l	linear growth rate
K_d	solid-liquid partition coefficient, dimensionless
K_w	liquid-gas partition coefficient, g/cm^3
L	depth of unsaturated zone, m
q_g	advective gas flux, m/a
q_l	advective liquid flux, m/a
q^*	lumped advection parameter : $q^* = q_l p_l K_w + q_g$, m/a
t	time, years
t_l	apparent time lag, years
t_0	time of zero concentration
z	depth, m
α	dispersivity, m
λ	decay constant, a
ε_a	gas-filled porosity, dimensionless
θ	volumetric water content, dimensionless
θ^*	lumped water content parameter: $\theta^* = \varepsilon_a + \theta p_l K_w + (1-\theta-\varepsilon_u) p_s K_w K_d$
p_l	density of the liquid phase, g/cm^3
p_s	density of the solid phase, g/cm^3
τ_g	gas-phase tortuosity, dimensionless
τ_l	liquid-phase tortuosity, dimensionless
z	depth, m

The CFC-profiles determined by Cook and Solomon (1995) are not necessarily valid in recent times. Since the early 1970s to the early 1990s the input function shows an approximate linear increase. Therefore Engesgaard et al. (2004) developed a linear correction model. They used the analytical solution for the case of linear increase in atmospheric concentrations provided by Carslaw and Jaeger (1959):

$$c_g(z,t) = k_l t + \frac{k_l \theta^* z(z-2L)}{2D^*}$$

Equation 10

The time must be set relative to t_0 which is the extrapolation of the linear growth phase. In the case of CFC-11 and CFC-12 t_0 would be approximately in 1962. Equation 10 then changes to:

$$c_g(z,t) = k_l (t-t_0) + \frac{k_l \theta^* z(z-2L)}{2D^*}$$

Equation 11

For the linear case the time lag is defined as:

$$c_g(z,t) = k_l (t - t_0 - t_l)$$

Equation 12

Substituting Equation 12 into Equation 11and only considering the time lag at the water table (z = L) Equation 11 simplifies to:

$$t_l = \frac{\theta^* \cdot L^2}{2D^*}$$

Equation 13

Excess air and microbial degradation have to be taken into account additionally in some cases. Degradation occurs primarily in anoxic environments, which means that the dissolved oxygen concentration is less than 0.5 mg/l. The degradation rate decreases with increasing fluorine content. Therefore CFC-11 is more rapidly degraded than CFC-12 and CFC-113. In oxic environments this process couldn't be observed yet (Plummer and Busenberg, 2000).

Excess air is air dissolved in groundwater under increased hydrostatic pressure occurring when the water table rises. This excess air is in solubility equilibrium with tropospheric air and may be enriched in CFC content. Usually excess air content is less than 6 cm^3/l (Wilson and Mc Neill, 1997). The effect of excess air is significant in aquifers with rapid focused recharge and fractured rocks. An important roll in this respect plays the content of CFC in water. The smaller the concentrations of CFCs are, the more sensitive they are to introduction of additional air (Plummer and

Busenberg, 2000). The effects of excess air can be determined from noble gas measurements, e.g. argon and neon (Stute and Schlosser, 2000).

An important process in fractured rocks may be the barometric pumping that transports trace gases. Nilson et al. (1991) found the rates of barometric pumping being one to two orders of magnitude greater than the rates of diffusive transport. Other processes, causing increased air-flow through the unsaturated zone, are periodic water table fluctuations leading to air pressure variations and by it to exchange of gases (Li and Jiao, 2005).

Cook et al. (1995) described sorption of CFC-113 relative to CFC-12. Results from CFC-12 transport agreed very well with tritium ages and therefore this process didn't seem to be important for CFC-12 and CFC-11 in most aquifers. Same authors described significant potential for sorption in limestone, which couldn't be found for sands.

3.4 DEUTERIUM AND OXYGEN-18

^{2}H and ^{18}O are stable isotopes of oxygen and hydrogen that are the constituents of the water molecule. Not retarded or adsorbed in the subsurface, they are ideal for tracing the hydrological cycle. Nevertheless fractionation processes occur as result of the differing physical and chemical properties (Clark and Fritz, 1997).

The basis for the determination of stable isotopes like D and ^{18}O was the development of the NIER-mass spectrometer in the forties of the last century and the creation of the worldwide "IAEA-WHO-Network for the Determination of the Isotopic Composition of Precipitation" that regularly publicises the data (temperature, precipitation, vapour pressure, concentrations of T, D, ^{18}O) in technical reports (IAEA, various years). The obtained precipitation-weighted pairs of variates are arranged in the so called meteoric water line first introduced by Craig in 1961. The $\delta^{18}O$ and $\delta^{2}H$ of fresh waters correlate on a worldwide scale. The δ-values describe the ratio of Deuterium or Oxygen-18 to the international standard SMOW (Standard Mean Ocean Water), which also was first introduced by Craig and later changed by the IAEA into the slightly different VSMOW (Vienna Standard Mean Ocean Water) (Clark and Fritz, 1997).

$$\delta^{18}O_{sample} = \frac{m(^{18}O/^{16}O)_{sample} - m(^{18}O/^{16}O)_{VSMOW}}{m(^{18}O/^{16}O)_{VSMOW}}$$

Equation 14

It refers to the composition of modern seawater, although the actual isotopic contents are somewhat different (Clark and Fritz, 1997). The δ-value in ‰ describes whether a sample compared to the reference is depleted (-) or enriched (+). It is calculated with the help of the following formula:

$$\delta^{18}O_{sample} = \left[\frac{\left({}^{18}O/{}^{16}O\right)_{sample}}{\left({}^{18}O/{}^{16}O\right)_{VSMOW}} - 1 \right] \cdot 1000‰ \text{ VSMOW}$$

Equation 15

The δ-values of ^{18}O and ^{2}H can be plotted in the so called Craig-Diagram. The resulting global meteoric water line (MWL) matches the equation

$$\delta^{2}H = 8.17\delta^{18}O + 11.27 \quad \text{(Rozanski et al, 1993)}$$

Equation 16

and results from the long-term averages of Deuterium and ^{18}O measured in the different IAEA stations.

The slope of this line depends from the surface temperature of the evaporating ocean and the moisture of the overlying air film (Jouzel, 1980). These conditions are not equal in all regions of the world due to varying precipitation and evaporation. Indeed the local MWL is an average of various local MWL. For this reason local MWL's must be calculated having differing slopes and axis intercepts due to fractionation processes dependent from temperature-, altitude-, latitude-, continental- effects as well as seasonal effects leading to fractionation and to an alteration of the slope of the MWL.

The most important influence to the $\delta^{18}O$ and $\delta^{2}H$ exerts the temperature, being responsible for evaporation and precipitation and is reflected by the MWL. A decrease in annual average air temperature of 1.1 - 1.7 °C corresponds to depletion in $\delta^{18}O$ of about 1 ‰. The global dispersion of warm and cold regions reflects this effect. (Clark and Fritz, 1997)

Altitude effect means that the isotopic composition is becoming lighter with higher altitudes. Mazor (2003) shows examples in Swiss and Greece where this effect lies between –0.26 ‰/100m and –0.44 ‰/100m for $\delta^{18}O$ in this case being an effective tool for tracing groundwater recharge in watersheds with highly differing altitudes.

The latitude effect, similar to the temperature effect, shows a decrease in ^{2}H and ^{18}O with increasing latitude due to the Raleigh rainout process. The continental effect is similar but the rainout does not occur from the equator to the poles but from the coast in direction to the continents. Seasonal effects in isotopic composition appear in regions where the seasonal extremes in temperature are larger, primarily in higher latitudes with continental climate. In regions with lower differences in summer/winter temperature but seasonal precipitation the amount effect can be observed. During the dryer months ^{18}O in precipitation is enriched whereas heavier rain events or larger monthly precipitation show a lighter composition of Deuterium and ^{18}O (Mazor, 2003).

The GMWL refers to precipitation data and not to surface or groundwater values (Clark and Fritz, 1997). Groundwater can have different δ-values due to water-rock-interactions leading to isotope exchange (Figure 19). These ratios plot above or below the MWL.

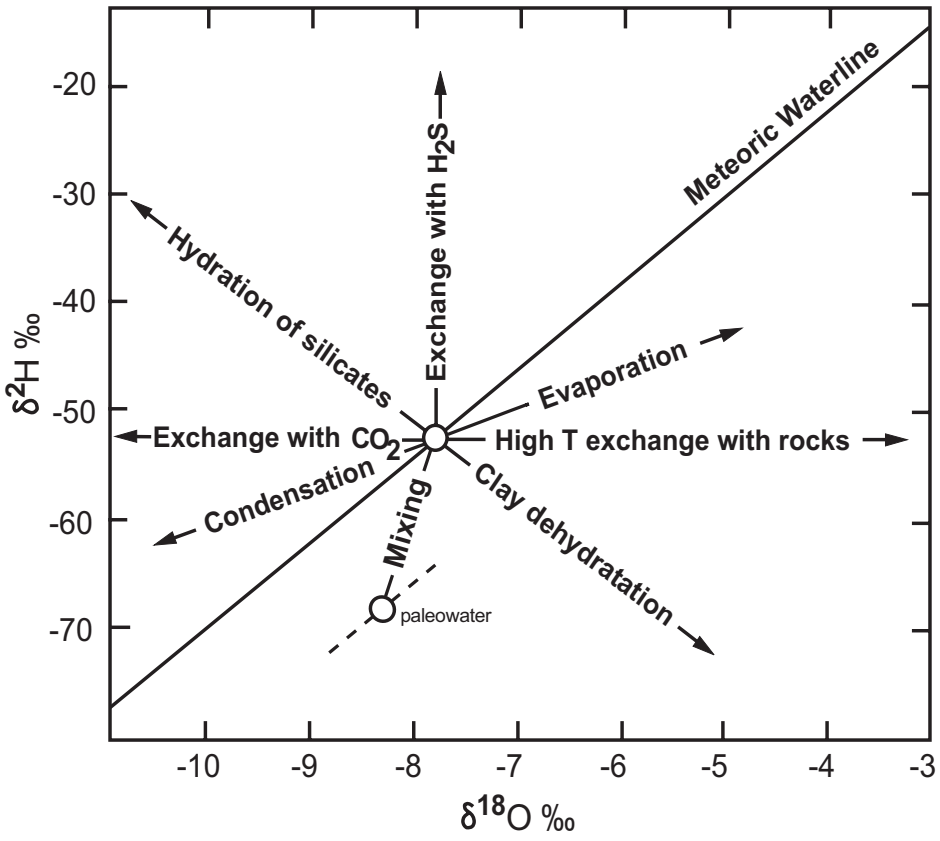

Figure 19: Isotope exchange processes and their effect on the composition of the waters (changed after Clark and Fritz, 1997 and IAEA, web)

3.5 CARBON ISOTOPES

Natural carbon consists of three isotopes. The two stable isotopes ^{12}C and ^{13}C show proportions of 98.89 % and 1.11 % respectively. The radioactive ^{14}C is only present in minor traces (Wagner, 1998). Radiocarbon is produced naturally in the lower stratosphere through the collision of high energy particles with atmospheric gases. This generates spallation and production of secondary neutrons, colliding with nitrogen and producing radiocarbon (Libby, 1955)

$$^{14}N + n \rightarrow {}^{14}C + {}^{1}H$$

The ^{14}C- Atoms oxidise to CO_2 and mix with the carbon dioxide of the atmosphere. The atmosphere shows a balanced $^{14}CO_2$- activity of 13.56 disintegrations per minute and gram of carbon, being approximately 1 ^{14}C-atom per 10^{12} stable atoms. In the past this rate was increased by nuclear bomb tests that also produced large quantities of radiocarbon.

The ^{14}C enters the groundwater via soil CO_2; being washed out with precipitation water in that the $^{14}CO_2$ is dissolved. A lot of CO_2 is absorbed by plants releasing CO_2 via their roots into the soil, where it is dissolved and enters the groundwater.

The ^{14}C- activity is expressed in relation to the $^{14}C/^{12}C$ ratio of the NBS oxalic acid standard and is defined as 95 % of the ^{14}C- activity of this standard in 1950 and is close to the activity of wood grown in 1890 in a fossil CO_2-free environment (Clark and Fritz, 1997). The measured activities are expressed as pmC (percent modern carbon). 100 pmC represent the activity of $^{14}CO_2$ of the atmosphere, although higher values due to anthropogenic enrichment are possible. The detection limit is about 1 pmC making this method appropriate for dating waters of a residence time up to 30000- 40000 years (Mazor, 2003).

The ^{14}C-concentration in the atmosphere is also affected by anthropogenic effects. The industrial revolution since the nineteenth century and the increased combustion of fossil fuels lead to a lowering of the $^{14}C/^{12}C$- ratio of about 10 % due to introduction of ^{14}C-free CO_2. Additional ^{14}C was produced between 1952 and 1963 by nuclear bomb testing. Similar to tritium a bomb peak of up to 200pmC can be observed (Mazor, 2003).

The radiocarbon of soil can be of organic (DOC) or inorganic (DIC) origin. The inorganic is gained by dissolution of atmospheric CO_2. The organic CO_2 originates from organic matter of soil which either is oxidised or biologically degraded with the help of microorganisms. The ^{14}C- content of groundwater can be measured in DIC and DOC alike. Both methods provide complications. Whereas inorganic carbon interacts with rocks, the organic carbon is soil-derived and interactions with humic substances or even coal have to be taken into account (Clark and Fritz, 1997).

For determining the MRT of groundwater by radiocarbon two features are necessary: the initial concentration of ^{14}C must be known and must have remained constant and the system has to be closed to loss or introduction of the parent radionuclide. If these assumptions are fulfilled the following decay equation can be applied:

$$a_t = a_0 \cdot e^{-\lambda t}$$

Equation 17

a_t …activity after time t
a_0 …initial activity
λ …decay constant

Because λ equals to $\ln 2/t_{1/2}$ and the half-life of ^{14}C is 5730 years the equation changes to:

$$t = -8267 \cdot \ln\left(\frac{a_t\,^{14}C}{a_0\,^{14}C}\right)$$

Equation 18

Estimation of the initial ^{14}C activity might be problematic because it changed considerably in the past not only due to bomb testing. The initial activity can be estimated by plotting tritium versus radiocarbon values (Verhagen et al., 1974). The initial ^{14}C activity corresponds to the intersection of the regression line with the detection limit of tritium. In this approach the assumption is made that tritium-free samples may not contain bomb ^{14}C.

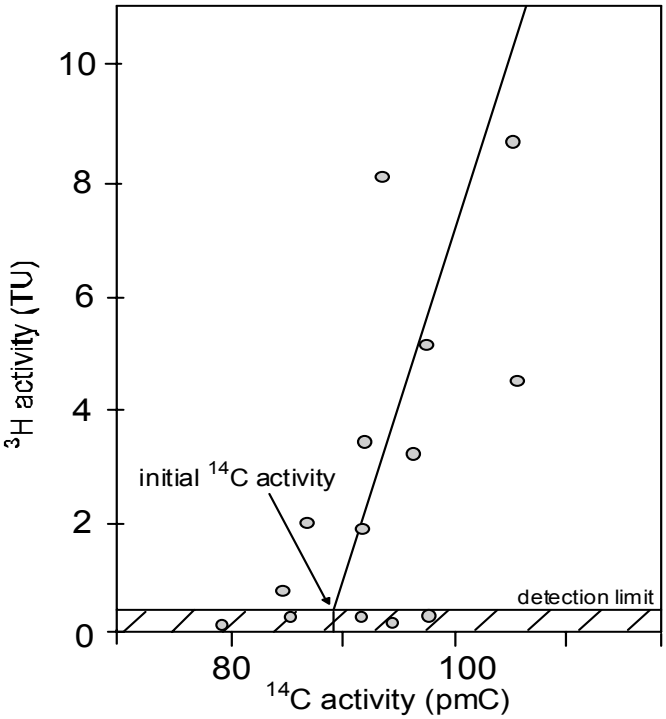

Figure 20: Plot of ^{3}H versus ^{14}C to estimate initial ^{14}C-activity (changed after Verhagen et al., 1974)

Carbon-13

The stable carbon-isotope ^{13}C is widely used to trace carbon sources and reactions because of its large variations in the different carbon reservoirs. Its abundance in rocks, water or organic material is expressed in permil deviation of the $^{13}C/^{12}C$- ratio from the PDB- standard, being a calcite structure of the fossil *Belemnitella Americana* from the Cretaceous Pee Dee Formation in South Carolina. The PDB $^{13}C/^{12}C$- ratio was determined by Craig (1957):

$$^{13}C/^{12}C = (1123\pm1) \cdot 10^{-5}$$

The VPDB is a hypothetical standard defined by the IAEA and is considered to be similar to PDB (Clark and Fritz, 1997). Marine carbonates have mostly values around 0‰ whereas plants have values of -12‰±2‰ or -23‰±3‰, being dependent on the photosynthetic cycle. Organic material and soils show values of -20‰ to -28‰ (Mazor, 2003).

Atmospheric CO_2 shows $\delta^{13}C$- values of about -7 ‰. The photosynthetic uptake leads to depletion in ^{13}C in the plants of 5 – 25 ‰. The depleted CO_2 is passed to the soil by root respiration or by disintegration of the plant material. Because the concentrations of CO_2 in soils are 10 to 100 times higher than in the atmosphere, further fractionation of about 4 ‰ by diffusion through air takes place. Another fractionation process happens during CO_2- hydration or dissolution of calcite or dolomite. Because calcite is enriched in ^{13}C it provides additional source of carbon to the DIC-pool of the water. Therefore groundwater flowing through carbonate rocks is more enriched in ^{13}C than groundwaters of silicate rocks which show more or less the conditions of the soil (Clark and Fritz, 1997).

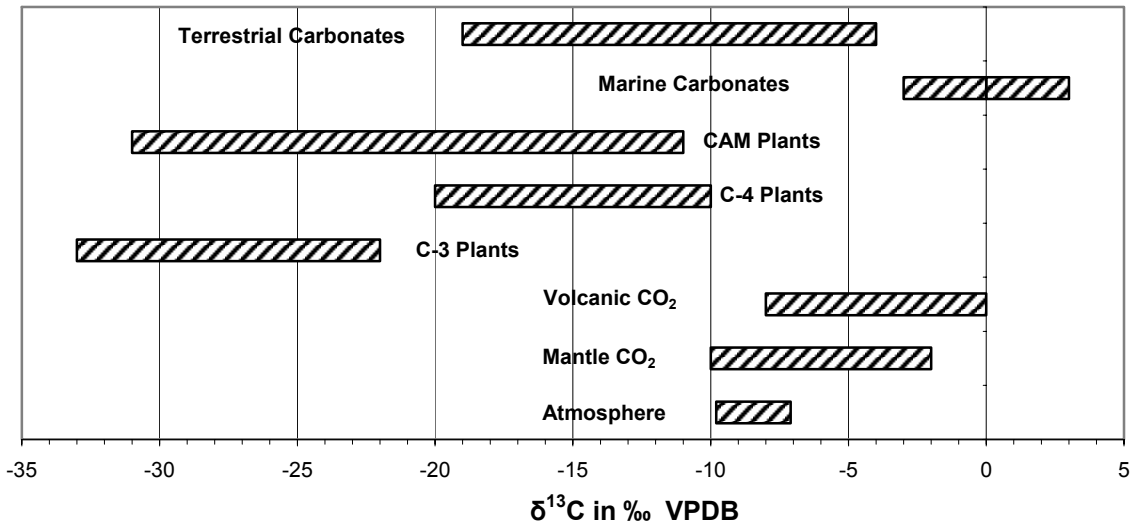

Figure 21: ^{13}C values of different reservoirs and materials. Isotope values for plant groups correspond to resulting soil CO_2 values (after Clark and Fritz, 1997; Rueedi, 2002; Wagner, 1998 and the quoted references therein)

The above figure shows some examples of common sources of carbon in groundwater and their influences on the $\delta^{13}C$ signature. Influenced by one or more of these materials or reservoirs, the groundwater may adopt the signature and flow paths can be determined if significantly different.

As well as rocks influence the $\delta^{13}C$ through reactions also the ^{14}C- activity can be changed. Dissolution of ^{14}C- free carbonic rocks with water containing $^{14}CO_2$ of 100 pmC would lead to a lowering of the activity in the resulting bicarbonates to 50 pmC (Mazor, 2003). This lowering is only valid under closed system conditions. Under open system conditions the initial ^{14}C-activity remains unchanged due to continuous exchange of DIC with the soil CO_2 (Clark and Fritz, 1997).

The standard of 100pmC is calibrated to wood grown in 1890 and has a $\delta^{13}C$ of -25 ‰. The fractionation process during photosynthesis also affects the concentration of ^{14}C. Saliège and Fontes (1984) determined the mass effect for ^{14}C being approximately 2.3 times larger with respect to ^{13}C- fractionation. The respiration through photosynthesis depletes the $\delta^{13}C$- ratio about at

18.5 ‰ what means that ^{14}C is depleted at about 42.5 ‰. Unpolluted atmospheric CO_2 would then contain 104.5 pmC (Clark and Fritz, 1997).

Because of various reactions like calcite and dolomite dissolution, matrix exchange, oxidation of organic material or diffusion of ^{14}C into the aquifer matrix, a correction of the calculated radiocarbon contents are necessary. There are various models to correct the influence of the carbonate dissolution to the ^{14}C- activity. Widely used is the correction of ^{14}C with the help of ^{13}C showing large differences between soil derived DIC and carbonate minerals in the aquifer. For this so called $\delta^{13}C$ mixing model (Clark and Fritz, 1997), which were first introduced by Pearson (1965) and Pearson and Hanshaw (1970), the $\delta^{13}C$ in soil and rock has to be determined alike. The $\delta^{13}C$ of infiltrating groundwater depends on temperature and pH, which change the fractionation of carbon isotopes. The $\delta^{13}C$-values for DIC of recharging groundwaters are defined as:

$$\delta^{13}C_{rech} = \delta^{13}C_{soil} + \varepsilon^{13}C_{DIC-CO_2(soil)}$$

Equation 19

$\delta^{13}C_{rech}$ …….. ^{13}C ratio in groundwater

$\delta^{13}C_{soil}$ …… $\delta^{13}C$ of soil CO_2

$\varepsilon^{13}C_{DIC-CO_2(soil)}$ … pH dependent enrichment between soil CO_2 and aqueous carbon

The $\varepsilon^{13}C_{DIC\text{-}CO2(soil)}$ is pH dependent. If an initial $\delta^{13}C_{soil}$ of -23 ‰ at pH 4 is assumed, the enrichment increases to approximately -16 ‰ at pH 7 and -14 ‰ at pH 8. The $\delta^{13}C_{rech}$ is used to calculate the $q_{\delta 13C}$:

$$q_{\delta^{13}C} = \frac{\delta^{13}C_{DIC} - \delta^{13}C_{carb}}{\delta^{13}C_{rech} - \delta^{13}C_{carb}}$$

Equation 20

The q- value is used in the decay equation which calculates the corrected residence times:

$$t = -8267 \cdot \ln \frac{a^{14}C_{DIC}}{q_{\delta^{13}C} \cdot a_0{}^{14}C}$$

Equation 21

The $\varepsilon^{13}C_{DIC\text{-}CO2(soil)}$ is dependent from further fractionation factors between CO_2 in gaseous and liquid phase and HCO_3 and CO_2 in the gaseous phase. It can be calculated with:

$$\varepsilon^{13}C_{DIC-CO_2(soil)} = mCO_{2(aq)} \cdot (\varepsilon^{13}C_{CO_2(aq)-CO_2(g)}) + mHCO_3 \cdot (\varepsilon^{13}C_{HCO_3-CO_2(g)})$$

Equation 22

Another approach is the statistical correction that may be applied in areas where the geochemical evolution can be averaged over the whole recharge area to estimate the initial ^{14}C activity of the carbonate. This calculated initial value represents the remaining ^{14}C activity after carbonate dissolution. The q-values are reported by Vogel (1970):

0.65 - 0.75	karstic systems
0.75 - 0.90	sediments with fine-grained carbonate (loess)
0.90 - 1.00	crytalline rocks

A further approach is the alkalinity model being only applicable in aquifers where the calcite dissolves under closed system conditions. As seen above, this leads to a q- factor of 0.5 (50 %). Because of its simplicity it is only of minor interest. Also for closed systems the chemical mass balance model can be used. In the calculation the DIC gained from dissolved soil CO_2 and from that measured in the sample are compared (Clark and Fritz, 1997).

Further models are developed by Fontes and Garnier (Fontes and Garnier, 1979) and Gonfiantini (Salem et al., 1980). These models also assume closed system conditions. In the investigated area because of possible irrigation return flow, intensive pumping and heavily fluctuating water tables this assumption can't be made. Testing the Gonfiantinis model q-factors of 0.2-0.3 are yielded. This means that the measured activity of for instance 100 pmC would have to be corrected to 500 – 333 pmC which is quite unrealistic since the highest atmospheric activities in the sixties were 200 pmC (Clark and Fritz, 1997).

3.6 STRONTIUM

Strontium is an alkali-earth metal occurring, besides the instable types, in four different stable forms: ^{84}Sr, ^{86}Sr, ^{87}Sr, ^{88}Sr. Only ^{87}Sr is radiogenic, originating from the disintegration of the radioactive alkali-metal ^{87}Rb which has a half-life of 48.8 x 10^9 (Neumann and Huster, 1974). Due to this, the concentrations of ^{87}Sr in minerals containing rubidium are gradually increasing. Strontium-87 has two origins: One was the forming during the primordial nucleosynthesis along with the other isotopes and the second is the radioactive decay of Rubidium-87. Generally groundwater has three primary strontium sources: the atmosphere, dissolution of Sr- bearing minerals and anthropogenic input (Négrel and Petelet-Giraud, 2005).

The $^{87}Sr/^{86}Sr$ ratio is a parameter to show the proportion between stable and radiogenic strontium and generally lies between 0.7 and 4 (Faure, 1972). The present day ratio of a strontium-bearing mineral is described by the following equation:

$$^{87}Sr/^{86}Sr_{present-day} = ^{87}Sr/^{86}Sr_{initial} + ^{87}Rb/^{86}Sr_{present-day}\,(e^{\lambda \cdot t} - 1)$$

Equation 23

λ = 1.42 x 10^{-11}

Geologically carbonates and plagioclases contain the least radiogenic strontium and potassium-feldspars and micas the most radiogenic. This is due to the substitution of potassium by rubidium. Water equilibrating with these rocks adopts the ratio (Clark and Fritz, 1997). Thus strontium that is derived from minerals shows the same $^{87}Sr/^{86}Sr$- ratio. Differences in the ratios of groundwaters originate either from varying mineralogy along contrasting flowpaths or from different relative amounts of Sr, derived from distinct minerals. The second situation arises during saturation of the water regarding to the minerals or the change of the water chemistry along the flow path provoking different dissolution rates. Furthermore the residence time and flow velocity of the water is important for strontium ratio and concentration. Groundwaters in relatively lightly soluble aquifers (calcite, hornblende, plagioclase) will equilibrate more readily and adopt the ratio than in poorly soluble media (quartz). The effective surface area of the minerals and coating may cause differences in water chemistry, isotope ratio and Sr-content (Bullen and Kendall, 1998). Precipitation of strontium and ion exchange don't affect the Sr-ratio in water. Therefore Sr-isotope ratios can provide information about the different sources of the solutes within the water (Gosselin et al., 2004).

Although strontium behaves in solution like calcium it can't be used as an indicator for high Ca-content. For example Na- plagioclase and K-feldspar contain little Ca but more strontium than Ca-plagioclase. (Bullen and Kendall, 1998)

The most important silicate minerals are feldspars, plagioclase, K-feldspar, hornblendes, micas, biotites, muscovits and clay minerals. Micas and clay minerals are low in Sr – concentration but are high in ^{87}Sr due to their increased Rb/Sr ratio. Non-silicates like carbonates, calcite, aragonite or dolomite contain high Sr concentrations but their $^{87}Sr/^{86}Sr$- ratio is low. Evaporite minerals like gypsum or anhydrite may have high contents of Rb (McNutt, 2000).

Similarly to the delta notation of other isotopes (e.g. $^{2}H/^{18}O$) also for strontium the reference to standard value was introduced. The δ-value for a sample relative to a standard is described by the following equation:

$$\delta^{87}Sr = \left(\frac{^{87}Sr/^{86}Sr_{sample}}{^{87}Sr/^{86}Sr_{\text{s tan }dard}} - 1 \right) \cdot 1000$$

Equation 24

For strontium, unfortunately, doesn't exist a uniform standard what complicates the comparison of different studies. A widely used standard is the metal SRM987 of the National Institute of Science and Technology (N.I.S.T) with a value of 0.71024 (Bullen and Kendall, 1998). Another standard is the strontium carbonate of the National Bureau of Standards with a value of 0.701 for the ratio of $^{87}Sr/^{86}Sr$ (Clark and Fritz, 1997).

The isotope ratios of lighter elements are mostly affected by thermodynamic fractionation. Sr isotopes are not affected by significant mass fractionation during phase separation regardless of temperature, biological processes or chemical speciation. Variations in atmospheric content also don't play any role, because Sr concentration is very low. The $^{87}Sr/^{86}Sr$ ratio is mainly controlled by water rock interactions. Changes in strontium isotope composition reflect either the production of ^{87}Sr through radioactive beta decay of ^{87}Rb or mass balance mixing (Ingraham et al., 1998; Bierman et al. 1998).

Silicate rocks can be distinguished into two groups. Most mantle-derived rocks show initial $^{87}Sr/^{86}Sr$ – ratios ranging from 0.703 to 0.706. Most granitic, metamorphic and detrital sedimentary rocks have initial $^{87}Sr/^{86}Sr$ – ratios between 0.709 and 0.725 (Faure and Powell, 1972). Limestones reflect the ratio of sea water at the time of their deposition which is intermediate between continental runoff values (0.7119) and basaltic hydrothermal components (0.703) (Bierman et al., 1998). Atmospheric Sr- ratios are similar to that of sea water or slightly more radiogenic. Freshwater carbonates may have higher isotopic values (> 0.71) reflecting the source of the water. Carbonate rocks like limestones and dolomites contain little Rb. Mostly the measured concentrations of rubidium originate from inclusions of other minerals like clay minerals (McNutt, 2000).

Generally carbonates like calcite and dolomite are more soluble than most silicates in aqueous solution. They also have higher Sr contents and lower $^{87}Sr/^{86}Sr$ – ratios. Therefore a groundwater having equilibrated in a carbonate aquifer will maintain its source signature flowing into a silicate aquifer which normally has higher ratios and lower concentrations. In reverse direction the silicate signature is lost quickly because the higher concentrated carbonatic water overwhelms the ratio of the low concentrated silicatic one. Nevertheless the second case can be helpful, because maintenance of the ratio in for example silicatic aquifers reveals the origin of the water (McNutt, 2000).

Besides water-rock-interactions and mixing the strontium ratios can also be affected by anthropogenic activities like agriculture. Böhlke and Horan (2000) found significant increased $^{87}Sr/^{86}Sr$ – ratios in the agricultural influenced recharge water. The higher values originate from increased use of fertilizers showing in this investigation a more radiogenic value (0.715) in comparison to the lower value (0.708) of the prevailing carbonates.

4 METHODOLOGY

4.1 PREPARATION

Information about geology, hydrogeology, soil and topography - previously obtained by reports of diverse agencies and universities (INEGI, CEAG, CNA, COREMI[1], Instituto de Ecología, SDA, Consejo de Desarrollo Regional del Agua, UNAM) - included in a Geographical Information System (GIS) served to chose the sampling sites. Furthermore these reports about geology, water chemistry, geophysics and vulnerability helped to understand the local conditions. Several parameters were important during the choice of the sampling areas: for instance geology (fractured rock/ sediments), hydrogeology (recharge areas/ aquifer type) and water chemistry (temperature).

The sampling points weren't chosen directly. Merely areas of approximately 1 km^2 could be determined to maintain the statistical distribution. In these areas no larger changes of morphology, geology, vegetation, soils or water chemistry were expectable. No samples were taken in the north of the study area because in the fractured rocks of the *Sierra de Guanajuato* only few wells are existent and if they are existent they are hardly accessible. To verify if the border of the watershed also falls together with the assumed border of the aquifer also outside of the study area at the north-western margin some samples were taken.

[1] now: Servicio Geologico Mexicano (SGM)

4.2 FIELD ACTIVITIES

Altogether 30 samples were taken, 28 of pumping wells and 2 of springs. The wells were partly in operation and could be sampled immediately. Those, who weren't in operation had to pump at least 15 minutes. The water chemical parameters (pH, conductivity, temperature, dissolved oxygen) were measured in a bucket filled with sample water (WTW Multi 350 I; pH-Electrode SenTix41, ConOx). The usage of a flow through cell was also tried but didn't yield reasonable results. Furthermore it wouldn't have been possible to use it in all wells due to sometimes difficult sampling conditions. Therefore the bucket-method was preferred.

For pH measurement a two point calibration with pH 4 and pH 7 buffer solutions (WTW) was made. Because of higher pH values this doesn't seem ideal but higher pH buffers weren't obtainable. The concentration of dissolved oxygen at 11 sampling points was measured later due to defects. Calibration of oxygen- and pH- probes was performed at every sampling point. The redox potential wasn't determined.

For later analysis of anions and cations water was filtered with the Nalgene® Filter Holder with Receiver and MILLIPORE 0.45 µm nitrocellulose filters and filled into new, three times prerinsed, plastic bottles; for cations with 1 ml concentrated HNO_3 (ultrapur) for preservation. For ^{13}C, alkalinity and strontium unfiltrated water was filled into plastic bottles and to the strontium sample solid NaOH (purification 99.8 %, CTR SCIENTIFIC MONTERREY), previously dissolved in deionised water (conc: 1 mol/l), added to precipitate the carbonates (pH > 12.5).

The samples of ^{14}C were filled into glass bottles with special membrane caps permitting the removal of air bubbles by pricking with a needle.

For analyses of CFC special vessels of the "Spurenstofflabor Harald Oster" were necessary, hindering interchange of water and atmospheric air. The glass bottles are preserved in tinned boxes surrounded also by sample water. To obtain this state, the box and the bottle inside were opened and put in a bucket. The water was conducted directly and slowly from the outflow into the glass bottle by a plastic tube until the whole bucket was filled and bottle and box are closed carefully. With this procedure the bottle was rinsed approximately ten times of its volume and contamination by the tube or vessel are improbable.

Figure 22: Sampling procedure for CFCs

The samples of ^{13}C, anions and cations were stored in an icebox cooled by ice cubes and later in a refrigerator until they could be analysed or shipped to the corresponding laboratory.

4.3 LABORATORY

4.3.1 Waterchemistry

The titration of the alkalinity was done usually directly at the evening after the sampling. Some couldn't be titrated sooner than 4 days after sampling. For the titration 0.02 N H_2SO_4 and the pH probe of WTW was used to control the pH. It was titrated to pH 4.3 to calculate the alkalinity. For estimation the following equation was used (Franson, M.A.;1976):

$$Alkalinity(mg/l) = \frac{A \cdot N \cdot 61}{B} \cdot 1000$$

Equation 25

A … ml of titrant to reach pH 4.3
B … ml of sample
N … Normality of acid

Analyses of major minor and trace elements were done in the *Laboratorio del Centro de Calidad Ambiental* of the *Tecnológico de Monterrey*. Elements were analysed after two methods: EPA 6010 C/2000 for As, Ba, Be, Cd, Ca, Cr, Sr, Fe, Li, Mg, Mn, PO_4^{2-}, Se, SiO_2 and Na (ICP AES) and EPA 300.1/1999 for Cl^-, F^-, PO_4^{2-}, NO_3^- and SO_4^{2-} (IC). Standard deviations for the methods and information about the used equipment were not provided by the laboratory.

Because of uncertainties concerning the reliability of the results the analysis of some elements was repeated by the hydrochemical laboratory of the *Technische Universität Bergakademie Freiberg*, Germany. Anions were analysed with the Eppendorf Biotronik IC2001 and Cations with the Merck Hitachi Equipment (L-6200A intelligent pump, D-6000A interface and L-3720 conductivity detector). The standard deviations for both methods illustrates Table 2. It was determined separately through 13 repeated measurements of certain samples.

Table 2: Determined standard deviations for IC-Methods in Freiberg

	Cations					Anions		
Elements	**Li^+**	**Na^+**	**K^+**	**Ca^{2+}**	**Mg^{2+}**	**Cl^-**	**NO_3^-**	**SO_4^{2-}**
1σ [mg/l]	0.016	2.51	0.68	0.53	0.22	0.11	0.77	0.81

4.3.2 Tritium

The analyses of tritium were made in the *Labor für natürliche Radionuklide/TriCar-Laboratory* at the *Technische Universität Bergakademie Freiberg*. Tritium was analysed through counting β-decay events in a liquid scintillation counter ("Quantulus"). The 300 ml samples were distilled and in cylindrical cells of the IAEA-type electrolytical enriched by the factor of 17±0.5. The detection limit of the method is 0.2 TU. In Appendix 19 standard deviations can be seen.

4.3.3 CFCs

CFCs were measured by *Spurenstofflabor Harald Oster*, Wachenheim, Germany, using an electron capture detector and gaschromatography (GC-ECD). To determine CFC concentrations in water samples, 20-40 ml of water is injected into a degassing chamber and sealed by a bellow valve. The dissolved CFCs are extracted by purging with CFC-free gas for 7 Minutes followed by pre-concentration of the tracers in a Peltier-element cooled trap (p.c. Harald Oster, Wachenheim). The subsequent chromatographic analysis is the same as described for standard GC-measurements (e.g. Oster et al., 1996; Kellner et al. 2005). The detection limit is 0.01 pmol/l for CFC-113. No information about the precision of the method was provided.

4.3.4 Deuterium and Oxygen-18

Deuterium and ^{18}O were analysed at the *Environmental Isotope Laboratory* (*EIL*) at the University of Waterloo, Canada. For deuterium analyses the sample water is reduced on hot manganese (512 °C) and by that the hydrogen gas is produced. For this procedure the sample is introduced to the evacuated reaction vessel which contains the manganese. Before the vessel is heated to 512 °C the water is frozen and the vessel re-evacuated. The precision of this method is ±2 ‰.The released hydrogen is analysed by GC-MS.

For oxygen-18 analyses 2-8 ml of sample water are equilibrated with CO_2 in a temperature controlled bath with continuous shaking for at least 3 hours. Preparation and extraction is done on a fully automated system of 30 ml vessels attached to the VG MM 903 mass spectrometer. For quality control the lab water standard EIL-12 is analysed frequently. No information was provided concerning the precision of the method.

The description of the methods was taken from the website of the EIL-laboratory: www.science.uwaterloo.ca/research/eilab/.

4.3.5 Carbon isotopes

As well as ^{2}H and ^{18}O analyses ^{13}C determination was performed by the *EIL*-laboratory. Carbon-13 samples were acidified with H_3PO_4 and the released CO_2 purified using cold distillation. The carbon dioxide was then transferred into mass spectrometric vessels and analysed on the MM-903 for $\delta^{13}C_{DIC}$ with respect to PDB. For calibration the internal standard EIL30 was used. There is no information about the precision of the method on the EIL-laboratory website.

Radiocarbon was extracted by the EIL-laboratory (same method as for ^{13}C) and sent in glass ampoules to the *IsoTrace Laboratory* at the University of Toronto. There the CO_2 was converted into graphite by reacting the carbon dioxide with molten lithium to form Li_2C_2 which produces acetylene when it is hydrolysed.

Graphite then was deposited epitaxially from the acetylene by a high voltage electrical discharge as 3 mm diameter discs (approximately 250 µg of carbon per disc) onto the two electrodes (targets). Every target contains one disc and is analysed separately with two ^{14}C standards (NBS Oxl) in different runs. Each target was scanned on 16 points in the AMS ion source and this procedure 10-12 times repeated.

The $^{13}C/^{12}C$ ratio being analysed at the same time is used to correct the $^{14}C/^{12}C$ ratio for isotope fractionation during analysis. The results for both targets of one sample are statistically compared and averaged. The average is then corrected for a background of 0.0077 pmC due to lithium contamination.

Further information wasn't provided by the laboratory

4.3.6 Strontium

The water of the strontium samples were filtered with paper filters (Whatman® ashless filter paper 125 mm, 1 µm) to separate the precipitated carbonates. The filters were dried (80 °C) and the carbonate filled in PE-bags for transportation.

At the laboratory for isotopic chemistry of the TU Bergakademie Freiberg the analysis of strontium was realised. First the determination of the $^{87}Sr/^{86}Sr$ – ratio in the precipitated carbonates was tried. For some samples only very small amounts of carbonates were filtered, which were considered not to be sufficient, because at least 20 mg are necessary for a reliable analysis. Unfortunately the filters and the NaOH contained measurable amounts of strontium: 80 ng/filter and 7,4 ng/ml respectively. The ratios were 0.678204 for the filter and 0.528166 for the sodium hydroxide, being significantly lower than the expected water ratios. To avoid effects of the filters and the sodium hydroxide solution it was tested to evaporate sample water directly. This method worked well and was used for all samples.

After evaporation to dryness the residue was dissolved by 1 ml 2.5 N HCl and 200 µL of this solution given in an ion exchange column (ion-exchange resin: Dowex 50 Wx 8). After adding 17 or 18 ml (dependently from the column size and calibrated flow properties) of 2.5 N HCl, which washes out the calcium, iron and rubidium fraction, other 4 ml are added and the strontium fraction can be picked up in teflon vessels. This fraction was evaporated again and separated a second time in the ion-exchange columns.

The residue now was dissolved with 5 µl deionised water and placed onto single tantalum filaments. In a special preparation unit the drop was dried and later the tantalum annealed. After this procedure the filaments could be loaded into the source of the thermal ionization (solid source) mass spectrometer Finnigan MAT 262.

For every sample then the spectrometer measured 5 blocks with 10 scans each and corrected the values to the $^{88}Sr/^{86}Sr$ – ratio of 8.375209 to eliminate the effect of isotopic fractionation during the analysis. The standard deviation was generally between 0.000052 and 0.000165. The laboratory provided 1-σ. In this report 2-σ was used to have consistency between the different analyses and therefore the above values were doubled. The blank of the whole method is below 1 ng strontium. During all measurements the SRM987 standard was determined five times. The values were between 0.71022 and 0.71034 with a 1-σ of 0.00010 to 0.00013, always comprising the international approved ratio of 0.71024.

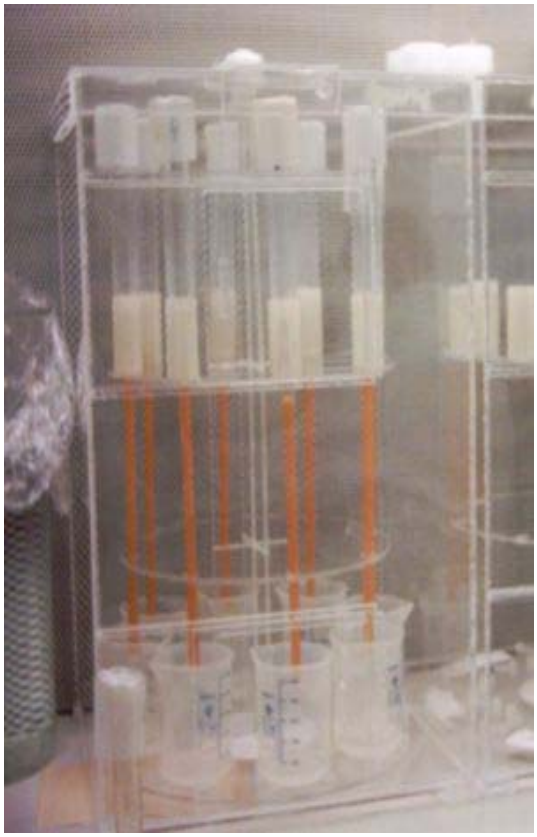

Figure 23: Ion exchange columns

Besides the waters also 5 samples of rock materials were taken and analysed. First 50 mg were dissolved by 2 ml 0.1 N HCl and the solution treated as the waters like described above. The undissolved residue was dried and 3 ml of a mixture of HF-HNO_3 was added. After 36 hours at 110 °C the liquid could be divided in the ion exchange columns. The analysis was the same process as described above. The blank for this method was determined between 0.7 and 1.2 ng strontium.

4.4 PROCEDURES

4.4.1 Waterchemistry

To validate the results of the chemical analyses the ion balance was calculated. For this procedure the program PHREEQC (Parkhurst and Appelo, 1999) with the wateq4f database was used. Because of uncertainties in titration of hydrocarbon, TIC values were used. The ion balance revealed large errors of up to 50 % (see Appendix 11) which impossibly could be due to sampling errors. Thus selected cations were reanalysed in February 2006 (Appendix 9). The values were in some cases (e.g. MIS 5 for Na and Ca) completely different and generally higher but the ion balance errors were even worse. Therefore major elements (Appendix 10) were analysed at a different laboratory (hydrochemical laboratory at the *TU Bergakademie Freiberg*). Although balance errors in only one third of the sampling points are below 5 %, data seem more reliable because there are also only three sampling points with errors above 10 %.

For interpreting and classifying of chemical data several statistical and graphical methods exist. Statistical methods are for instance principal component, cluster or factor analysis. Graphical approaches include Collins bar diagram, Stiff pattern diagram, pie diagram or Piper diagram (Domenico and Schwartz, 1990). In this thesis Cluster analysis and Piper diagram are used to detect possible groups of groundwater.

Piper diagram

The Piper diagram (Piper, 1941) consists of three individual diagrams. The abundances of cations and anions are plotted into triangles containing Na^++K^+, Ca^{2+}, Mg^{2+} and Cl^-, SO_4^{2-}, HCO_3^-+CO_3^{2-} respectively. The concentrations are transformed to relative abundances (% meq/l). It is assumed that Na, K, Ca and Mg equal 100% of the cations. The quadrilateral field is defined by straight lines projected from the two triangles. Figure 24 gives an impression of a Piper diagram.

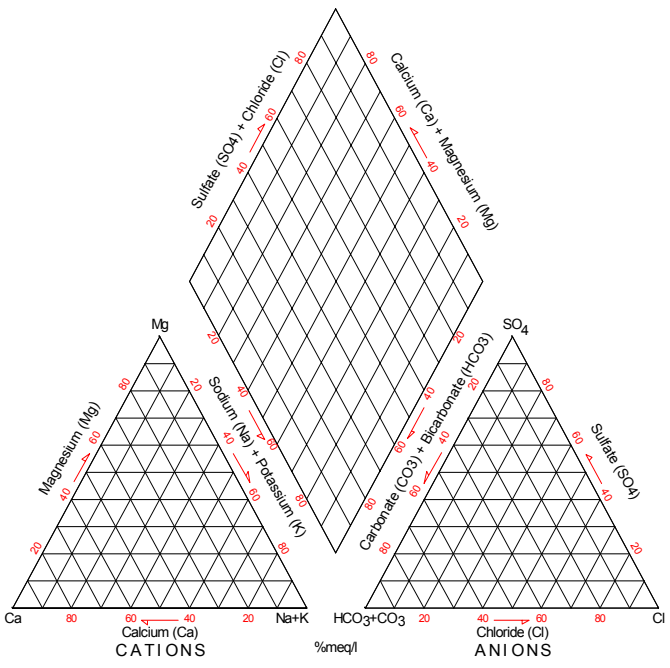

Figure 24: Piper diagram

The Piper diagram is very adequate when data are noisy (Domenico and Schwartz, 1990) which is the case in this investigation. Usually waters are classified into facies which is an approach of smoothing chemical data (Back, 1961). The disadvantage of Piper diagrams is the limited number of possibilities for classifying. In some cases this may eliminate local variability. Templates for classifying waters can be seen in Figure 25. Water facies result from single cation and anion facies.

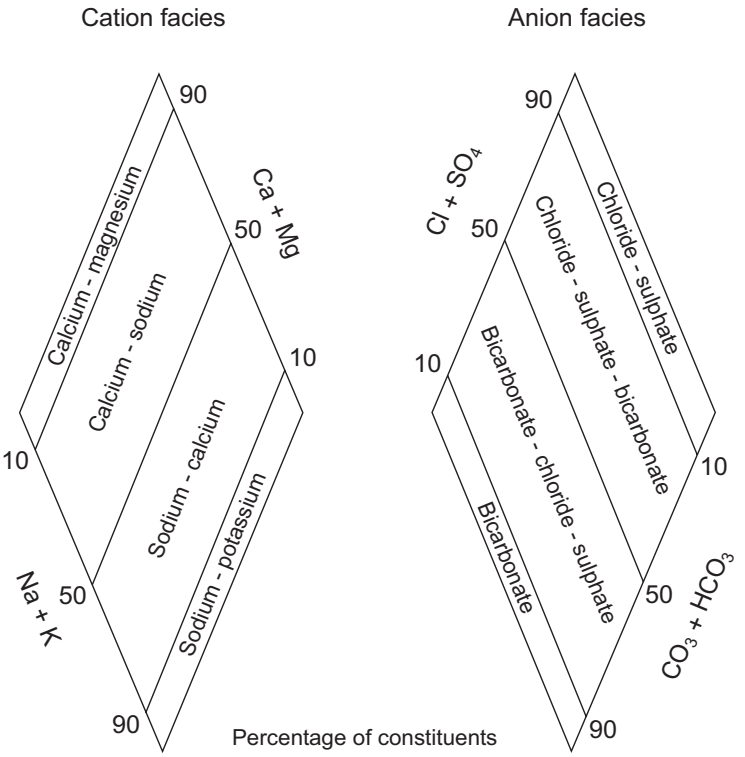

Figure 25: Templates for classifying cation and anion facies (changed after Back, 1961)

Cluster analysis

Cluster analysis is a widely used technique for classifying objects. It attempts to maximize the homogeneity within the clusters and the heterogeneity between the clusters (Hair et al., 2006). The objects (e.g. samples) are aggregated stepwise according to their variables (e.g. elements). It exist hierarchical and non-hierarchical methods to group objects. Hierarchical cluster analysis combines objects according to their distances from or similarities to each other. For non-hierarchical cluster analysis so called seeds have to be chosen from which cluster formation starts by attributing objects with the closest distance to the cluster centroid (Otto, 1999). Furthermore it has to be differentiated between cases and variables. Cases may be sampling points being clustered according to parameters like pH or element concentrations. Variables are for instance the measured parameters clustered according to their name or number.

Data of this investigation was classified with hierarchical cluster analysis using the ward algorithm and squared Euclidean distances with the program SPSS14. Because of different dimensions standardisation was accomplished which means that from every value the mean of the corresponding variable is subtracted and this term divided by the standard deviation.

It is possible to look for significant differences between the newly formed groups. This was done by analysis of variance (one-way-ANOVA) and the program SPSS14. Testing for normal distribu-

tion (Shapiro-Wilk-Test and P-P-plot) revealed that only bicarbonate shows normal distribution. A logarithmic transformation didn't yield normal distribution for all variables (e.g. temperature and conductivity). That's why the Kruskal-Wallis-Test was used to validate significant differences of the means.

Chloride- mass- balance (CMB)

The chloride-mass balance (CMB) is a relatively easy method for estimating groundwater recharge in semiarid and arid regions. Nevertheless some pre-conditions have to be fulfilled to use this approach: (a) the chloride in the groundwater originates only from precipitation; (b) chloride behaves conservative in the aquifer; (c) there is no change of mass-flux of chloride over time; (d) no recycling or concentration of chloride within the aquifer occurs. If these conditions are present the areally averaged recharge flux to the aquifer is expressible as a linear relationship (Wood, 1999):

$$q = \frac{P \cdot Cl_p}{Cl_{gw}}$$

Equation 26

P is the average annual precipitation (mm), *q* the recharge flux (mm), Cl_p the average precipitation- weighted chloride concentration in mg/l and Cl_{gw} the average chloride concentration of the groundwater. If surface runoff *R* is taken into account Equation 26 changes to:

$$q = \frac{(P - R) \cdot Cl_p}{Cl_{gw}}$$

Equation 27

Data of surface runoff were not obtainable. The river *Guanajuato* has a discharge of 115 million m^3 which is 10 % of average mean precipitation. For river *Silao* no discharge is known. Furthermore a certain proportion of wastewater, not being of atmospheric origin, has to be taken into account. Discharge of groundwater by springs is very small due to deep water tables and may be neglected. For overall surface runoff a value of 10 to 20 % of mean annual precipitation will be assumed in this thesis.

There are no continuous chloride measurements in the investigation area obtainable. Only single determinations were accomplished. The Cl_p-value of 0.9 mg/l is the mean of three former reports: CEASG (1999), SAPAL (2001) and COREMI et al. (2004). Measured values can be seen in Appendix 14.

As stated above chloride has to originate only from precipitation for applying the CMB. In COREMI et al. (2004) a natural background of 15 mg/l in the study area is assumed. Taking analytical uncertainties into account all samples having more than 20 mg/l are not considered in the CMB.

4.4.2 Tritium

For the investigation area it doesn't exist a regional input function. Former analyses of tritium in precipitation weren't obtainable. For constructing an input function the two closest stations of the IAEA-GNIP-network (IAEA-GNIP, web) were used.

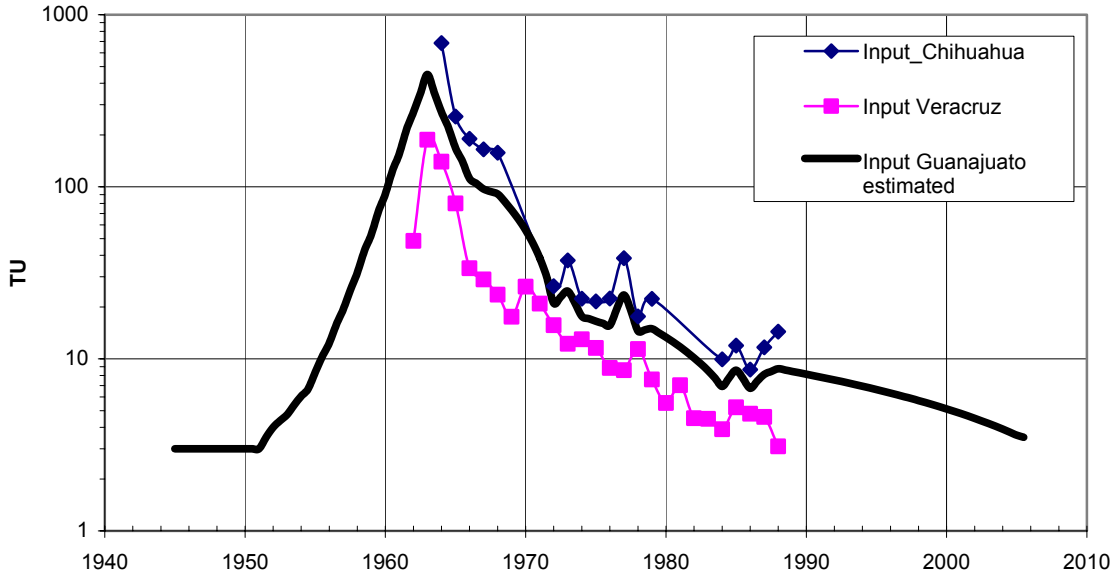

Figure 26: Construction of the input function from measurements of the two IAEA-GNIP stations Veracruz and Chihuahua

It didn't seem appropriate to use one of the input functions directly because of very different site conditions and large distances. Chihuahua is situated in the north of Mexico; about 900 km from Guanajuato and Veracruz is more than 400 km away in south-eastern direction at the coast of the Gulf of Mexico. Input values of Chihuahua (28.63 °N and 106.07 °W) may be influenced by nuclear bomb testing at the Nevada Test Site (36 °N and 116 °W) in the north of Las Vegas , which could have led to an increase also in Chihuahua. Close to Veracruz (19.2 °N and 96.13 °W), in Laguna Verde, the only Mexican nuclear power plant is operated. Nevertheless this hadn't any influence to the data because production started in 1990. Atmospheric values between 1990 and 2005 may be higher than the estimated ones but measurements of tritium in precipitation after 1990 were not obtainable. Unpublished climatic data (CNA Celaya; station Guanajuato) show for the year 2005 prevailing wind directions from north and southwest. If these are the primary wind directions, no influence of Laguna Verde would have to be taken into consideration.

To construct an input function the mean of the annual mean input values of the two obtainable GNIP-stations was calculated. Unfortunately the data are very poor because in some years only one measurement was made which therefore is heavily affected by seasonal variations of tritium activity in the atmosphere and calculation of an infiltration-weighted average as proposed by Zuber (1986) is not possible. Because the measurements started in 1962 and ended in 1988, input values before and after this interval had to be estimated. For input values before 1962 an exponential function for calculating tritium activities was used assuming that the natural production before 1952 was 4 TU. Between 1962 and 1988 some years exist without measurements, which were interpolated linearly. After 1988 an annual decrease of the tritium activity of 5.5 % was assumed (Clark and Fritz, 1997).

4.4.3 CFCs

The measured concentrations in water and the calculated corresponding air contents are summarised in Appendix 21.

The air mixing ratios were calculated using Equation 1-4 and the constants of Table 1. Because the total pressure was unknown and not measured, the relation of List (1949), valid for altitudes less than 3000 metres, was used: ln P = -H/8300. For recharge temperature the mean annual air temperature of the investigation area (18.5 °C) and as recharge the elevation 1800 metres were assumed. Salinities were measured during the field campaign and could be included in Equation 4 and Equation 6. They were taken into consideration although their influence on the calculation didn't seem significant in most cases due to low values. For instance to leave out the salinity in MIS 30 (0.3 ‰) would change the mixing ratios from 8.89, 36.09 and 6.00 pptv to 8.86, 35.98 and 5.98 pptv for CFC-11, CFC-12 and CFC-113 respectively. In MIS 7 with the highest salinity values of 1.4 ‰ the ratios would decrease by 1.5, 4.1 and 0.6 pptv. Nonetheless this could change the apparent ages by several years if the waters where from the 1950s or the 1990s because of low slopes of input functions.

The water table in the valley of Silao-Romita shows a depth of more than fifty metres, in some cases more than 100 metres. Like stated above, in such cases the concentration directly at the water table is considered to be lower than actual atmospheric values. Therefore the two former introduced correction models were applied to find the time lag. A couple of unknown parameters had to be estimated to use Equation 9 for the exponential correction and Equation 13 for the linear model. The following table lists the used parameters.

Table 3: Used parameters for correcting time lags (* values taken from Cook and Solomon, 1995)

D_l^0 [m^2/a] *	α [m] *	D_g^0 [m^2/a]	k_w	k_d *	τ_l *	τ_g *	ε_a *	θ *
0.03	0.02	260 (CFC-11) 285 (CFC-12) 230 (CFC-113)	0.34 0.09 0.10	0.02 0 0.1	0.15	0.19	0.2	0.15

Furthermore liquid and gas flow (q_l, q_g) were set to zero, because the transport is considered to occur through diffusion only and also no degradation is taken into account (λ = 0). The density of liquid (ρ_l) is considered to be 1 g/cm^3 and for the density of the solid phase (ρ_s) 2.65 g/cm^3 was assumed, which is the density of quartz.

The water table depth was measured in each well during the field campaign. Unfortunately the wells often were pumping and the measured values include the drawdown. Nonetheless in some cases this may represent real conditions, because wells producing potable water are pumping permanently. But the majority of all wells are for agricultural use. Because of water shortage already some restrictions were imposed to the farmers who are only allowed to extract groundwater in certain hours and therefore farmers only irrigate their land during this time. If the field measures are used for calculating the time lag, in some wells with very deep water tables generated by pumping, senseless values are obtained.

Data of the local water agency (CEASG) of water table measurements in the dry season show the phenomenon of heavily fluctuating water table values between 2001 and 2004. During one year a drawdown of up to 50 metres was measured, which impossibly can be caused by overexploitation. Probably these data originate from non-static water table conditions due to pumping during the readings.

Nonetheless the values of 2003 were compared with the values of 2004 and in cases of similar coordinates but much higher water table they were corrected to these unsaturated zone depths. The corrected values can also be seen in Appendix 22.

A source of errors in determining the time lag may also be the declining water table. The unsaturated zone thickness hasn't been constant in the last 50 years. Therefore the time lag must be considered as the maximum possible value and real time lags probably are smaller.

4.4.4 Deuterium and Oxygen-18

The GMWL is an average of lots of LMWL's of different stations with very differing site conditions. If existent the LMWL should be used to compare groundwater data. In the Transmexican Neovolcanic Belt the LMWL of Cortés et al. (1997) is widely used. They calculated the local MWL from various former studies for Central Mexico matching the equation:

$$\delta^2 H = 7.97\delta^{18}O + 11.03 \qquad (n = 85;\ r^2 = 0.97)$$

Equation 28

This report primarily takes into consideration studies being carried out in the basin of Mexico. Therefore the actual LMWL may be slightly different due to local effects of differing climate. In section 5.4 also precipitation data of the study area are taken into account to validate the LMWL.

4.4.5 Carbon isotopes

From the great variety of correction models for taking the carbon solubility and therefore too low ^{14}C activities into account, two were chosen. First the statistical correction using q-values of Vogel (1970) was applied. This is only a very rough estimation and therefore the $\delta^{13}C$-mixing model also was used for correction. To account for bomb-^{14}C in estimating initial activities, tritium values were taken into consideration. Sampling points with tritium activities below 0.5 TU were considered as tritium-free and therefore also don't contain bomb-^{14}C. The initial activity was set to 105 pmC. Sampling points presenting more than 0.5 TU may contain certain amounts of water affected by bomb-tritium and therefore also include increased ^{14}C-concentrations. Initial activity of these samples was set to 120 pmC. An exception is the spring MIS1 because it is considered to discharge only recently recharged waters and not to contain bomb-^{14}C. Initial ^{14}C-activity was also set to 105 pmC.

The second model ($\delta^{13}C$ model) needs besides the initial activity some additional parameters. The $\delta^{13}C$ of soil generally is set to -25 ‰ (Clark and Fritz, 1997). In the investigation area considerable amounts of CAM- (e.g. Cacti) and C4-plants (e.g. maize) are present and soil ratio may be increased. Therefore a $\delta^{13}C_{soil}$ of -20 ‰ was presumed. The $\delta^{13}C_{carb}$ of the prevailing carbonates was set to 0 ‰ which is equal to the value of marine carbonates. Because of relatively low strontium ratios being in the range of mantle derived rocks the presence of marine carbonates can't be proved (see section 1.1). Nonetheless 0 ‰ were supposed due to lacking measurements of $\delta^{13}C$ in carbonates.

For calculating the $\varepsilon^{13}C_{DIC\text{-}CO2(soil)}$ further fractionation factors and concentrations of the different carbonate species are necessary to fulfil Equation 22. The carbonate species were determined with the program PHREEQC (Parkhurst and Appelo, 1999).The temperature and pH dependent factors were calculated after the following equations taken from Clark and Fritz (1997) who correspond to Vogel et al.(1970) (Equation 29), Mook et al. (1974) (Equation 30) and Deines et al. (1974) (Equation 31):

$$10^3 \ln \alpha^{13}C_{CO_{2(aq)}-CO_{2(g)}} = -0.373 \cdot \left(\frac{10^3}{T}\right) + 0.19 \approx \varepsilon^{13}C_{CO_{2(aq)}-CO_{2(g)}}$$

Equation 29

$$10^3 \ln \alpha^{13}C_{HCO_3-CO_{2(g)}} = 9.552 \cdot \left(\frac{10^3}{T}\right) - 24.1 \approx \varepsilon^{13}C_{HCO_3-CO_{2(g)}}$$

Equation 30

$$10^3 \ln \alpha^{13}C_{CO_3-CO_{2(g)}} = 0.87 \cdot \left(\frac{10^6}{T^2}\right) - 3.4 \approx \varepsilon^{13}C_{CO_3-CO_{2(g)}}$$

Equation 31

The enrichment factor ε is not really equal to the fractionation factor $10^3 ln\alpha$, but for values close to the reference the difference is negligible (Clark and Fritz, 1997).

4.4.6 Strontium

With the help of strontium it is intended to detect different mixtures of waters. Isotopic compositions like that of strontium mix conservatively, they are intermediate between the endmembers in a two component mixture. Mixtures of elements having different isotope ratios and different concentrations (e.g. Sr, Nd, Pb) form hyperbolas (see Figure 27), if they are plotted in diagrams of their ratios versus concentrations. This approach developed by Faure (e.g. Faure and Mensing, 2005) can be used for any element containing stable radiogenic isotopes or whose isotope composition varies due to fractionation. The mixing hyperbolas can be transferred into lines if the inverse concentration 1/Sr is used. Processes like fractionation would produce a curve and not a line. Fractionation affects primarily lighter elements like N or O and can be checked plotting the concentration logarithmically which then would also appear as a curve (Kendall and Caldwell, 1998).

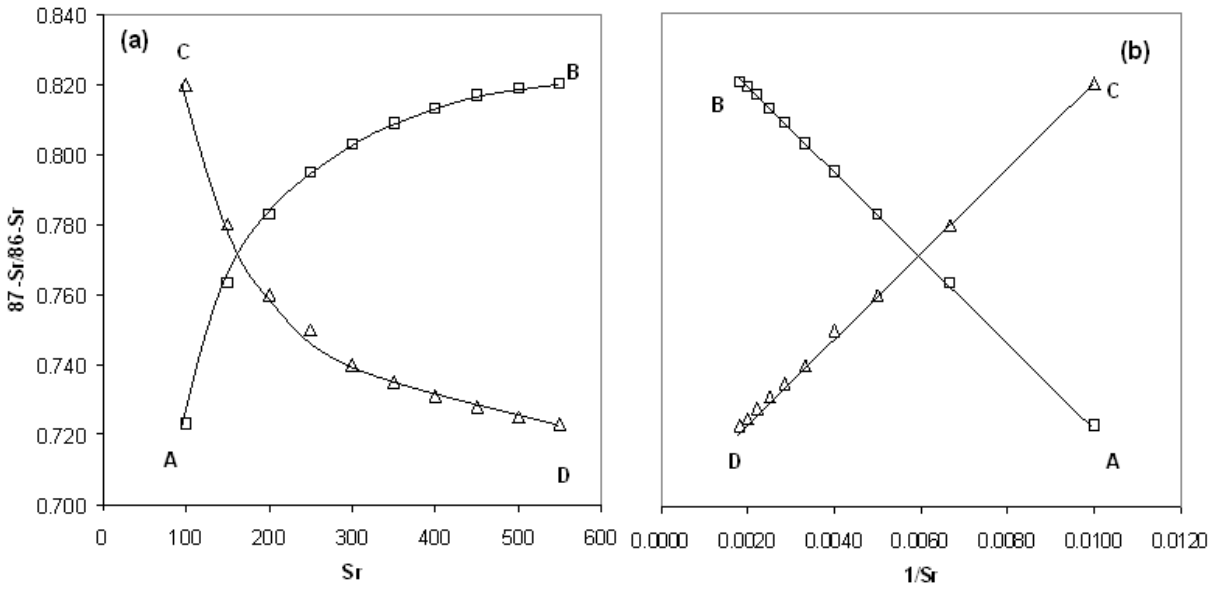

Figure 27: (a) Hyperbolas formed by mixing of two components having different concentrations and ratios dependent from the mixing ratio and their conversion (b) into lines

Faure and Mensing (2005) also introduce an example for three component mixing which can be solved with the isotope ratios of two elements; in this case strontium and neodymium. There the three endmembers form a triangle with the mixtures in-between. The solution is difficult, because the mixing lines have curvature depending on concentrations of the used elements.

5 RESULTS AND DISCUSSION

5.1 WATERCHEMISTRY

During the field activities 30 sampling sites were investigated, from that 28 are wells and 2 are springs. The water is used for irrigation (21) and drinking water (6) primarily. Furthermore 2 wells are used for swimming pools and one spring isn't used.

Besides the hydrochemical parameters like temperature, conductivity, oxygen and pH that were analysed in the field, samples for the analysis of major, minor and trace element samples were taken (see Appendix 7-10). The following interpretation refers to the third analysis for major cations and anions (Na^+, K^+, Ca^{2+}, Mg^{2+}, NO_3^-, Cl^-, SO_4^{2-}, HCO_3^-) accomplished by the hydrochemical laboratory of the *Technische Universität Bergakademie Freiberg*, Germany. Minor cations like Sr, Fe and Mn refer to the second analysis. Although errors have similar dimensions, values seem more reliable than those from the first analysis, because precipitation of carbonates for strontium determination showed a certain quantity of precipitates which is not reflected by the first analysis but can be more or less well confirmed by the second one. Interpretation of trace elements refers to the first analysis. Because there wasn't a repetition no validation of these data is possible.

Concerning the hydrochemical parameters the first distinctive features become apparent. The temperature ranges from 16 °C to 96 °C whereas the majority shows values between 22 °C and 29 °C. Two wells (MIS 29 and MIS 30) and one spring (MIS 2) can be called "thermal" because their temperatures were about 30 °C. Actually there are three other wells with temperatures above 29 °C (MIS 6, MIS 18, and MIS 28) which is very close to 30 °C. The second measurement showed a deviation of temperature to the first measurement of generally 0.5 to 1 °C, in one case up to 5 °C. Therefore it is possible that there exist more thermal waters. The limit of 30 °C does not base on a special rule but was fixed highhandedly.

It is remarkable that almost all wells present temperatures above the annual mean air temperature of 18.5 °C. Maybe the seasonality of rain leads to higher groundwater temperatures because the majority precipitates in summer when higher air temperatures are present. The precipitation-weighted mean of air temperature between May and October is 20.8 °C. Taking this average into account, the watertemperature of eleven sampling points (MIS1, MIS3, MIS5, MIS7, MIS9, MIS11, MIS14, MIS15, MIS17, MIS20, and MIS23) correspond to the normal geothermal gradient of 3 °C/100m.

The conductivity normally ranges between 430 and 1400 µS/cm. In two cases the values with 2450 (MIS 28) and 2740 (MIS 7) are more than twice as much than the rest of the measurements. These two sampling points show also increased sulphate, sodium and calcium values. This can be an indicator for a distinctive origin.

The pH showed values between 7.2 and 7.8 at almost all sampling points. One exception was the thermal spring MIS2 with 8.7 but this value might be erroneous because due to high temperatures it was measured after cooling down.

Oxygen values are between 2.8 and 7.1 mg/l. This would normally prove oxic conditions but sampling wasn't ideal. On the one hand pumping could have introduced air into the water. On the other hand oxygen content was measured in a bucket and during filling water into the bucket this may also have introduced additional oxygen. Therefore oxygen values are quite uncertain.

The values of the major, minor and trace elements don't show large abnormalities else. Concerning the Mexican norm for drinking water (NOM-127-SSA1-1994) with its modification from October 2000, in the wells, which are obviously used for drinking water, the limits for the different listed substances are not exceeded.

Relatively high nitrate concentrations with 154 mg/l shows the spring MIS1 and MIS14 with 129 mg/l which are not used for production of potable water. MIS1 is situated down-gradient to a small village (*Sangre de Cristo*) in the mountains and possibly influenced by the waste waters of this settlement and its graveyard which are only a few hundred metres away. Higher calcium (94.6 mg/l), sulphate (307 mg/l) and chloride contents (68.4 mg/l) corroborate this assumption.

In the agricultural wells occasionally occur increased values of certain elements. Arsenic is slightly increased in well MIS 18 (59 µg/l) and MIS 19 (31 µg/l). Regarding the recommendations of the WHO there is no quantifiable health risk up to 50 µg/l.

The sulphate values are low too and don't violate the norm for potable water in drinking water wells. Mostly values range between 11 and 80 mg/l. Two agricultural wells show very high sulphate concentrations: MIS7 with 689 mg/l and MIS28 with 1832 mg/l. Solution of gypsum and anhydrite are the reason for these high contents. Because of volcanic activities in the study area also influences of volcanic gases are probable.

The sodium values, with one exception (MIS18: 255 mg/l), are generally below the limit of 200 mg/l. Potassium shows normal values too (mean 9.3 mg/l). Remarkable is the relatively high concentration in MIS18 with 58.3 mg/l.

Phosphate and beryllium never were detected and selen only one time in the spring MIS 1 (37 µg/l). Cadmium and chrome also were detected rarely, whereas in the sample MIS 19 the cadmium value was slightly increased (10 µg/l).

Silicon concentrations were also determined. They vary from 0.5 mg/l in MIS21 to 66 mg/l in MIS2. Mean SiO_2 concentrations of near surface groundwater normally range between 12 and 17 mg/l (Merkel and Sperling, 1996). Generally Silicon can be used to determine the origin of waters by applying the SiO_2- geothermometer. Unfortunately the geothermal gradient is very uncertain in the investigation area, which would be needed to conclude from SiO_2 formation at certain temperatures to the depth of formation.

Piper diagram

Figure 28 shows the distribution of all samples in the Piper Diagram. Although for some analyses relatively high ion balance errors were calculated, all sampling points are plotted in the diagram. To differentiate analyses, data sets with more than ten percent error are red, those from 5 to 10 percent are green and below 5 percent symbols are plotted black.

The diagram in this case classifies primarily mixing types of waters. After Back (1961) half of the sampling points can be classified as Ca-Na-HCO_3-Cl-SO_4^{2-}- type from which 5 analysed waters (MIS7, MIS15, MIS20, MIS22 and MIS28) are calcium-dominated. A second group contains 9 samples of Na-Ca-HCO_3-Cl-SO_4^{2-}- type. It differs from the first group by dominating sodium/potassium content compared to calcium and magnesium. Sampling point MIS1, MIS7 and MIS11 belong to the Ca-Na- SO_4^{2-}-Cl-HCO_3 – facies having dominating percentages of sulphate-ions. The only sampling point corresponding to the Na-Ca-Cl-$SO_4^{2-}HCO_3$ – facies is MIS18 with high sodium/potassium percentage. MIS28 could be classified as calcium-sulphate water but high ion balance errors make this classification questionable. Same problem arises in MIS25 which normally belonged to sodium-calcium-bicarbonate- type.

Interesting in this respect is the fact that the calcium and bicarbonate dominated group is only present in the centre of the basin. Second facies waters which are sodium and bicarbonate dominated except for MIS17 and MIS30 can be found in the southern bordering regions.

The sulphate- dominated waters (MIS7, MIS11, MIS18, MIS25 and MIS 28) may originate from leaching of gypsum and anhydrite which are present in calcareous medium. The calculated saturation indices (see Appendix 12) for gypsum and anhydrite are generally below 0 which means that due to insufficient reaction time or low content of these phases in rocks no saturation occurred. Only MIS28 is equilibrated regarding gypsum having a SI of -0.1. Between -0.2 and +0.2 generally equilibrium is assumed (Merkel and Planer-Friedrich, 2005). Because of large variability of sulphate concentrations, different sources are possible. The higher concentrated waters may refer to faults and intrusions which provoke mixing with waters of volcanogenic origin and that generally show higher sulphur contents. Also anthropogenic effects are thinkable which may be present in MIS1 and MIS11. Besides increased Ca (95 and 144 mg/l) and SO_4 (307 and 330 mg/l)

also higher NO_3- values (154 and 55 mg/l) were detected which might be an indication for human impacts.

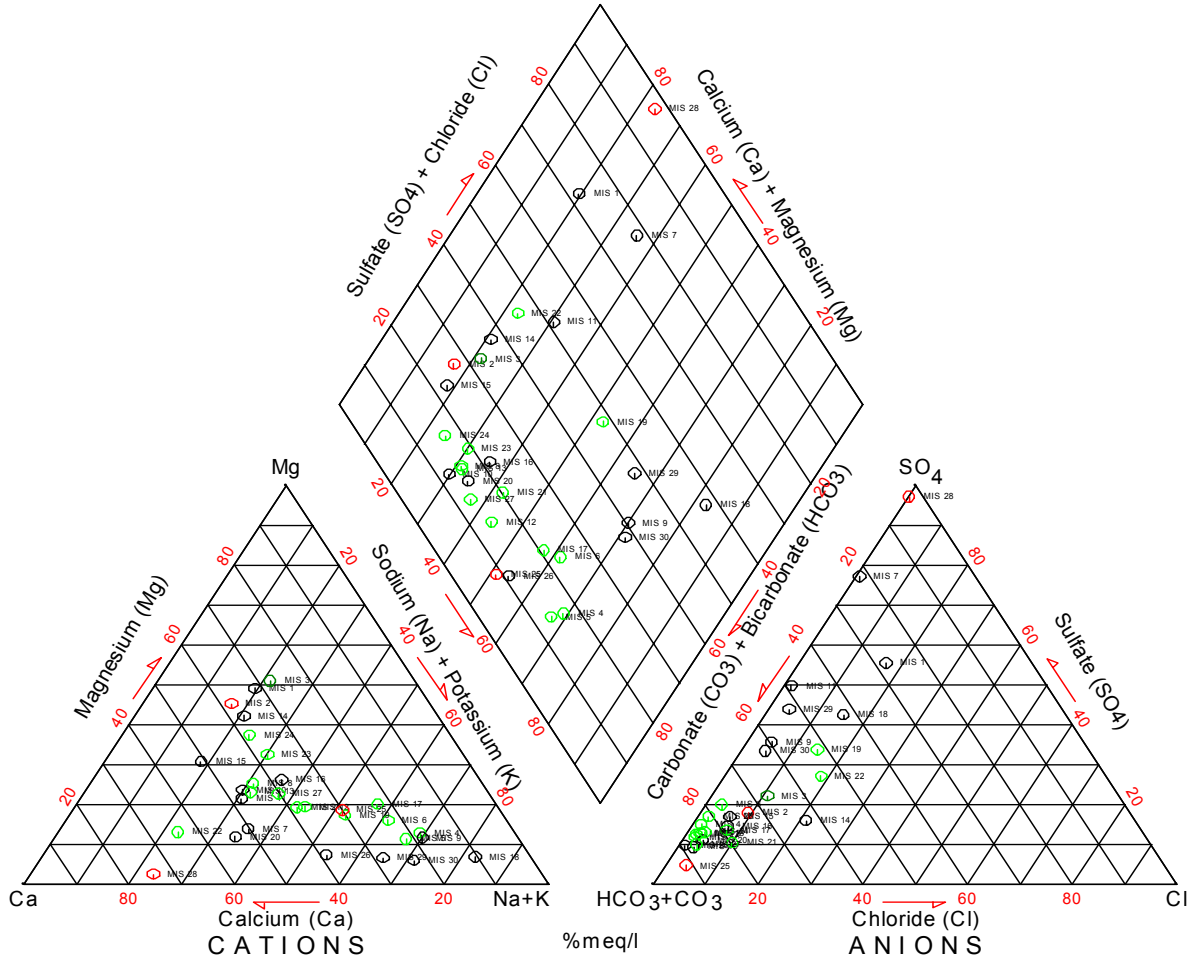

Figure 28: Piper diagram of all sampling points. Red circles correspond to analyses with ion balance errors of more than 10 %, green circles to errors between 5 and 10 % and black circles to balance errors below 5 %. The construction of the diagram was done with the program RockWorks 2004.

Cluster analysis

Cluster analysis was performed for the cases of two to ten clusters. Because of “outliers” the first steps yield clusters with only one or two members and one large cluster containing the remaining sampling points. If analysis of variance (Kruskal-Wallis) is taken into consideration classification of 9 clusters shows most significant differences for seven out of ten parameters. Nevertheless seven-cluster-model seems more appropriate. Relatively high ion balance errors make classification into 9 clusters unreliable because of small distances.

The seven-cluster-model also matches well with the facies of the Piper diagram. Cluster 3 corresponds to the Na-Ca-HCO_3-Cl-SO_4^{2}- type which can be found primarily in the southern part of the investigation area (see Figure 29). Cluster 5 contains almost the same sampling points like Ca-Na-HCO_3-Cl-SO_4^{2-}- type, which prevails in the centre of the basin. Remarkably means of most ionic concentrations and conductivity are substantially higher in the centre (see Table 4). The difference between the two groups is also reflected by saturation indices of calcite and aragonite. Cluster 3 members show values of -0.6 to 0.1 which represents equilibrated or undersaturated conditions. Cluster 5 members are in equilibrium or slightly supersaturated (-0.1 to 0.4) regarding the two mineral phases.

Table 4: Centroids of seven-cluster classification. Bold values indicate statistically significant differences (Kruskal-Wallis, p = 0.05) within these variables.

Cluster	Members	Temp [°C]	Cond [µS/cm]	Na [mg/l]	K [mg/l]	Ca [mg/l]	Mg [mg/l]	SO_4 [mg/l]	Cl [mg/l]	NO_3 [mg/l]	HCO_3 [mg/l]
1	2	19.5	**1288**	57.3	10.0	**93.0**	**76.5**	193.6	73.1	**141.5**	296.0
2	1	96.3	**619**	26.0	4.7	**56.1**	**40.7**	47.6	17.9	**27.6**	222.0
3	8	27.2	**594**	62.2	5.8	**33.5**	**12.7**	47.4	11.1	**14.7**	198.8
4	1	24.0	**2740**	137.0	10.7	**176.0**	**29.6**	689.0	5.1	**8.3**	249.0
5	16	26.1	**707**	70.9	7.9	**65.1**	**21.2**	73.4	10.6	**28.4**	316.4
6	1	29.0	**1318**	255.0	58.3	**32.1**	**12.7**	285.0	74.5	**9.4**	360.0
7	1	**29.0**	2450	**173.0**	**14.5**	501.0	10.6	**1832**	**3.0**	13.6	63.0

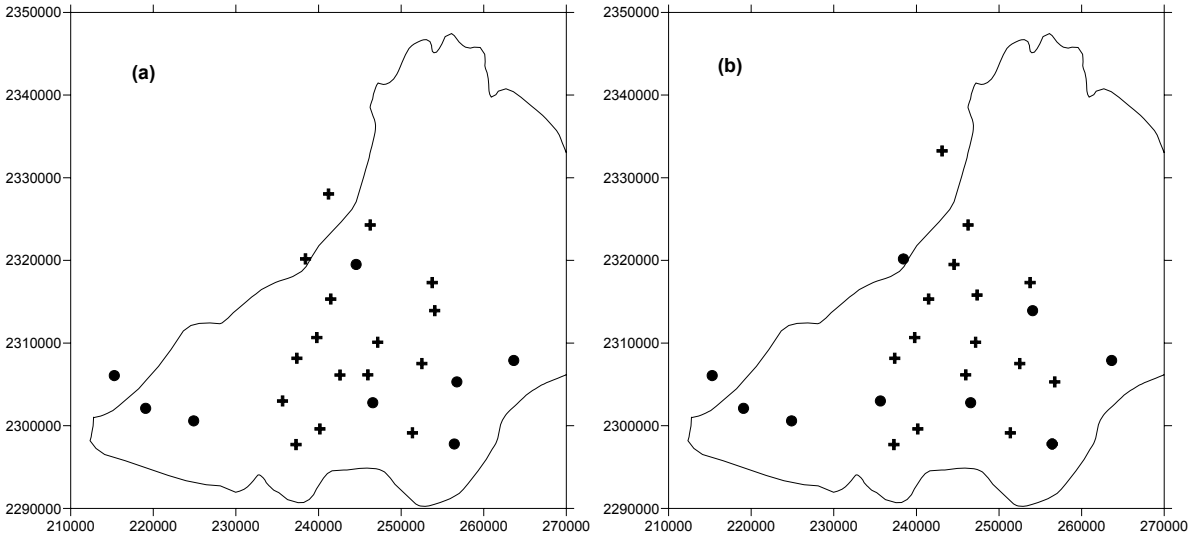

Figure 29: Comparision of dispersion of clusters (a) and water facies (b). Crosses correspond to cluster 5 in (a) and the Ca-Na-HCO_3-Cl-SO_4^{2-} -facies in (b), circles to cluster 3 in (a) and the Na-Ca-HCO_3-Cl-SO_4^{2}-facies in (b).

Chloride-mass-balance (CMB)

MIS1 (68.4 mg/l), MIS14 (77 mg/l), MIS18 (74.5 mg/l), MIS19 (46.3 mg/l) and MIS22 (25.6 mg/l) are affected by higher chloride contents. The latter three are situated in the vicinity of Irapuato in the south-east. They might be influenced by surface water, because the reservoir *El Conejo* is close which possibly supplies increased recharge to the aquifer and by it also constituents of superficial runoff. Whether fertilizers contribute to the chloride content is not provable. Most farmers use P_2O_5 (UREA 18-46-00) fertilizers (various personal comments of farmers). Only one person confirmed the use of KCL but in this well (MIS15) no significant increase in Cl is noticeable (17.6 mg/l). Generally potash fertilizers, which contain Cl, are quite common all over the world but their use in the study area couldn't be observed. Nevertheless the tendency of higher Cl-values inside the basin and lower values at the margin is apparent.

Geogenic effects don't seem to play a roll. Lithium contents are relatively low (< 0.05 – 0.59 mg/l). Sampling points showing high Cl- concentrations have low Li-contents. They are below detection limit in MIS1, MIS14 and MIS22. After Heier and Billings (1970) brines show values between 0.04 and 100 mg/l. After this theoretically geogenic Cl-influence is possible. Lithium occurs primarily in acidic volcanites and in these cases often with chlorine (Merkel and Sperling, 1998). Nonetheless chloride and lithium don't correlate. They show a negative correlation coefficient (-0.25) and a p-value of 0.8 (non-parametric, Spearman).

Furthermore Na and Cl don't show significant correlation (p-value: 0.08; corr. coef.: 0.33; Spearman). If halite dissolution took place, a Na/Cl ratio of 1 would have to be visible. Figure 30 shows a largely scattering distribution with generally higher sodium concentrations in comparison to chloride. Therefore sodium must have different sources like weathering of plagioclase, ion exchange or impact from wastewaters.

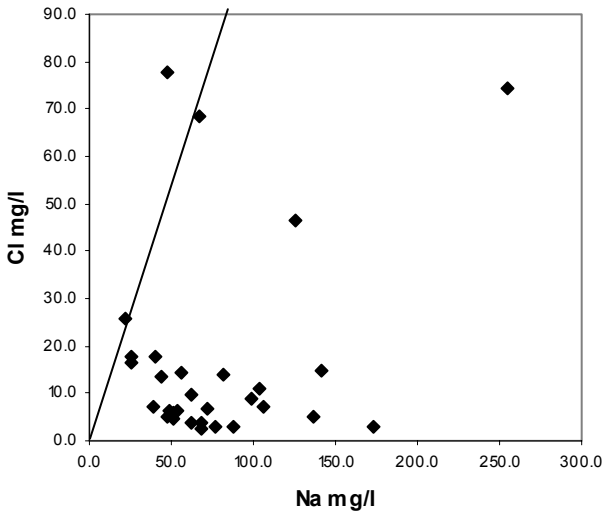

Figure 30: Bivariate plot of Cl versus Na. The line represents dissolution of halite

Applying the CMB recharge values of 32 mm (MIS15) to 217 mm (MIS26) are obtained if surface runoff is not taken into account. Considering runoff would reduce calculated recharge by 10 to 20 %. Since the CMB is a linear relationship, recharge shows the same dispersion like chloride values (see Figure 31). Calculated recharge rates in the centre of the basin seem to be quite low.

Irrigation return flow, which certainly is affected by evaporation and therefore also by enrichment of chloride, possibly changes chloride contents there. By it also fertilizers would reach the groundwater table. This return flow may be considerable. Assuming that one third (650 km^2) of the study area is irrigated by approximately 350 million m^3/a (CEAG, 2003) 500 mm of irrigation waters are pumped to the fields.

A slight geogenic effect is not excludable. The thermal spring MIS2 shows Cl-contents of 18 mg/l being similar to those of the basin. Because original groundwater flow direction was from north to south (COREMI et al., 2004) admixture of these waters is imaginable. The surrounding hills show recharge rates of 130 to 220 mm. Since the precipitation is about 620 mm and the real evapotranspiration approximately 500 mm these rates are possible.

It has to be mentioned in this respect that plots in this thesis are processed by the program Surfer8 using the gridding method of Kriging. The program adopted a linear variogram but this doesn't seem reliable because of heavily fluctuating distances (see Appendix 15). Because of this it is also useless to try to adapt for instance a spherical or logarithmic variogram. Therefore the isoline plots can only be considered as rough estimations and are used to visualise the dispersion of the particular variable. Calculated values outside the region bounded by the sampling points are senseless. Nevertheless plots are sufficient to illustrate analysed concentrations and dispersion patterns and to deduce tendencies.

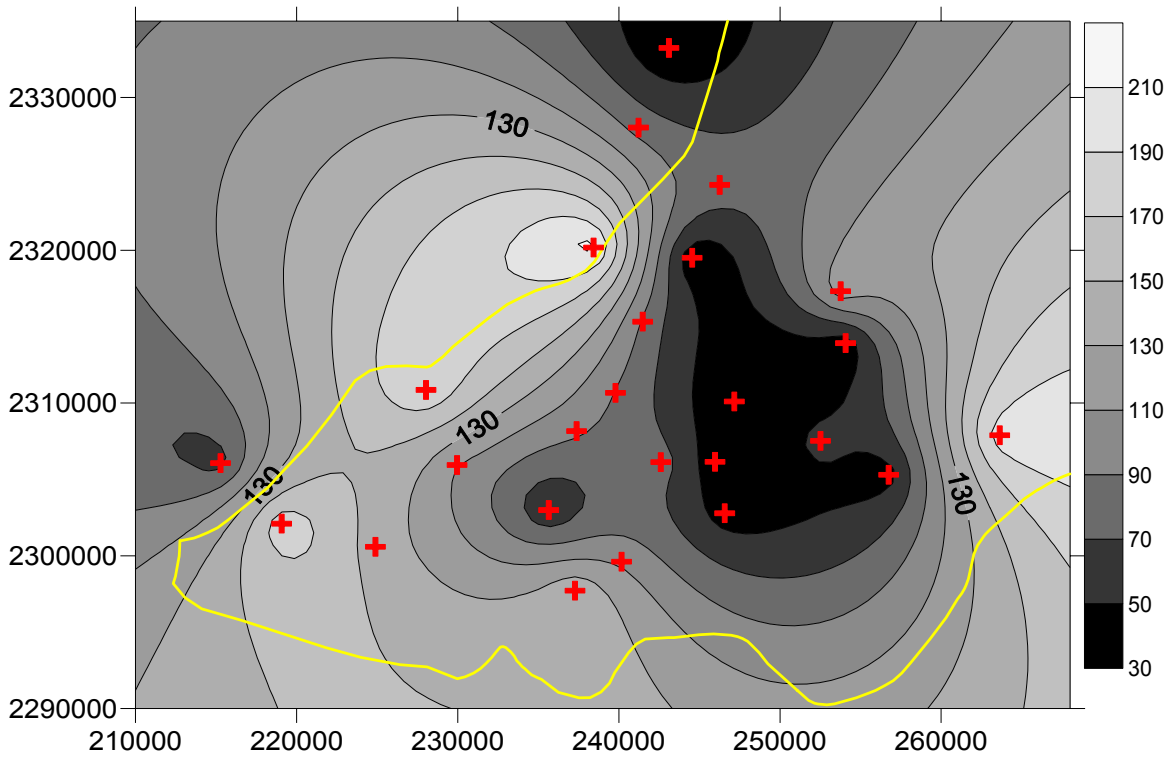

Figure 31: Recharge (mm) calculated by the CMB method (calculation without surface runoff).

5.2 TRITIUM

The analysis of tritium in sample water led to relatively low values which can be seen in Appendix 19. Almost half of the results present 2-σ being larger than the measured activities. Only seven samples show more than 1 TU. Figure 32 illustrates the distribution in the study area.

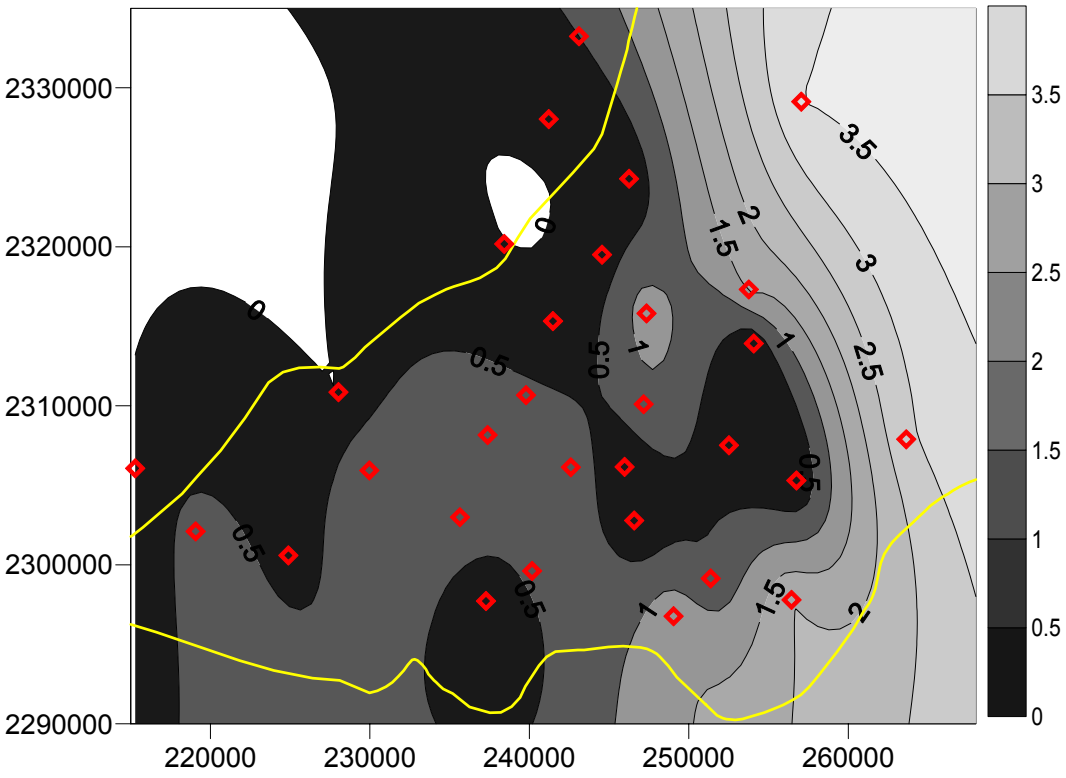

Figure 32: Tritium (units in TU) in the study area

The highest values were measured at the edge of the *Sierra de Guanajuato*. The sampling point MIS 1 with 3.5 TU is an exception. This well is a boundary spring between impermeable consolidated diorite superposed by fractured permeable andesite. It can be assumed that the residence time there is relatively short and the determined activity corresponds to the actual atmospheric tritium content. The estimated local input function shows the same value for the year 2005.

In the centre of the basin and in north-western direction the lowest tritium activities are found. At the border to the neighbouring watershed (León) no difference can be observed. The superficial differentiation doesn't seem to exist in the underground. These waters have residence times being larger than 50 years or the share of "young" water is very small.

To determine the residence times the geometry of the aquifer has to be taken into account. Like stated above (section 3.1) mathematical models or so-called box-models are used to describe flow dynamics of different aquifers. The simplest one is the piston flow model. Using the meas-

ured activities and Equation 1 the decay curve can be calculated and plotted together with the input function. The intersection of the decay line and the input curve correspond to the recharge date. The following figure shows the decay lines of all samples having more than 1 TU.

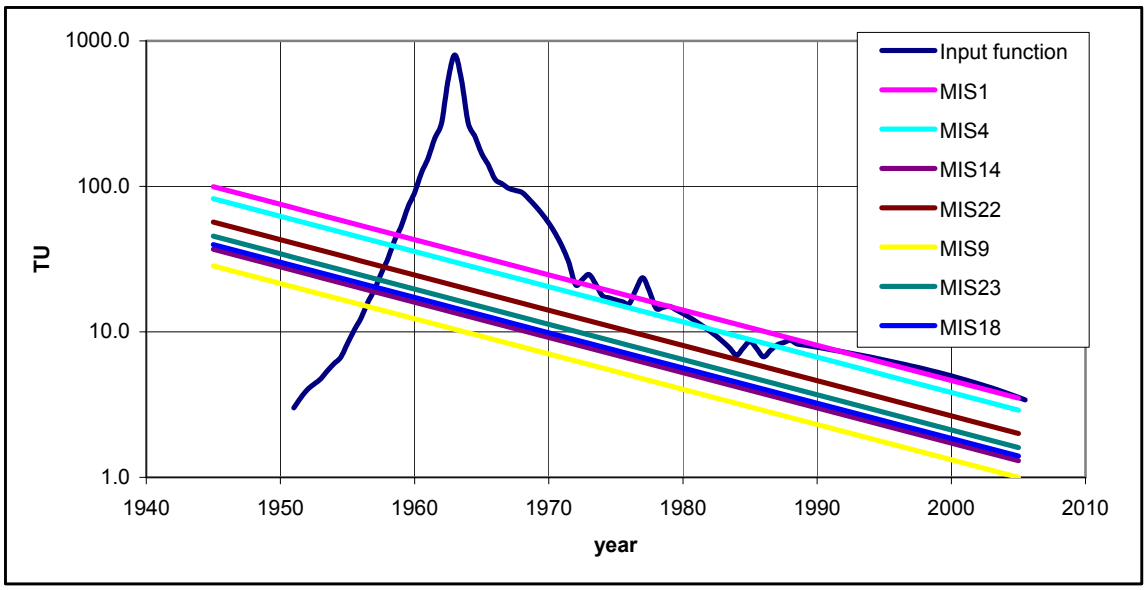

Figure 33: Decay lines for seven sampling points assuming piston flow.

Four of the samples (MIS9, MIS14, MIS18 and MIS23) have unambiguous residence times of approximately 50 years. For MIS1, MIS4 and MIS22 several interpretations are possible (see Table 5, making it difficult to estimate the recharge date. Although MIS1 could have 8 different residence times, the most probable is the lowest one because of the prevailing geology. Normally these “ages” can be validated using the results of CFC analysis. This is discussed in section 5.3.

The above used piston flow is an ideal assumption only valid for confined aquifers with a small recharge area which is far away. Because of these conditions it can be considered that the water has already the same constitution as at the time of recharge. In the investigated basin the aquifer is mostly unconfined and the wells penetrate the saturated zone to a depth of sometimes 300 m. They are almost always screened completely. Precipitation water also can infiltrate in the whole basin. These conditions match best with the exponential model. The application of this model yields so called mean residence times, which is the weighted mean of the hypothetical “ages” of all different flow lines.

Table 5 shows the results for the samples having an activity of more than 1 TU. The mean residence times for the exponential model are within the range of 73 and 300 years. These values can only be considered as a rough estimation. For example MIS9 has a 2σ of ±0.4 TU. This would correspond to a residence time of 200-500 years.

Table 5: Calculated residence times for piston flow (PM) and exponential model (EM). Value for MIS1 in brackets because exponential flow is unlikely there

Sample	Activity [TU]	Residence time PM [years]	Mean residence time EM [years]
MIS1	3.5	0, 14, 27, 28, 30, 32, 34, 47	(50)
MIS4	2.9	19, 21, 24, 48	73
MIS9	1	50	300
MIS14	1.3	49	220
MIS18	1.4	49	200
MIS22	2	21, 48	130
MIS23	1.6	49	170

5.3 CFCs

The results of the CFC-analysis, the corresponding air mixing ratios and calculated time lags are shown in Appendix 21. The residence times were calculated for piston flow and exponential flow conditions. The aquifer is assumed to be largely unconfined and precipitation water can infiltrate almost everywhere. Furthermore the wells are screened completely. The most probable model for these conditions is the exponential model as already stated above. Time series of tracer measurements could verify this but they are not existent. Therefore another method will be used in this chapter.

The application of piston flow leads to residence times of 21-47, 13-55 and 17-36 years for CFC-11, CFC-12 and CFC-113 respectively. The analytical error from 1-σ was transformed to deviation in years and amounts to 0.5-3, 0.5-12 and 2-17 years. Within these analytical errors the ages of CFC-12 and CFC-113 are more or less consistent. CFC-11 shows a significant deviation from CFC-12 and CFC-113. If 2-σ was applied only in few cases differences between the CFC-types would be visible

The value of 1065 pptv for CFC-11 indicates contamination in well MIS24 because it is four times as high as the peak in 1994 with 278 pptv. Maybe in MIS11 and MIS14 contamination by CFC-12 occurred because tracer pairs plot well outside the curve-bounded regions (see also Figure 34). Depletion of CFC-11 might also be possible in MIS14. There the calculated MRT (EM) differs by 24 years. In MIS11 calculation of residence time yields almost equal values for CFC-11 and CFC-113 respectively corroborating the assumption of increased CFC-12 concentrations.

Generally CFC-11 shows the highest and CFC-113 the lowest residence times. CFC-12 and CFC-113 seem to be more consistent than CFC-11. This phenomenon can also be seen in Figure 34. In (a) the samples plot primarily below the curves. This lower CFC-11/CFC-12 ratio may be due to degradation of CFC-11 (Lindsey et al., 2003). It could also be possible that CFC-12 is enriched but in (b) the tracer pairs of CFC-12 and CFC-113 plot within the regions bounded by piston and exponential flow curves and furthermore these compounds are less degraded in groundwater (Plummer and Busenberg, 2000). The measurements of dissolved oxygen present values

above 0.5 mg/l. Oxygen values below 0.5 mg/l normally are an indicator for microbial degradation. Although O_2 contents are higher, anoxic conditions in the aquifer are possible. Through pumping an intensive mixing inside the well is provoked and atmospheric air could be introduced, falsifying real conditions. The arrangement of the tracer pairs along the exponential model line in Figure 34(b) corroborates the decision for this model because most points plot at this curve.

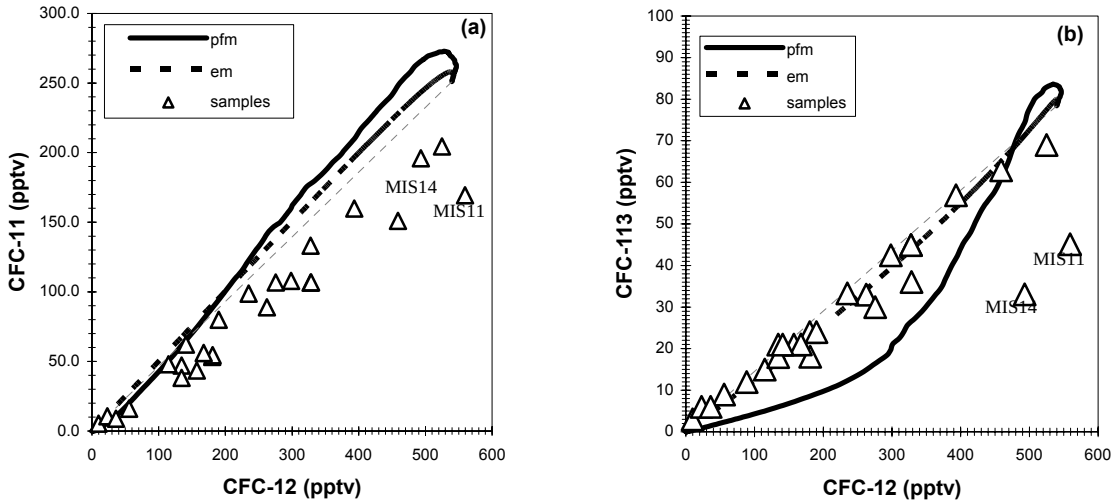

Figure 34: Tracer concentrations plotted for piston flow and exponential flow (curves end at date of sample) and measured tracer pairs CFC-11/CFC-12 (a) and CFC-113/CFC-12 (b). The dotted grey line doesn't represent a function, but only the connection between starting and end point.

The exponential model yields mean residence times of 19-1570 years for CFC-11, 0-1500 years for CFC-12 and 11-1500 years for CFC-113. Exemplary for all CFCs in Figure 35 the diversity of the calculated MRTs of CFC-12 is plotted. Sampling point MIS 4 is not taken into consideration there due to different conditions and resulting large exponential-model-ages. After Figure 35 in the centre of the basin we would find the youngest and in direction to the margins the older groundwaters. This result is contrary to tritium, where the largest residence times are found in the inner part of the watershed.

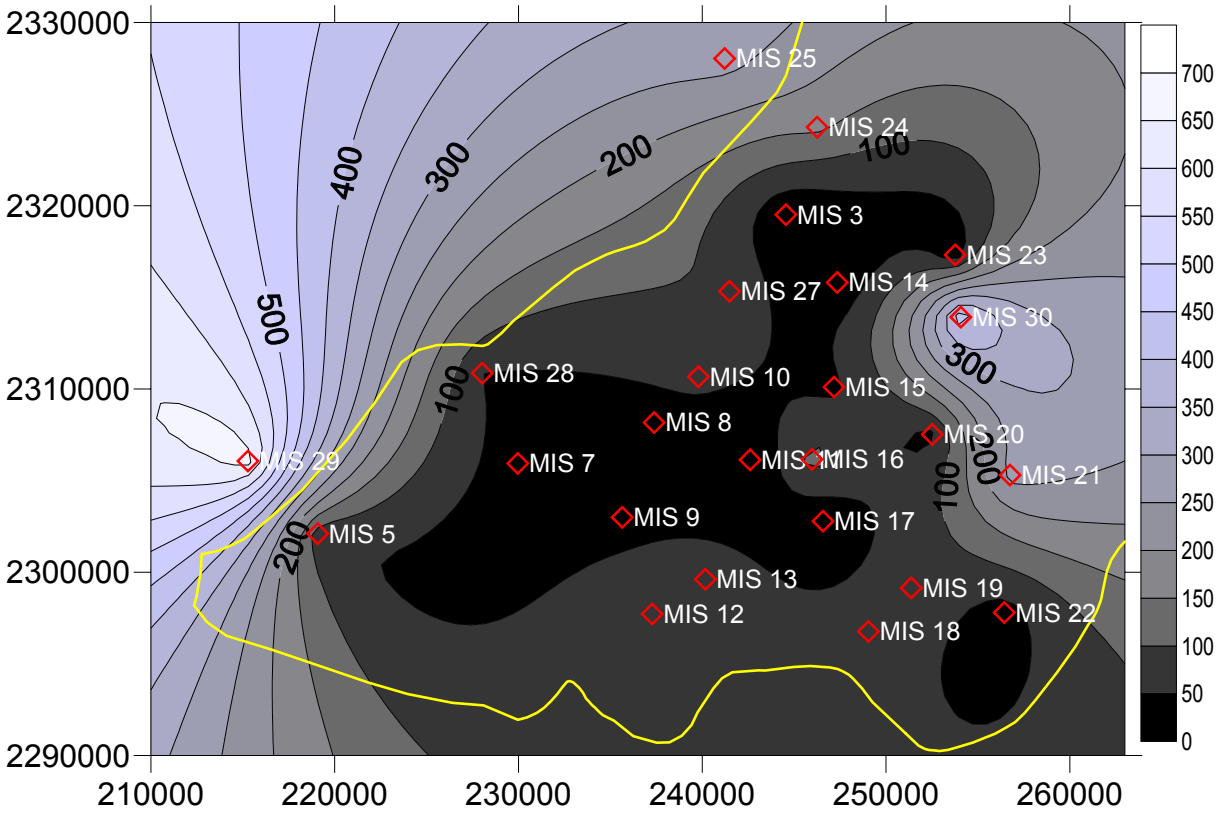

Figure 35: Mean residence times (exponential model, units in years) in the investigation area for CFC-12.

Time lags

The calculated time lags for the exponential correction model are 15-57 years (CFC-11), 12-44 years (CFC-12) and 17-68 years (CFC-113). The application of the linear model yields to 15-138 years for CFC-11 and 14-128 years for CFC-12 ages (see Appendix 22). The linear model wasn't applied for CFC-113 because of the very short linear phase of 5 years between approximately 1985 and 1990 (Engesgaard et al., 2004). The comparison of both methods shows incredibly high values for the linear model in deep wells. Whereas the results to an unsaturated zone thickness of approximately 60 meters are consistent within 6 years, the difference increases up to 90 years in well MIS 4 having a measured water table depth of 135 metres. The exponential time lag was estimated to be 57 years for CFC-11 and 139 years applying the linear model.

Since the unsaturated zone thickness always is very large, it can be assumed that above the water table rather the air mixing ratios of the exponential increase of tropospheric tracer content are present than the concentrations of the linear increase phase. Therefore these values were used to correct the calculated residence time. Nevertheless the application of this correction model yields to senseless negative residence times in half of the wells if the piston flow model is considered. Twenty percent of the wells have negative values if the exponential flow model is applied. Possibly the effect of the rapidly declining water table would also have to be taken into

account but prior to 1998 no piezometric measurements were done in the study area, to estimate at least an average zone thickness of the last 50 years.

To validate the calculated residence times, tritium can be used. Similar to Figure 34, in Figure 36 tritium units are plotted versus corresponding air mixing ratios of CFC-12.

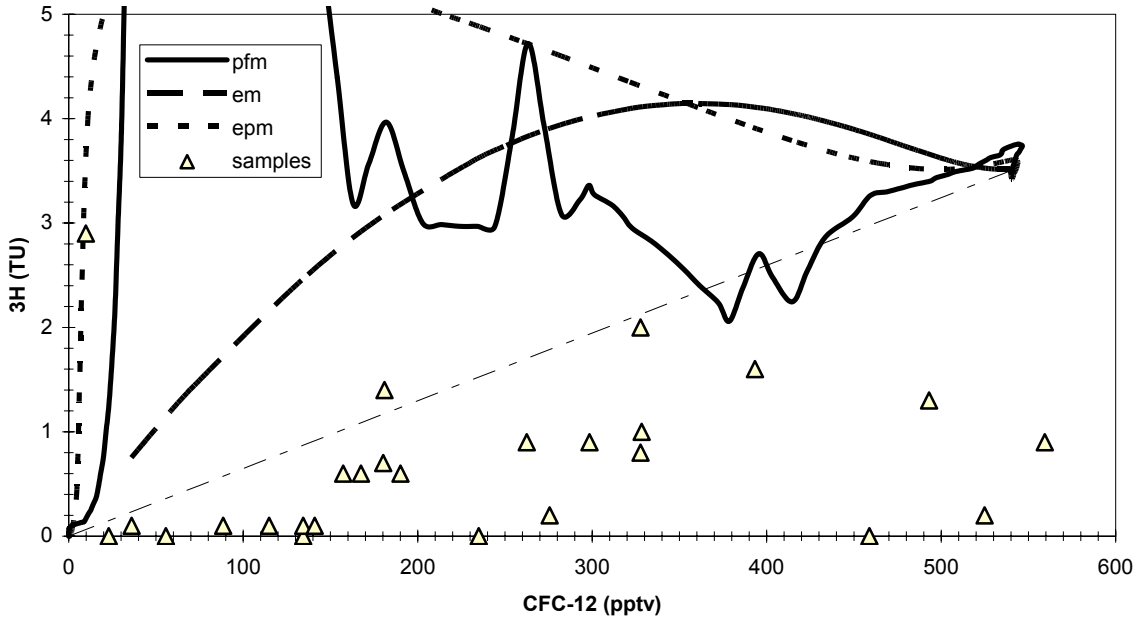

Figure 36: Hypothetical concentrations of exponential and piston flow models of tritium activities are plotted against the same mixing models for CFC-12 and sample values are included.

In this diagram most CFC-12 values are increased compared to tritium values in the same well because they are not enclosed by the curves. Tritium values are considered to be more reliable because they don't undergo processes like degradation or are affected by introduction of air or unsaturated zone thickness. Therefore it is more probable that CFC-12 concentrations are increased. This can be provoked by several processes. Most likely pumping and the fluctuating water table in the vicinity of the well cause introduction of tropospheric air into the water. The pump type doesn't seem to have great influence to the enrichment because submergible pumps show increased concentrations as well as wells working with external pumps ("Johnson"- pump).

This enrichment process can also be seen in Table 6. There the mean residence times of the CFCs are almost always lower than the mean tritium derived residence times. One exception is sampling point MIS4. There the reverse tendency is apparent; the tritium MRTs are smaller than the CFC residence times. This phenomenon may originate from different aquifer conditions. CFCs don't seem to be enriched there. Maybe this well is pumping more constantly because of domestic/ drinking water usage and no irrigation takes place there. In Figure 36 the tracer pair of MIS4 plots above the piston flow line and matches very well with an exponential-piston flow model. This model – in this case – considers that 50 % of the aquifer has an exponential distribu-

tion and 50 % can be approximated by piston flow (see section 3.1) (Böhlke, 2004). Maybe in the vicinity of the well confined conditions of the aquifer prevail, whereas in the upper area unconfined conditions allow distributed recharge, corresponding to the exponential model. If the time lag is taken into account the point shifts to the right and also piston flow or exponential model conditions could be possible.

Assuming the residence time in the unsaturated zone is very short also enrichment through irrigation return flow could be possible, because the tritium activity doesn't change in the short period of being above ground but CFCs interchange with tropospheric air. A rapid flux could also introduce higher CFC concentrations to deeper unsaturated zones. This may lead to more CFC in the soil air because equilibration of enriched water with undersaturated air would increase CFC content and by that a decrease of the gradient in the soil column is provoked. Therefore the time lags possibly are overestimated because correction methods of Cook and Solomon (1995) and Engesgaard (2004) don't regard this aspect.

Contamination was observed in well MIS24 with CFC-11 values never existed in natural environment and maybe in well MIS11 concerning CFC-12. Whether other wells show contamination can't be proved, because concentrations are within the possible range and differences between the obtained residence times of the three CFCs are within standard deviations.

Furthermore the calculation of air mixing ratios contains large uncertainties. The average annual air temperature of 18.5 °C was presumed. All wells featured temperatures above this level. The groundwater equilibrates with CFCs directly at the water table. All water samples had higher temperatures than the mean annual air value. Regarding these higher values in the calculation this would lead to CFC mixing ratios plotting above the input functions in Figure 18.

Table 6: Comparison of exponential model (EM) mean residence times (MRT) corresponding to tritium and CFCs (CFCs corrected)

	Tritium	CFC-11		CFC-12		CFC-113	
Sample	**MRT (EM) [years]**	**correction [years]**	**MRT (EM) [years]**	**correction [years]**	**MRT (EM) [years]**	**correction [years]**	**MRT (EM) [years]**
MIS4	73	56	1514	44	1456	68	1432
MIS9	300	19	37	14	15	21	18
MIS14	220	26	-5	20	-10	30	14
MIS18	200	20	107	16	54	23	71
MIS22	130	42	-1	33	-4	51	-22
MIS23	170	16	14	13	8	19	0

5.4 DEUTERIUM AND OXYGEN-18

The results of stable isotope analysis are given in Appendix 22. Oxygen-18 values range from -10.20 to -8.79‰ and deuterium from -80.14 to -69.94‰. The analyses were made twice for almost all deuterium samples and for six ^{18}O samples. Oxygen-18 deviates between 0.04 and 0.19‰ (mean 0.11‰) from the first analysis and ^{2}H from 0.02 to 1.73‰ (mean 0.04).

Figure 37 is obtained by plotting these values in the Craig diagram. Generally tracer pairs plot below the LMWL. The regression line has a slope of 5.4. After Clark and Fritz (1997) a slope of 5.5 clearly shows evaporation. Additionally some records of atmospheric ^{2}H and ^{18}O – values were plotted in Figure 37, taken from CEASG (1999) and COREMI et al., 2004 (see also Appendix 24).The precipitation data are mostly inside the range of the statistical uncertainty of ±2‰ δD, but plot always above the LMWL. They show also a very wide range maybe due to strongly differing topography in the investigation area provoking altitude effects or due to seasonal variations.

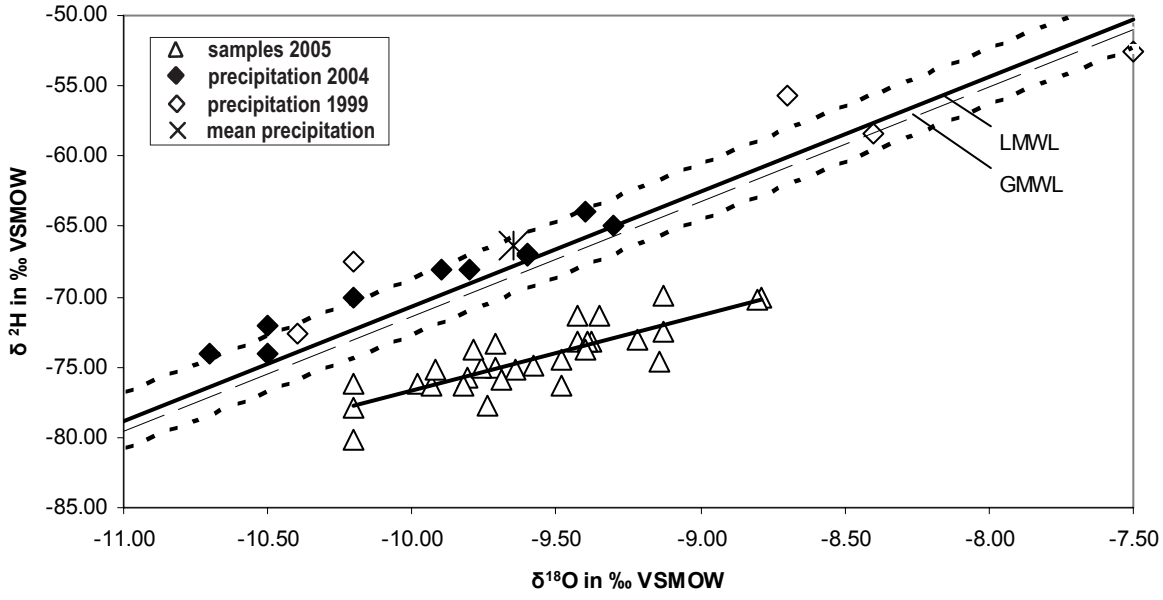

Figure 37: ^{2}H and ^{18}O values of groundwater samples and precipitation data of former studies.

The samples don't reflect the great variances of the precipitation data. The narrower range may either be due to similar recharge conditions for the whole basin or to very well mixing. The sampling points MIS7, MIS9, MIS11, MIS22 and MIS23 show the most enriched values for both ^{2}H and ^{18}O which could be an indicator for evaporative effects. Comparing these wells with the most depleted ones (MIS27, MIS10 and MIS15) no tendency concerning the water table depth or total depth of the well is visible. Generally between the towns of Silao and Romita these depleted values are found and the enriched ones are situated in the southwest and east of the sampling area.

If the tritium activities are taken into account the samples enriched in deuterium and oxygen-18 have values between 0.9 and 2 TU, whereas the two most depleted ones have 0.1 (MIS27) and 0.6 TU (MIS 10). Generally a shift of the mean tracer concentrations from the depleted "older" ones (tritium free: < 0.4 TU) to the enriched "younger" values (high tritium content: > 0.9 TU) parallel to the LMWL is apparent. The mean of the samples with tritium activities in-between (low tritium content: 0.4-0.9 TU) also plots on a virtual mixing line between the young and old ones but these tracer pairs show the largest variance (see Figure 38). Nevertheless it is possible that they are a mixture of tritium free waters and those having more than 1 TU.

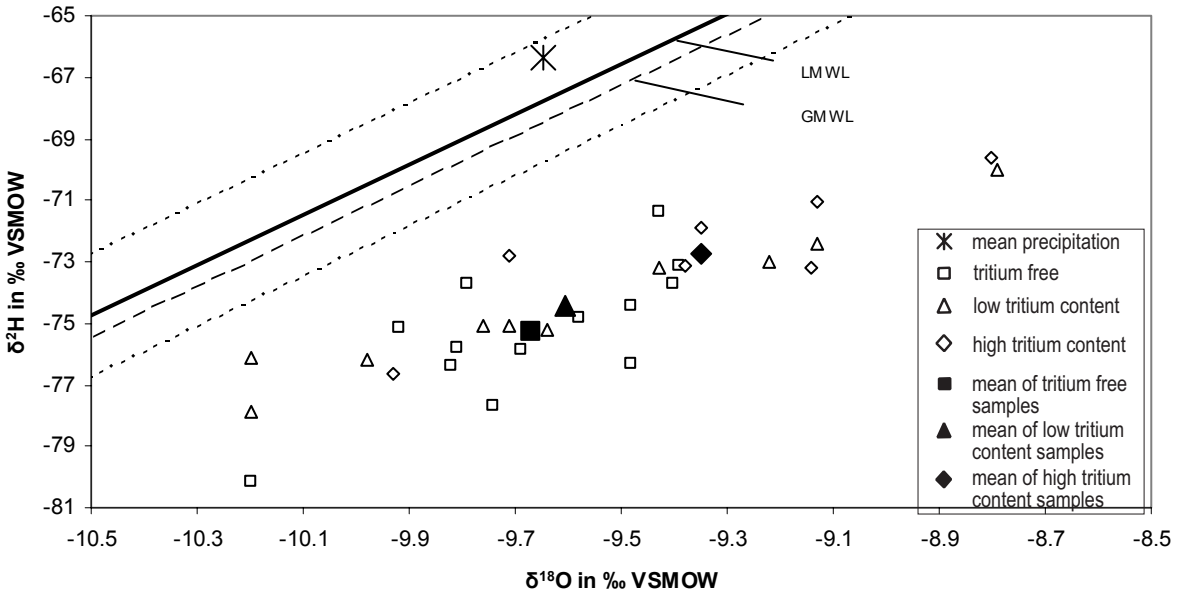

Figure 38: Comparison of tracer pairs with regard to their tritium content

Like stated above evaporation seems to be the most apparent effect on the groundwaters. It increases, the younger the waters are. This may either be due to differing climatic conditions in the past or to possible influences of irrigation waters. The extracted waters are evaporated to a certain extend and infiltrate without changing their tritium signature, because tritium is not affected by fractionation processes.

Between chloride and ^{18}O values no correlation exists which could prove evaporative effects. Testing for significance (Spearman-Rho, significance level 0.05) yields a correlation coefficient of -0.14 and a p-value of 0.44.

If evaporation was the only influence the regression line of all water samples would have to intersect in the vicinity of the mean precipitation point, or at least there would have to exist at least some measurements in the vicinity of the intersection of regression line and LMWL. Even if there were more data it is not likely that the mean was that heavily depleted (^{2}H ~ -87 ‰ and ^{18}O ~ -12 ‰). Depleted groundwaters of low tritium activity may also be mixed with paleowaters. IAEA

(web) considers that for instance Pleistocene paleowaters had a differing MWL being below the actual MWL.

The geothermal exchange with calcareous rocks may also be likely if the reaction temperatures are sufficiently high. After Clark and Fritz (1997) at least 100 °C are needed to alter the ^{18}O signature significantly. Since the groundwater temperature is higher than the mean annual air temperature in the sample area, geothermal effects may play a role and provoke an alteration in ^{18}O content.

The shift of $\delta^{18}O$ to more enriched concentrations in comparison to a former study (CEASG, 1998; see Figure 39) possibly are provoked by exploitation of deeper waters and/ or admixture of more isotopically exchanged waters due to declining water table. Unfortunately no data exist about geothermal gradients in the investigation area and therefore this approach may be speculative. Enrichment through increased proportions of irrigation return flow might be another explanation.

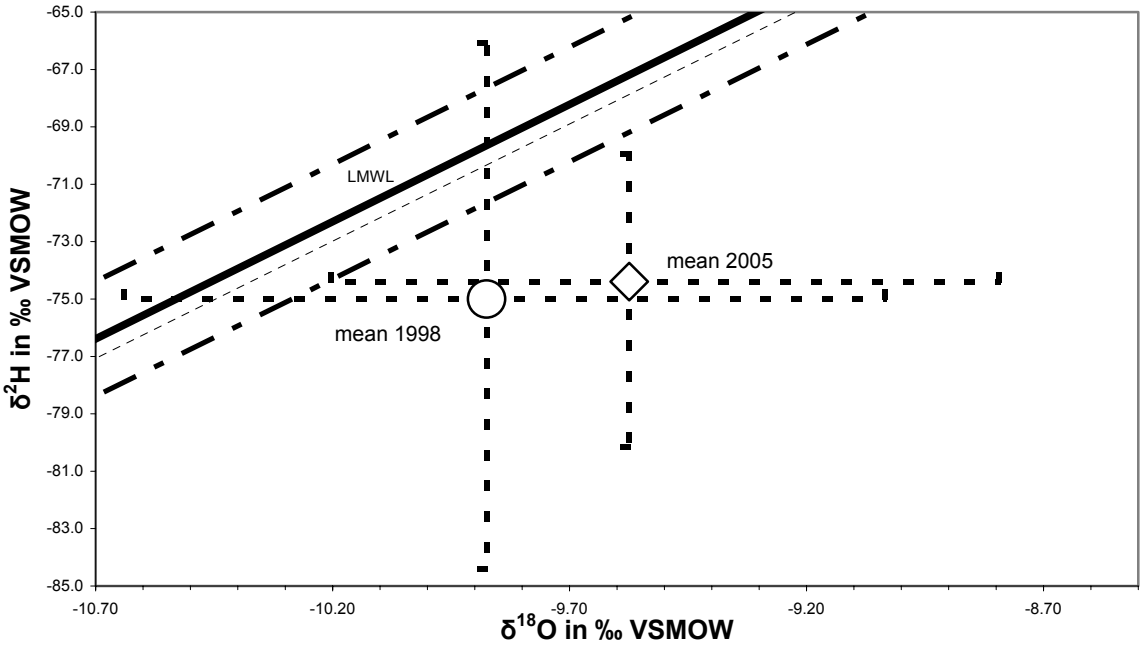

Figure 39: Comparison of range and mean of $\delta^{18}O$ and $\delta^{2}H$ data with a former investigation (CEASG, 1998) in the study area

Rademacher et al. (2002) found an increase of 1.2 ‰ for $\delta^{18}O$ and 11 ‰ for $\delta^{2}H$ in water recharged between 1960 and 1990 in a high elevation basin in the *Sierra Nevada* of California. The temperature increase in the same time span was about 1.3 °C being not sufficiently high to explain the observed increase. They assume that changes in atmospheric circulation pattern account for the increase. No data have been found about climatic changes in the study area but this aspect might also play a role.

5.5 CARBON ISOTOPES

The $\delta^{13}C$-ratios range between -6.8‰ and -11.91‰. At the upper scale volcanic, mantle and atmospheric CO_2 possibly influence the ratios. At the lower end CAM and C-4 plants are likely to change the $\delta^{13}C$. Samples which primarily might be influenced by plants and terrestrial carbonates are MIS1, MIS3, MIS7, MIS11 and MIS28. The remaining sampling points don't show influences of plants but may be affected by the other mentioned reservoirs. All samples are within the range of terrestrial carbonates (see Figure 40).

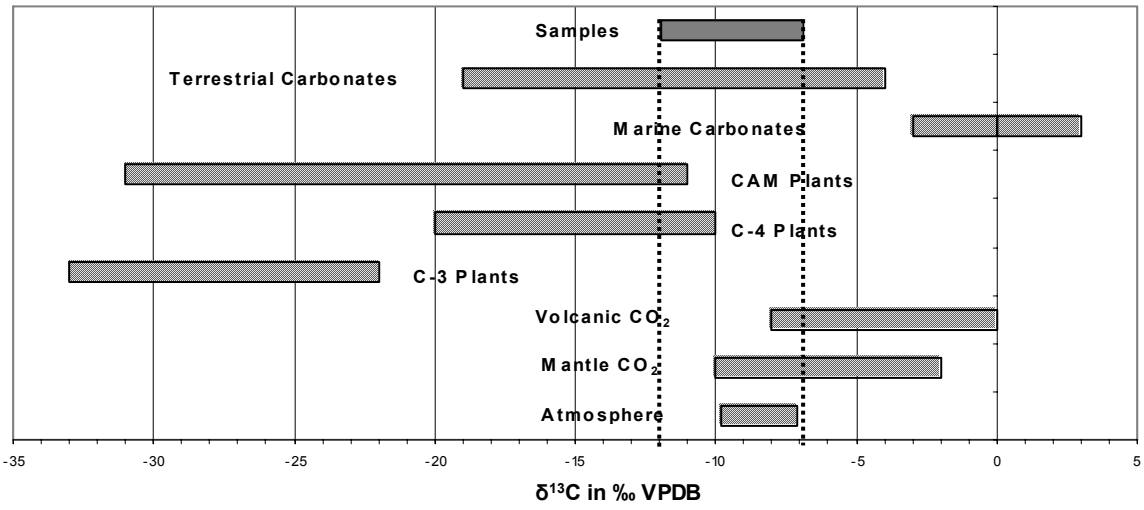

Figure 40: Range of ^{13}C ratios in the samples and possibly influencing reservoirs (after Clark and Fritz, 1997; Rueedi, 2002; Wagner, 1998 and the quoted references therein)

Plotting radiocarbon activities versus ^{13}C ratios a tendency becomes apparent. The samples with lower activities show higher ^{13}C-values and the "modern" samples the lowest ratios. This might strengthen the above made supposition because deep waters normally have higher residence times and deep origin may have provoked interaction with mantle or volcanic CO_2. Reversely recent waters possibly are more influenced by plants than deep CO_2.

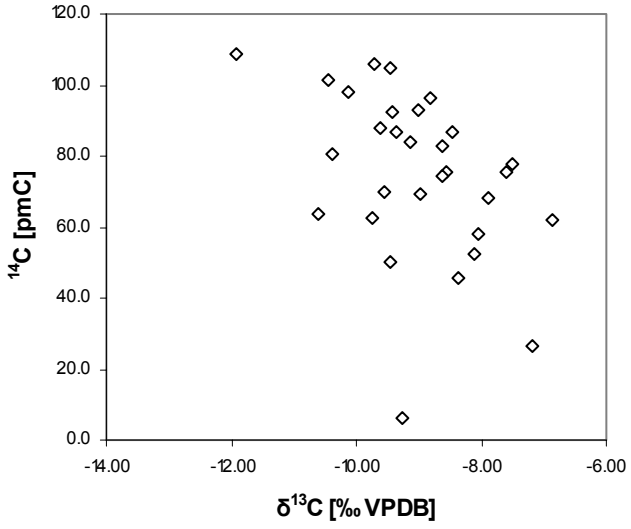

Figure 41: ^{14}C concentrations versus $\delta^{13}C$ ratios.

The measured ^{14}C activities range between 6 and 109 pmC. This clearly indicates the presence of fossile waters having recharged some thousand years ago. Nevertheless these values need correction due to carbonates which provide ^{14}C-free carbon to the DIC-pool of the groundwater. Therefore residence times are overestimated. Two correction models were applied: Vogels concept and the ^{13}C model.

The only parameter which has to be estimated for statistical correction after Vogel is the initial activity. The approach of Verhagen et al. (1974) didn't yield reasonable results (see also Figure 20). A regression line does not hit the detection limit at all. Therefore estimation was performed as described in section 4.4.5. For correction, q-values of 0.75 and 0.9 were chosen to account for carbonate content. Since the measured activity in some wells (e.g. MIS3, MIS14, MIS15) is greater than 100 pmC correction yields lower initial activities than actually present in the wells and partly negative residence times are obtained (see Appendix 26). This may either be due to the simple approach not considering geochemical reactions or also to the fact that bomb ^{14}C could have affected the measured activity. Due to different q-values the corrected residence times deviate 1000-1500 years from each other. For instance if a q-value of 0.75 in MIS4 is considered, the corrected residence time is 2318 years. A q-value of 0.9 yields 3826 years. Corrected residence times reach up to 22361 years in MIS2.

Normally more appropriate is the ^{13}C mixing model. It takes fractionation processes between carbonate species and water into account. The disadvantage of this model is the need for more parameters which weren't determined during this campaign. Besides the initial activity also the $\delta^{13}C$-ratios in soil and carbonate had to be estimated which produced huge errors in estimating residence times. Only changing the soil $\delta^{13}C$ by 1 ‰ altered the corresponding residence time by 700 years. Therefore the calculated residence times are very speculative and uncertain.

Nevertheless data reveal tendencies of different residence times. Obviously MIS2 has a very large component of fossil waters. The tritium activity (0.5 TU) is in the range of the detection limit. The time of recharge, with some caution, must have been more than 10000 years ago. MIS30 and MIS17 also show relatively low ^{14}C activities with values of 26 and 46 pmC. In these cases the residence times are certainly also greater than 1000 years. A "young" component is not present or quantities are very small since the tritium activities are below 0.1 TU.

Further sampling points being almost tritium- free and showing radiocarbon values up to 75 pmC are MIS6 (53 pmC, 0.4 TU), MIS12 (75 pmC, 0.0 TU), MIS16 (70 pmC, 0.1 TU), MIS21 (75.7 pmC; 0.0 TU), MIS25 (62 pmC, 0.1 TU, MIS27 (75 pmC, 0.1 TU), MIS28 (63.9 pmC, 0.0 TU) and MIS29 (58.2 pmC, 0.1 TU). These samples certainly have residence times larger than 50 years and do not contain larger shares of recently recharged (rain-) water.

MIS20 (92.5 pmC; 0.2 TU), MIS24 (83.8 pmC; 0.1 TU) and MIS26 (86.6 pmC; 0.0 TU) are also tritium free although radiocarbon values are more or less “modern”. Even though mean residence times must be greater than 50 years fractions of fossil waters probably are small.

MIS13 (70 pmC, 0.6 TU), MIS18 (63 pmC, 1.4 TU) and MIS19 (50 pmC, 0.6 TU) contain admixtures of certain quantities of waters being recharged in the last 50 years because even if standard deviations of tritium (0.4 TU) are taken into consideration some tritium remains. In these low ^{14}C samples possibly admixture of radiocarbon-free geothermal waters plays a roll. Geothermal waters may contain measureable tritium contents (Gonfiantini et al., 1998). Nevertheless temperatures are not extraordinary increased in comparison to the other sampling points to corroborate this assumption.

The samples MIS3 (109pmC, 0.2TU), MIS14 (106pmC, 1.3TU) and MIS15 (105pmC, 0.9TU) are reflected by high ^{14}C activities but are tritium free or show moderate tritium contents. Carbonate correction of ^{14}C would lead to higher activities. The “old” fraction of these waters may be lower and therefore the mean residence time of the whole mixture is smaller. Higher tritium values and “modern” ^{14}C- activities are an indication for admixture of “younger” waters possibly influenced by bomb ^{14}C.

Very special seems MIS4 (68 pmC, 2.9 TU). At first view the high tritium values are not reflected by radiocarbon activities. But correcting the assumed initial ^{14}C activity (120 pmC) by the calculated q-factor (^{13}C model) of 0.6 results in a recharge activity of 72 pmC which is quite close to the measured activity. MIS4 maybe is the only sampling point where ^{14}C, CFC and tritium values match together and effects like irrigation return flow or pumping do not play a roll.

The remaining sampling points (MIS5, MIS7-MIS11) are reflected by ^{14}C-activities between 75 and 100 pmC and tritium values of 0.6 to 1 TU. Contents of radioisotopes reflect intensive mixing of groundwater. Because of measurable tritium values also bomb-^{14}C might be present which changes estimated residence times considerably.

5.6 STRONTIUM

The measured $^{87}Sr/^{86}Sr$ ratios are within a relatively narrow range between 0.7043 and 0.7062 (mean/median 0.7047). The majority of these samples have almost equal ratios if 2-δ is taken into consideration. Only the samples MIS1, MIS2 and MIS4, are significantly different (see Figure 43 and Appendix 27). Furthermore MIS3, MIS21, MIS23 and MIS 25 show differences. Samples of carbonate rocks which were also collected during this campaign are mostly within the range of the water samples. Solely MIS1G is clearly far away from all rock and water ratios with values of 0.7073 and 0.7082 for carbonates and residues respectively.

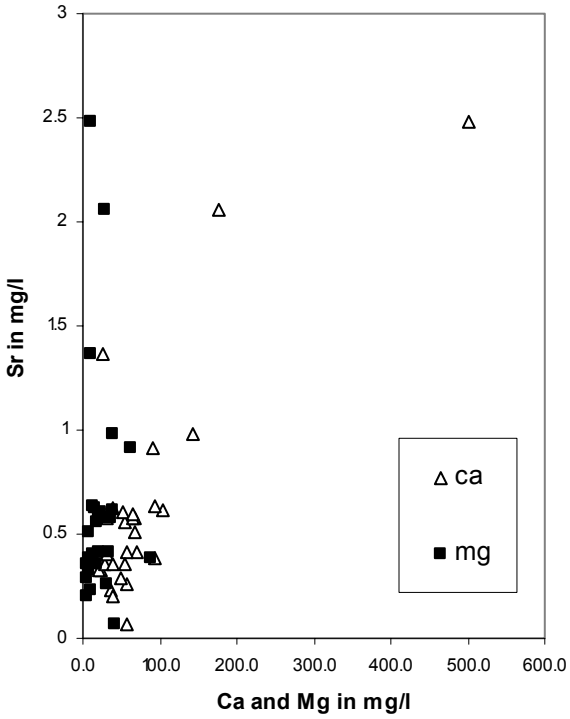

Figure 42: Bivariate plot of strontium versus calcium and magnesium.

The rock samples were analysed twice, first the carbonate fracture and second the residue, because they appeared very clayish and clay normally represents higher strontium ratios (Faure and Powell, 1972). Nevertheless there is no great variance between carbonate and residual fraction. This may be due to the lacustrine origin of these sediments having equilibrated in the same medium, in this case lake water, and later precipitated together.

The main source of Sr probably is dissolution of carbonates. A bivariate plot of Sr versus Ca and Mg (Figure 42) displays possible correlation between strontium and calcium but not between strontium and magnesium. The non-parametric test for correlation (Spearman-Rho) proves significant relation between Sr and Ca (p-value: 0.006; corr. coef: 0.5) but no correlation for Sr and Mg (p-value: 0.7; corr. coef: 0.06). Therefore possibly dissolution of calcium bearing rocks like limestone or gypsum plays the main roll in releasing strontium.

The signature of the water samples is well within the range of volcanic rocks of the upper mantle which is between 0.702 and 0.706. MIS1G are sediments of the JsVs stratigraphical unit. The carbonates of this unit represent marine conditions during deposition. This is also reflected in the Sr ratio. The oceans today show signatures of 0.7091 on average. In the Jurassic period the low-

est values of $^{87}Sr/^{86}Sr$ were 0.7067 (Faure and Powell, 1972). MIS1G lies inside this interval. Anyway, such high ratios weren't found again during this campaign.

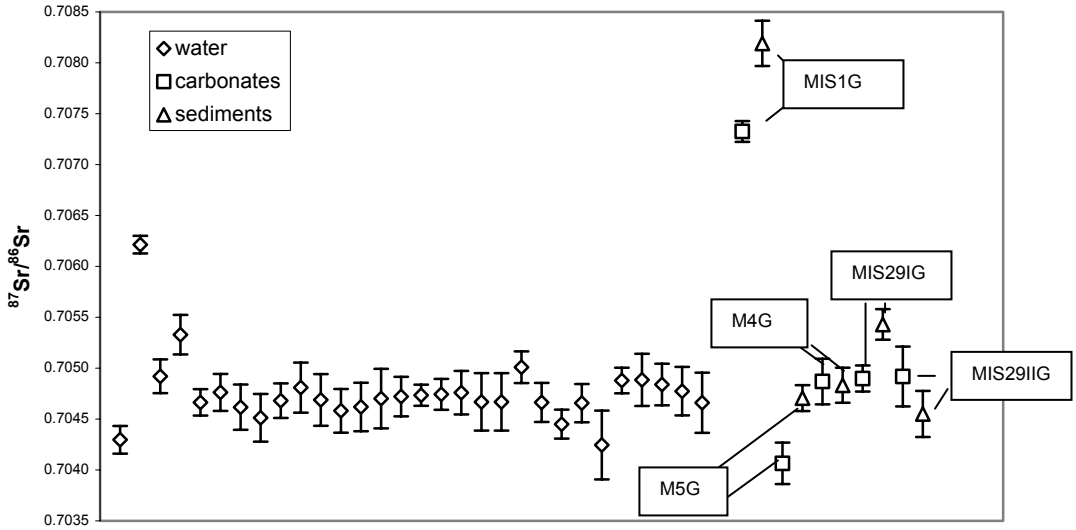

Figure 43: $^{87}Sr/^{86}Sr$ ratios of groundwaters and some rock samples (errors refer to 2σ).

Because of high carbonate and therefore strontium contents, ratios are relatively similar in the study area. Nevertheless two mixing lines might be determined (see Figure 44). It is important to note that these lines don't represent flow paths but only theoretical mixing of groundwater concerning Sr (Faure and Mensing, 2005).

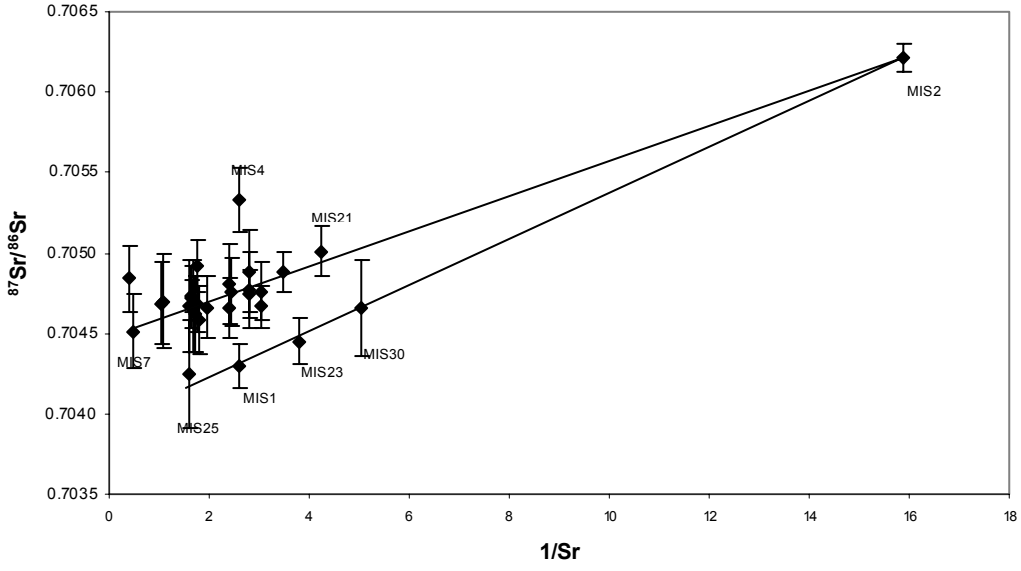

Figure 44: Possible mixing lines of groundwaters concerning strontium.

One endmember of all lines is MIS2 appearing most radiogenic but having the lowest Sr content. This sampling point represents the hydrothermal deep component of the groundwater which might be present in the whole watershed. One distinct mixing line is formed by MIS25, MIS1, MIS23 and MIS30. MIS25 acts as the other endmember with the lowest strontium ratio of all samples and high Sr concentrations, representing groundwaters having equilibrated with the existent calcareous rocks. All members of this mixing line are close to the *Sierra de Guanajuato* and therefore mixing is quite possible. Calculating the fractions of water from MIS2 of the single members, MIS30 would have a share of 76 %, MIS23 of 64 % and MIS1 of 57 %.

A second mixing line could be drawn from MIS7 to MIS2. Most samples would fall within the range of these two endmembers and theoretically the fraction of MIS2 would be up to 91 % (MIS21). The differences between the members of the two mixing lines are not really significant and determination is very speculative. Furthermore the assumed endmembers are not necessarily real endmembers. Detection of endmembers could be accomplished if $^{87}Sr/^{86}Sr$-ratios and concentrations of solid phases were determined. Wood and Macpherson (2005) used solid phase content to calculate (e.g. PHREEQC) the theoretical concentration in solution and therewith estimated properties of the endmembers.

After Faure and Mensing (2005) also detection of ternary mixing is possible if two stable isotopes are used. Figure 45 illustrates $\delta^{13}C$ values versus strontium ratios. Again MIS2 with high Sr- ratio and MIS25 with low Sr ratio but high $\delta^{13}C$ may represent endmembers. A third component reflects low strontium ratios and low $\delta^{13}C$ values. The possible endmember, representing this fraction, could be infiltrating water.

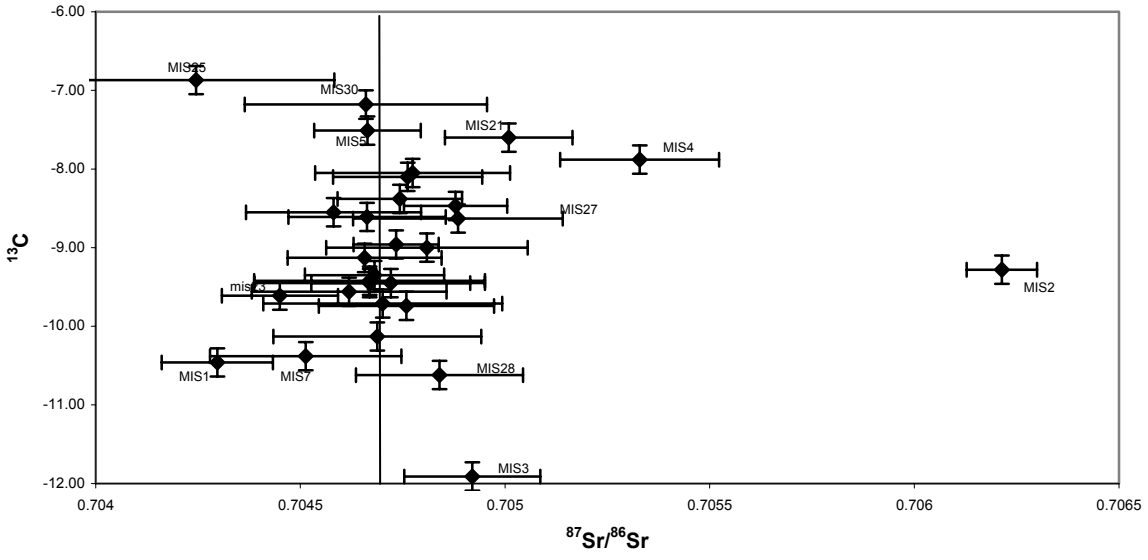

Figure 45: $\delta^{13}C$ versus $^{87}Sr/^{86}Sr$ ratios. $\delta^{13}C$-errors represent the mean deviation of a repeated analysis of six samples (0.18‰). The vertical line illustrates the mean/median of 0.7047.

The line in Figure 45 represents the mean and median of strontium ratios. Taking 1-σ (provided by the laboratory) into account 18 sampling points may be represented by this value of 0.7047. If 2-σ is considered two further sampling points could theoretically have this value (MIS27 and MIS28). These sampling points are plotted blue in Figure 46. Despite this consistency in strontium a wide range in $\delta^{13}C$ between sampling points is existent. All samples have interacted with the same carbonate sediments which are present in the centre of the basin. These strata might also be perforated by the wells at the south-western margin of the study area. Nevertheless $\delta^{13}C$ ratios indicate influences of further reservoirs. MIS11 and MIS28 possibly receive C4-plant-CO_2. The remaining 18 sampling points are not in the range of plant-CO_2 but could be affected by atmospheric and mantle CO_2. MIS5 and MIS30 are additionally in the range of volcanic CO_2. The dispersion of this group and corresponding $\delta^{13}C$ ratios in the study area are illustrated by the following figure.

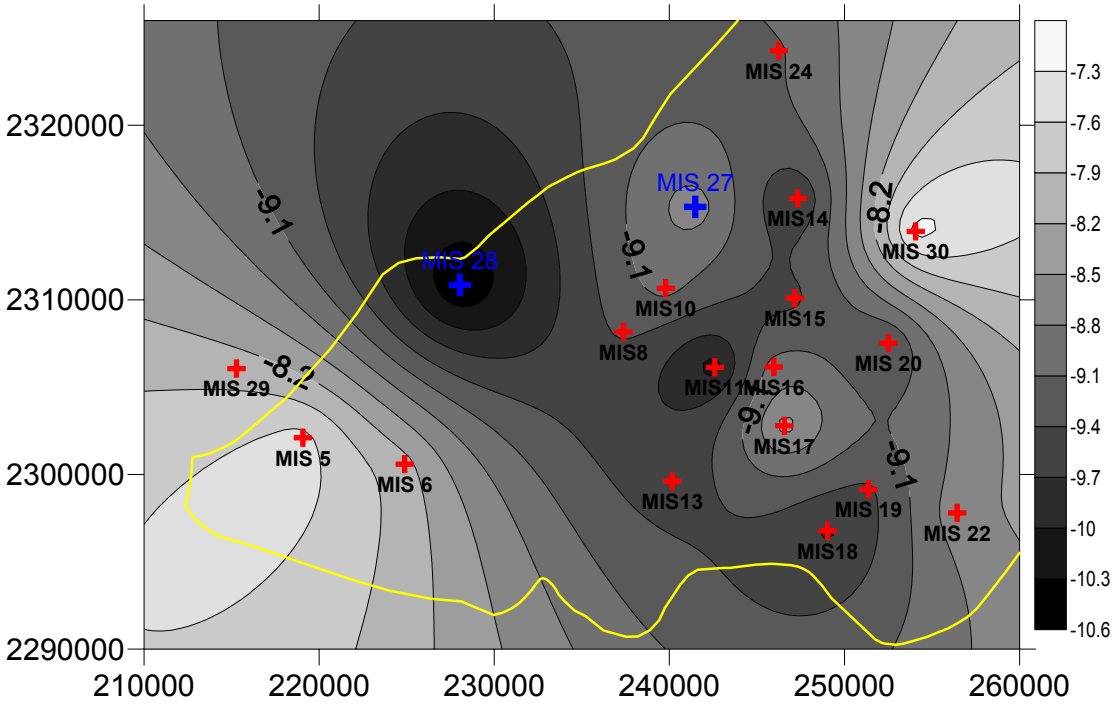

Figure 46: Dispersion of samples having the same $^{87}Sr/^{86}Sr$ ratio and corresponding $\delta^{13}C$ values (units in ‰ VPDB)

6 CONCLUSIONS

Environmental isotopes, gaseous tracers and hydrochemistry were analysed to derive information on groundwater flow, residence time, mixing and recharge conditions in the aquifer of Silao-Romita. Problems during sampling and analysis and specific field conditions limit the interpretation of the results. Nevertheless it was possible to get an insight into recharge and mixing patterns of waters and an estimate on residence times.

Analysis of major-, minor- and trace elements was somewhat problematic. Ion-balance errors were relatively high, especially in the first analysis. Therefore major anions and cations were determined a second and a third time. The third measurement which seemed most reliable revealed different groups of waters. Grouping of Cluster analysis and Piper diagram agree relatively well. One large group is present in the centre of the watershed and represents Ca-HCO_3 dominated waters. The second larger group is primarily present in the south-western and southern part of the study area and represents Na-HCO_3 dominated waters. Most of the element concentrations of the group inside the basin are twice the amount of the southern group. This tendency is also reflected in the saturation indices of mineral phases like calcite which develop from slightly undersaturated at the margins to supersaturated in the basin. This trend may also be a hint to the prevailing recharge flow direction. The chloride mass balance shows similar tendencies with the highest recharge values in the mountains (e.g. *Sierra the Guanajuato).* The calculated values of 30-220 mm may be influenced by anthropogenic effects like irrigation return flow and fertilizing. The CMB also reveals recharge at the north-western margin. Tritium activities in turn do not indicate any changes in activity in direction to the adjacent aquifer of León. Therefore recharge by rain is very unlikely because this would increase tritium activities. Connections to the adjacent aquifer are probable.

Obviously the recharge amount in the central part of the basin is very small. Tritium values indicate mean residence times of more than fifty years which means that very small fractions of recent meteoric waters can be found in the groundwater. Possibly the main source of recharge is irrigation return flow there because tritium activities are not affected by this in contrast to CFC, ^{2}H and ^{18}O. On the one hand CFCs are most enriched in the centre of the basin which may originate from enrichment through exposure to the atmosphere. On the other hand deuterium and ^{18}O ratios there are slightly increased in comparison to the margins of the basin which, in this case, is an indication for evaporative effects.

In general evaporation seems to play an increasing role the younger the waters are. Samples containing more tritium are more enriched in ^{2}H and ^{18}O than those presenting low or no tritium activity. This aspect may also corroborate the assumption of changing ^{2}H and ^{18}O contents in the atmosphere due to changing climatic conditions as proposed by various authors (e.g. Rademacher et al. 2002, COREMI et al., 2004) because the increase in temperature leads to “heavier” rain. This effect is even visible between samples of 1998 (CEASG, 1998) and those of this study. Increasing enrichment of tracers through irrigation which cannot be detected by tritium measurements is very possible.

Stable isotope results may also demonstrate mixing with paleowaters because deuterium values are depleted and samples plot below the LMWL. The measurements of ^{14}C activity are not appropriate to support this assumption. First radiocarbon values illustrate similar dispersion patterns like CFCs with the highest activities in the centre of the basin near Silao. Enrichment by atmospheric or soil CO_2 may be expected through pumping or irrigation. Furthermore carbonate correction leads to huge uncertainties in estimating residence times making it impossible to determine real “ages”. Mixture with fossil waters was shown, for instance in MIS2 and MIS30, but the relative portion could not be calculated. Those samples have very low ^{14}C activities and residence times of more than 10000 years in MIS2. A determination of $\delta^{13}C$ in soil and carbonates would allow for a better correction, and estimations of residence times would only depend on one uncertainty (initial ^{14}C activity in atmospheric CO_2).

Carbon-13 ratios in waters reveal different possible sources of DIC in groundwater. Terrestrial carbonates seem to be the origin in most sampling points although plant-CO_2, volcanic, mantle and atmospheric CO_2 could also be important. Low strontium ratios confirm this assumption and marine carbonates may be neglected in the basin. In the *Sierra de Guanajuato* they are present but they don’t play any role for strontium or ^{13}C ratios in the sampled wells. Groundwaters inside the basin are well equilibrated with calcareous rocks. Saturation indices for calcite and aragonite are primarily above zero and strontium ratios are almost identical. At the margins ratios differ more and saturation indices are below zero due to distinct geology and increased recharge amounts.

Groundwaters in the investigation area are quite well mixed due to intensive exploitation and resulting drawdown. Detection of different mixing components through strontium is difficult due to high carbonate content of the sediments in the basin, as high strontium concentrations of waters having equilibrated with carbonate rocks and their ratio obscure signatures of groundwaters with lower strontium content. Yet at the border to the *Sierra de Guanajuato* mixing becomes obvious, because there are less carbonate rocks. A mixture of waters originating from fractured rocks and which have low concentrations but higher ratios mix with a second component. This second type represents waters which contain more strontium but present lower ratios. The second component

contains waters that equilibrated with calcareous rocks. If the $\delta^{13}C$ is plotted versus $^{87}Sr/^{86}Sr$ a third component with a low carbon-13 and a low Sr-ratio is visible, possibly representing infiltrating waters.

The following sketch illustrates the assumed sources of recharge in the investigation area. Besides measured precipitation and discharge data also the estimated (CMB) recharge rates were included, although they are relatively unreliable.

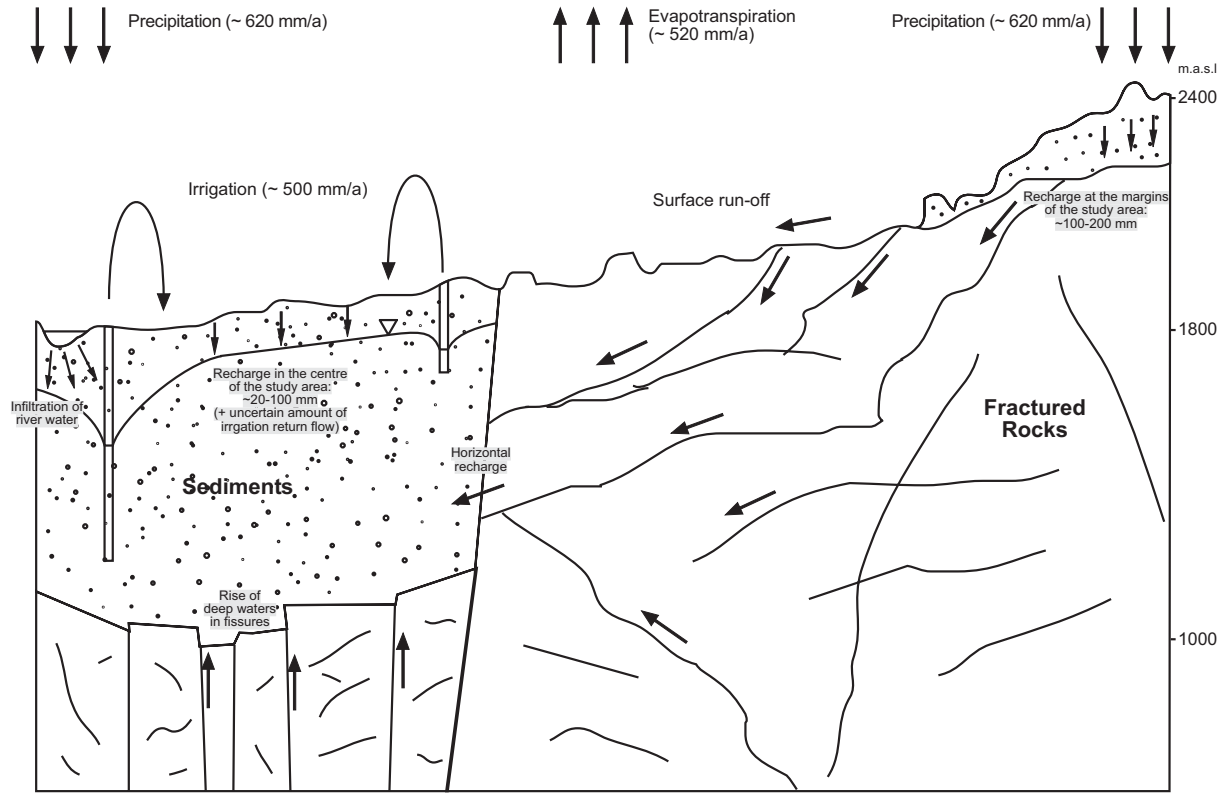

Figure 47: Schematic cross-sectional view illustrating possible sources of recharge.

7 RECOMMENDATIONS

Interpretations in this thesis largely base on relatively unreliable data and therefore are in some cases only rough estimations or possibly are wrong. To avoid similar problems in following investigations some recommendations will be done at the end of this report.

During preparation it was very disadvantageous that numbering of the existent wells was not consistent and in every report different naming was used. Furthermore data about registered geology, well depth, filter screens etc. was very poor and if existent no coordinates were obtainable. More insights into hydrogeology could be obtained if it was possible to choose special wells with known geology and construction beforehand. This also failed due to limited accessibility of many wells.

Sampling in the pumping wells, which are also mostly screened completely, possibly provoked the difficulties with CFCs. Observation wells are not existent or not accessible in the study area. Therefore at least partly screened wells with different pumping depths should be chosen and they should work with submergible pumps. Maybe better would be the sampling at the end of the rain season when most pumps are not in operation and there are no depression cones. In this case maybe an own pump would have to be used but it would be possible to perform depth-dependent low-flow sampling and the usage of a flow-through-cell would be less problematic.

Apart from $^{2}H/^{18}O$ analyses no isotope determination was done in the investigation area in the past. This fact is also reflected by the obtainable data. For tritium no measurements in precipitation exist and the input function had to be estimated. Monthly analyses of some precipitation samples in different parts of the area or at least determination of tritium concentration in some lakes would give an idea about the magnitude of the actually existing atmospheric activity.

Apart from non-ideal sampling in pumping wells CFC interpretation may suffer from uncertain anthropogenic impact. Local measurements in precipitation or air could exclude or confirm anthropogenic effects and also enlighten possible local deviations of the input values. Measurements of CFC in soil air in different depths would also be extremely helpful to determine and calibrate the possible time lags although this may be very expensive and time consuming.

Strontium interpretation was problematic due to relatively similar values resulting from interaction of groundwater with carbonates. Depth-dependent sampling of groundwater may give a better insight into mixing and detection of possible flow paths as well as sampling in the fractured rocks of the *Sierra the Guanajuato* and along the interface between fractured and sedimentary rocks may be helpful. Furthermore some samples of superficial water and determination of strontium concentration in carbonate rocks would be interesting. By that calculation and detection of end-members of different mixing lines may be possible.

The origin of groundwaters can be estimated by applying the silica-geothermometer if the geothermal gradient is known. Up to know no data about the gradient in the study area has been obtainable. Temperatures and corresponding extraction depths let consider a differing gradient throughout the investigation area. The estimation would provide valuable information to validate the results of the other isotopes (^{2}H, ^{18}O, strontium, ^{13}C).

The determination of mean residence times of groundwater with ^{14}C was problematic due to carbonate correction. Two variables had to be estimated which yielded quite unreliable results. Analysis of $\delta^{13}C$ in carbonates and in soil air or soil water would eliminate the two uncertain parameters. Furthermore atmospheric ^{14}C content must be known. An analysis of superficial or rain water would give an idea about the current atmospheric radiocarbon activity in the territory and would make the whole method more reasonable.

The chloride-mass-balance generally is an effective method to estimate the recharge. To use it correctly in the study area more measurements of chloride in precipitation would be necessary. Monthly analyses of rain water during several years are needed instead of single measurements to estimate reliable recharge values. Problematic is the unknown agricultural influence through fertilizing. Bromide has similar conservative properties like chloride and could also serve to calculate the mass balance if it would be determined in precipitation.

8 ACKNOWLEDGEMENT

My time in Mexico was one of the most interesting and instructive periods of my life. To have the opportunity to work abroad and to complete my study was possible thanks to the following people.

Prof. Dr. Broder J. Merkel initiated this thesis by making the contact to the CEA in Monterrey and supported my desire to go abroad. Furthermore I want to thank him not only for proofreading but also for always being available for discussions and professional advice in case of questions.

I want to thank Dr. Jürgen Mahlknecht for giving me the opportunity to work out a thesis in Mexico and his amicable support in all situations not only concerning scientific questions. He enabled all the important contacts which were indispensable for realising the sampling campaign in Guanajuato and helped me struggling through Mexican bureaucracy.

I like to thank the DAAD for financing the time of my fieldwork in Mexico. Without its support it would have been almost impossible to realise this thesis. Furthermore I'm grateful to the CONCyTEG who financed large parts of the analyses in the scope of the project 04-12-A-044.

José Chávez Guevara and Lizeth Oliva who accomplished the sampling with me and with whose help and knowledge the wells were much more easily accessible. I'm very grateful for the patience they had with me, especially when I was heavily diseased…

All my friends in Mexico who welcomed me with amity, cordiality and hospitality and made my residence in Mexico a unique experience. Muchas Gracias mis amigos! Nunca olvidaré a ustedes!

Dr. Marion Tichomirowa, who enabled the work in the isotope laboratory (Freiberg, Germany) and gave valuable hints concerning the interpretation of strontium results. Furthermore I thank Mrs. Braun, Mrs. Liebscher, Mrs. Mühlberg and Mr. Bomberg for their enduring and amiable help in introducing me in strontium analysis.

Prof. D. Hebert and the *TriCar laboratory* in Freiberg (Germany) for the tritium analysis and the interesting discussion around the interpretation of the results.

H.J. Peter who analysed the anions and cations in Freiberg (Germany).

I thank the Spurenstofflabor of Dr. Harald Oster, Wachenheim (Germany) for CFC determination.

The *Laboratorio del Centro de Calidad Ambiental* in Monterrey (Mexico) for analyses of major, minor and trace elements.

The *Environmental Isotope Laboratory* in Waterloo and *IsoTrace Laboratory* in Toronto (Canada) for isotope analyses of ^{2}H, ^{18}O, ^{13}C and ^{14}C.

Dr. Britta Planer-Friedrich who - although far away in Canada – always was available (there's no Sunday…) if I couldn't solve the problems with PhreeqC.

Dr. Susanne Stadler for near-term English-correction of some parts of this thesis.

All my friends for just being there when I needed them.

Last but not least I thank my mother for always believing in me and for giving me the support and freedom to realise almost impossible dreams.

9 REFERENCES

BACK, W. (1961): Techniques for mapping of hydrochemical facies: U.S. Geol. Surv. Prof. Paper 424-D, p.380-382

BAUER, S., Fulda, Ch., Schäfer, W. (2001): A multi-tracer study in a shallow aquifer using age dating tracers ^{3}H, ^{85}Kr, CFC-113 and SF_6 – indication for retarded transport of CFC-113; *Journal of Hydrology,* **248***,* 1-4, p. 14-34

BIERMAN P.R., A. Albrecht, M.H. Bothner, E.T. Brown, T.D. Bullen, L.B. Gray and L. Turpin: Erosion Weathering and Sedimentation; In: Kendall and McDonnell (1998) p. 647-678

BÖHLKE, J.K. (2004): TRACERMODEL1. Excel workbook for calculation and presentation of environmental tracer data for simple groundwater mixtures. In: IAEA Guidbook on the Use of Chlorofluorocarbons in Hydrology. International Atomic Energy Agency, Vienna, in press.; obtainable through internet: http://water.usgs.gov/lab/software/tracer_model/

BÖHLKE, J.K. and M. Horan (2000): Strontium isotope geochemistry of groundwaters and streams affected by agriculture, Locust Grove, MD; *Applied Geochemistry,* **15**, p. 599-609

Bullen, T.D. and C. Kendall: Tracing of weathering reactions and water flowpaths: A multi-isotope approach. In: Kendall and McDonnel (1998)

BU X. and Warner M.J. (1995): Solubility of chlorofluorocarbon 113 in water and seawater. *Deep-Sea Research* **42(7)**, 1151–1161.

BUSENBERG, E., and Plummer, L.N. (1992) Use of chlorofluorocarbons (CCl3F and CCl2F2) as hydrologic tracers and age-dating tools; the alluvium and terrace system of central Oklahoma, *Water Resources Research*, v.**28**, n.9, p.2257-2284

CARSLAW, H.S. and J.C. Jaeger (1959): Conduction of heat in solids. Oxford University Press, Oxford, UK.

CMA (Chemical Manufacturers Association) (1983): CFC-11 and CFC-12 production release data, 14 pp., Washington, D.C.

CEAG (2003): Cuantificación del volumen de extracción a partir del Análisis de Imágenes de Satélite y Verificación de Campo en el Acuifero Silao- Romita, Gto; elaborado por Gondwana Exploraciones S.C.

CEASG (COMISIÓN ESTATAL DE AGUA Y SANEAMIENTO DE GUANAJUATO)(1998): Estudio Hidrogeologico y Modelo Matemático del Acuífero del Valle de Silao Romita, Gto. Contrato CEAS-APA-GTO-97-025, realised through Lesser y Asociados SA de CV

CEASG (1999): Estudio isotópico para la caracterización del agua subterránea en la zona de La Muralla, Guanajuato. CEASG; Contrato CEASXXVI- OD-UNAM-99-088, realizado por el Instituto de Geofísica de la Universidad Nacional Autónoma de México para la CEASG. Guanajuato, Gto. 74 pp.

CFE-SIB (Subgerencia de Ingenería Básica de la Comisión Federal de Electricidad (1979): Estudio Isotópico para determinar el origen y causas del geotermismo en la región de la Planta Termoeléctrica de Salamanca, Gto (internal report)

CLARK, I.A. and P. Fritz (1997): Environmental Isotopes in Hydrogeology, Lewis Publishers, New York, 328 p.

COOK, P. and A.L. Herczeg (2000): Environmental Tracers in Subsurface Hydrology, Kluwer Academic Publishers, Boston a. o., 529 p.

COOK, P.G.; D.K. Solomon, L.N. Plumer, E. Busenberg, S. L. Schiff (1995): Chlorofluorocarbons as tracers of groundwater transport processes in a shallow, silty sand aquifer, *Water Resources Research*, Vol. **31**, No. 3, p. 425-435

COOK, P.G. and D.K. Solomon (1995): Transport of atmospheric trace gases to the water table: Implications for groundwater dating with chlorofluorocarbons and Krypton 85, *Water Resources Research*, Vol. **31**, No. 2, p. 263-270

COREMI/ CONCyTEQ/ CENICA, Dirección Tecnica , Subdirección De Apoyo Técnico, Gerencia De Estudios Especiales, Subgerencia de Geohidrología y Geotecnica (2004): Potencial geohidrológico del Graben De Leon, Pachuca, HGO

CORTÉS, A., J. Durazo and R.N. Farvolden (1997): Studies of isotopic hydrology of the basin of Mexico and vicinity: annotated bibliography and interpretation, *Journal of Hydrology* **198**, p. 346-376

CORTÉS, A., Espinosa, G., Golzarri, J.I. (2001): Estudio Isotópico e Hidrogeoquímico de la Zona de León Río Turbio"; Sistema de Agua Potable de León, (SAPAL), Guanajuato (Proyecto de colaboración con el Instituto de Geofísica, UNAM),

CRAIG, H. (1957): Isotopic Standards for Carbon and Oxygene and correction Factors for Mass-spectrometric Analysis. *Geochim. Cosmochim. Acta*, **12**, p. 133

CUNNOLD, D.M., R.G. Prinn, R. Rasmussen, P.G. Simmonds, F.N. Alyea, C. Cardelino, A. Crawford, P.J. Fraser, R. Rosen (1986):Atmospheric lifetime and annual release of $CFCl_3$ and CF_2Cl_2 from 5 years of ALE data, *Journal of Geophysical Research*,**91**, pp. 10797- 10817

CUNNOLD, D.M., P.J.Fraser, R.F. Weiss, R.G. Prin, P.G. Simmonds, B.R. Miller, F.N. Alyea and A.J. Crawford (1994): Global trends and annual releases of CCl_3F and CCl_2F_2 estimated from ALE/GAGE and other measurements from July 1978 to June 1991, *Journal of Geophysical Research,* Vol. **99 D1,** p 1107-1126

DEINES, P., D. Langmuir and R.S. Harmon (1974): Stable carbon isotope ratios and the existence of a gas phase in the evolution of carbonate groundwaters. *Geochimica et Cosmochimica Acta*, **38**, p. 1147-1164

DERRA, S. (1990): CFC's – No easy solutions. *Res. Develop.*, **32**, p. 54-66

DICKINSON, R. and Cicerone, R., 1986. Future global warming from atmospheric trace gases. *Nature* **319**, p. 109–115

DOMENICO, P.A. and F.W.Schwartz (1990): Physical and chemical hydrogeology; John Wiley & Sons, New York a.o.; 824 p.

ELKINS J.W. (ed), J.H. Butler, T.M. Thompson, S.A. Montzka, R.C. Myers, J.M. Lobert, S.A. Yvon, P.R. Wamsley, F.L. Moore, J.M. Gilligan, D.F. Hurst, A.D. Clarke, T.H. Swanson, C.M. Volk, L.T. Lock, L.S. Geller, G.S. Dutton, R.M. Dunn, M.F. Dicorleto, T.J. Baring, A.H. Hayden (1996): Nitrous oxide and halocompounds. In: Climate Monitoring and Diagnostics Laboratory No. 23, Summary Report 1994-1995. eds. D.J. Hofmann, J.T. Peterson

and R.M. Rosson, U.S. Department of Commerce, NOAA Environmental Research Laboratories, p. 84-111

ENGESGAARD, P; A.L. Højberg, K. Hinsby, K.H. Jensen, T. Laier, F.Larsen, E. Busenberg, L.N. Plummer (2004): Transport and Time Lag of Chlorofluorocarbon Gases in the Unsaturated Zone, Rabis Creek, Denmark; *Vadose Zone Journal* **3**; p. 1249-1261

Faure G. and T.M. Mensing (2005)Isotopes, Principles and applications. 3rd Edition, John Wiley & Sons Inc., Hoboken, New Jersey, 896 p.

FAURE, G.; J.L. Powell (1972): Strontium isotope geology, Springer-Verlag Berlin, 188 p.

FRANSON, M.A. (ed.), 1976: Standard Methods for the Examination of Water and Wastewater; 14.Edition; American Public Health Association, Washington; 1193 p.

FRITZ, P. and J.Ch. Fontes (1980): Handbook of Environmental Isotope Geochemistry, Volume 1; The Terrestrial Environment, A; Elsevier, Amsterdam a.o.; 545 p.

FRITZ, P. and J.Ch. Fontes (1986): Handbook of Environmental Isotope Geochemistry, Volume 2; The Terrestrial Environment, B; Elsevier, Amsterdam a.o.; 557 p.

FONTES, J.Ch. and J-M. Garnier (1979): Determination of the initial ^{14}C activity of total dissolved carbon: A review of existing models and a new approach. *Water Resources Research*, **15,** p. 399-413

GAMLEN, P. H.; Lane, B.C.; Midgley, P.M.; Steed, J.M. (1986): Production and release to the atmosphere of CCl_3F and CCl_2F_2 (chlorofluorocarbons 11 and 12) *Atmos. Environment*, **20**, 1077-1085

Geofísica de Exploraciones Guysa S.A. de CV, 1998: Estudio hidrogeológico y modelo mathemático del aquífero del Valle de León, Gto; informe técnico, inédito (technical report, unpublished)

GODWIN, H. (1992): Half-life of radiocarbon. *Nature* **195**, p. 984

GONFIANTINI, R, K. Fröhlich, L. Araguás-Araguás and K. Rozanski (1998): Isotopes in groundwater hydrology. In: Kendall and McDonnell, 1998.

GOSSELIN, C.G., F.E. Harvey, C. Frost, R. Stotler, P.A. Macfarlane (2004): Strontium isotope geochemistry of groundwater in the central part of the Dakota (Great Plains) aquifer, USA, *Applied Geochemistry* **19**, p 359-377

HAIR Jr., J.F.;W.C. Black., B.J. Babin, R.E. Anderson and R.L. Tatham (2006): Multivariate data analysis, Pearson Prentice Hall, 6th ed., 899 p.

HEBERT, D. (1989): Tritium in der Atmosphäre – Quellen Verteilung, Perspective-,VEB Deutscher Verlag für Grundstoffindustrie, Leipzig, 78 p.

HEIER, K.S. and G.K. Billings (1970): Lithium; In: Wedepohl, K.H.: Handbook of Geochemistry; Springer Verlag Berlin a.o., Part II-1

IAEA (editor)(various years): Environmental Isotope Data- World Survey of Isotope Concentration in Precipitation. Tech. Rep. Series (various editions), IAEA, Vienna

IBARRA-OLIVARES JG (2004) Un modelo del Funcionamiento del Sistema Acuífero de Silao-Romita, Edo. de Guanajuato. Msc. Thesis, Universidad de Guanajuato, Guanajuato, Mexico, 87 p.

INGRAHAM, N.L., E.A. Caldwell and B.T. Verhagen: Arid catchments; In: Kendall and McDonnell, (1998)

JOUZEL, J, 1980: Isotopes in Cloud Physics: Multiphase and Multistage Condensation Processes Chapter 2. In: Fritz and Fontes (1980)

KELLNER, R. (ed.), J.-M. Mermet, M. Otto and H.M. Widmer (2005): Analytical Chemistry; Wiley-VCH, Weinheim a.o., 941 p.

KENDALL, C. and J.J. McDonnell (eds) (1998): Isotope tracers in catchment hydrology, Elsevier, Amsterdam a.o., 839 p.

KENDALL, C. and E.A. Caldwell (1998): Fundamentals of isotope geochemistry; In: Kendall and McDonnell, 1998

LI, H. and J.J. Jiao (2005): One-dimensional airflow in unsaturated zone induced by periodic water table fluctuation, *Water Resources Research*, Vol. **41**, W04007, 10 p.

LINDSEY, B.D., S.W. Phillips, C.A. Donnelly, G.K. Speiran, L.N. Plummer, J.K. Böhlke, M.J. Focazio, W.C. Burton and E. Busenberg (2003):Residence times and nitrate transport in ground water discharging to streams in Chesapeake Watershed; Water-Resources Investigation Report 03-4035

LIST, R.J. (1949): Smithsonian Meteorological Tables. Sixth ed., Smithsonian Institution Press, Washington, DC, 527 p

LOVELOCK, J.E. (1971): Atmospheric fluorine compounds as indicators of air movements, *Nature*, **230**, p. 379

Lucas, L.L. and M.P. Unterweger (2000): Comprehensive review and critical evaluation of the half-life of Tritium; *Journal of research of the National Institute of Standards and Technology*; **105**, p. 541

MAHLKNECHT, J.;J.F. Schneider, B.J. Merkel, I. Navarro de León and S.M. Bernasconi (2004): Groundwater recharge in a sedimentary basin in semi-arid Mexico; *Hydrogeology Journal* **12**; p. 511-530

MAZOR, E. (2003): Chemical and isotopic groundwater hydrology. Marcel Dekker Ltd.; third edition; 352 p.

MCCARTHY, R.L.; Bower, F.A.; Wade, R.J. (1977): The fluorocarbon- ozone theory, 1, production and release: World production and release of CCl3F and CCl2F2 (fluorochlorocarbons 11 and 12) through 1975, *Atm. Environment*, **11**, p. 491-497

MCNUTT, R.H.: Strontium Isotopes, In: Cook and Herczeg (2000), p. 233-260

MERKEL, B. and B. Planer-Friedrich (2005): Groundwater Geochemistry; Springer Verlag Berlin, Heidelberg; 200 p.

MERKEL, B. and B. Sperling (1996): Hydrogeochemische Stoffsysteme Teil I; DVWK-Schriften 110, *Kommissionsvertrieb Wirtschafts- und Verlagsgesellschaft Gas und Wasser mbH*, Bonn, 288 p.

MERKEL, B. and B. Sperling (1998): Hydrogeochemische Stoffsysteme Teil II; DVWK-Schriften 117, *Kommissionsvertrieb Wirtschafts- und Verlagsgesellschaft Gas und Wasser mbH*, Bonn, 397 p.

MIBUS, J., P. Szymzcak, D.Hebert and H. Oster (2002): Kombinierter Einsatz FCKW und Tritium als Tracer. In: Isotope und Tracer in der Wasserforschung: proceedings zum Workshop am Geologischen Institut der TU Bergakademie Freiberg am 21. Juni 2002; 53. Berg- und Hüttenmännischer Tag, Jahr der Geowissenschaften, Freiberger Geo- Tage; *Institut für Geologie: Wissenschaftliche Mitteilungen,* 111 p.

MOLINA, M. and F.S. Rowland (1974). Stratospheric sink for chlorofluoromethanes: Chlorine atom catalyzed destruction of ozone. *Nature* **249**, p. 810–812

MOOK, W.G., J.C. Bommerson and W.H. Staverman (1974): Carbon isotope fractionation between dissolved bicarbonate and gaseous carbon dioxide. *Earth and Planetary Science Letters*, **22**, p. 169-176

NÉGREL, Ph. and E. Petelet-Giraud (2005): Strontium isotopes as tracers of groundwater-induced floods: the Somme case study (France), *Journal of Hydrology* **305**, p. 99-119

NEUMANN, W. and H. Huster (1974): The half-life of ^{87}Rb measured as a difference between the isotopes ^{87}Rb and ^{85}Rb. *Z. Phy*. **270**, p. 121-127

NILSON, R.H., E.W. Peterson, K.H. Lie, N.R. Burkhard, J.R. Hearst (1991): Atmospheric Pumping: A mechanism causing vertical transport of contaminated gases through fractured permeable media, *Journal of Geophysical Research*, Vol.**96**, B13, 21933-21948

OSTER H., Sonntag C. and Munnich K.O. (1996) Groundwater age dating with chlorofluorocarbons. *Water Resour. Res*. **32(10)**, p. 2989–3001.

PARKHURST, D.L. and C.A.J Appelo (1999): User's guide to PhreeqC (Version 2)- a computer program for speciation, batch-reaction, one-dimensional transport and inverse geochemical calculations. US Geol. Surv. Water Resour. Inv. Rep. 99-4259, 310

PERSON, F.J. (1965): Use of C-13/C-12 ratios to correct radiocarbon ages of material initially diluted by limestone. In: Proceedings of the 6th International Conference on Radiocarbon and Tritium Dating, Pulman, Washington 357.

PERSON, F.J. and B.B. Hanshaw (1970): Sources of dissolved carbonate species in groundwater and their effects on carbon-14 dating. In: Isotope Hydrology 1970, IAEA Symposium 129, March 1970, Vienna: 271-286

PLUMMER, L.N. and E. Busenberg (2000): Chlorofluorocarbons. In: Cook and Herczeg, 2000

RADEMACHER, L.K.; J.F.Clark and G.B.Hudson (2002): Temporal changes in isotope composition of spring waters: Implications for recent changes in climate and atmospheric circulation; *Geology*, Vol. **30**, no. 2, p. 139-142

ROZANSKI, K.; L. Araguás-Araguás, R. Gonfiantini (1993): Isotopic patterns in modern global precipitation. In: P.K. Swart, K.C. Lohmann, J. McKenzie and S. Savin (eds) Climate change in continental isotopic records. Geophysical Monograph 78, American Geophysical Union, Washington, D.C., p. 1-36

RUEEDI, J. (2002): Groundwater dating by 14C. In: UNEP/DEWA/RS.02-2: A survey of methods for groundwater recharge in arid and semi-arid regions

SALIEGE, J.F., Fontes, J.-Ch., (1984): Essai de déterminacion expèrimentale du fractionnement des isotopes ^{13}C et ^{14}C du carbone au cours de processus naturels. *International Journal of Applied Radiation and Isotopes*, **35**, p. 55-62

SALEM, O., Visser, J.H., Dray, M., Gonfiantini, R. (1980): Groundwater flow patterns in the western Libyan Arab Jamahiriya, evaluated from isotopic data, Arid Zone Hydrology: Investigations with Isotope Techniques (Proc. Advisory Group Mtg Vienna, 1978), IAEA, Vienna 165- 180

SISTEMA DE AGUA POTABLE Y ALCANTARILLADO DE LEÓN (SAPAL), 2001. Estudio Isotópico e Hidrogeoquímico de la Zona de León-Río Turbio. Contrato realizado por el instituto de Geofísica de la Universidad Nacional Autónoma de México para el SAPAL. León, Gto., México. 75 pp.

SPARKS, Samantha (1988): Pesticides in Mexico. *Multinational Monitor,* Vol. 10, No. 10 (obtainable through internet: http://multinationalmonitor.org/hyper/issues/1988/10/mm1088_06.html)

STUTE, M. and P. Schlosser: Atmospheric noble gases. In: Cook, P. and A.L. Herczeg (2000): Environmental Tracers in Subsurface Hydrology, Kluwer Academic Publishers, Boston and others, 529 p.

TOTH, J. (1963): A theoretical analysis of groundwater flow in small drainage basins. *Journal of Geophysical Research* **68**, p. 4795-4812

UNTERWEGER, M.P., Coursey B.M., Shima F.J. and Mann W.B. (1980): Preparation and calibration of the 1978 National Bureau of Standards tritiated water standards. *International Journal of Applied Radiation and Isotopes*, **31**, p. 611- 614.

VERHAGEN, B.Th., E. Mazor and J.P.F. Sellshop (1974): Radiocarbon and tritium evidence for direct recharge to groundwaters in the northern Kalahari, *Nature*, 249, p. 643-644

VOGEL, J.C., Grootes, P.M.; Mook, W.G. (1970): Isotope fractionation between gaseous and dissolved carbon dioxide, *Z. Phys*., **230**, p. 255-258

VOLK C.M., Elkins J.W., Fahey D.W., Dutton G.S., Gilligan J.M., Loewenstein M., Podolske J.R., Chan K.R. and Gunson M.R. (1997): Evaluation of source gas lifetimes from stratospheric observations. *J. Geophys. Res. – Atmos*. **102(D21)**, p. 25543–25564

WAGNER G.A. (1998): Age determination of young rocks and artefacts. Springer Verlag Berlin a.o., 466 p.

WARNER M.J. and Weiss R.F. (1985): Solubilities of chlorofluorocarbons 11 and 12 in water and seawater. *Deep-Sea Res. 32*, p. 1485–1497.

WEISS, R.F. and B.A. Price (1980): Nitrous oxide solubility in water and seawater. *Marine Chemistry*, **8**, p. 347-359

WILSON G.B. and G.W. Mc Neill (1997): Noble gas recharge temperatures and excess air component. *Applied Geochemistry* **12**, 747-762

WMO, 1988. The Montreal Protocol on substances that deplete the ozone layer. WMO Bull. **37**, pp. 94–97.

WOOD, K.H. and G.L. Macpherson (2005): Sources of Sr and implications for weathering of limestone under tallgrass prairie, northeastern Kansas, *Applied Geochemistry*, **20**, p. 2325-2342

WOOD, W.W. (1999): Use and misuse of the chloride-mass balance method in estimating ground water recharge, *Ground Water*, Vol. **37**, No. 1; p. 2-3

ZUBER, A. (1986): Mathematical models for the interpretation of environmental radioisotopes in groundwater systems In: Fritz and Fontes (1986)

Maps:

Instituto Nacional De Estadistica Geografía E Informatica (INEGI): Carta Uso Del Suelo y Vegetacion, 1:250000, Guanajuato, F14-7 (Map of landuse and vegetation)

INEGI: Carta Topográfica, 1:250000, Querétaro F14-10

INEGI: Carta Topográfica, 1:250000, Guanajuato F14-7

Visited internet pages:

EPA, Part 141:National Primary Drinking Water Regulations, http://www.access.gpo.gov/nara/cfr/waisidx_02/40cfr141_02.html

IAEA: www-naeb.iaea.org/napc/ih/volumes.asp ; Mook, W.G.(editor) (2004) : Environmental Isotopes in the Hydrological Cycle, Principles and Applications.

IAEA 2: http://www.iaea.org/programmes/rial/pci/isotopehydrology/docs/intercomparision/half_life.pdf

IAEA-GNIP: http://isohis.iaea.org/Login.org

INEGI: htttp://www.cuentame.inegi.gob.mx/territorio/default.asp#

NASA: ftp://e0srp01u.ecs.nasa.gov/srtm/version2/SRTM3

Norma Oficial Mexicana NOM-127-SSA1-1994, „Salud Ambiental, Agua Para Uso Y Consumo Humano-Limites Permisibles De Calidad Y tratamientos A Que Debe Someterse El Agua Para Su Potabilizacion: http://www.salud.gob.mx/unidades/cdi/nom/127ssa14.html

Trinkwasserverordnung 2001: http://www.dvgw.de/wasser/rechtsvorschriften/trinkwasserverordnung/index.html

WHO: http://www.who.int/water_sanitation_health/diseases/arsenicosis/en/

10 ABBREVIATIONS

AES	atom emission spectrometry
AMS	accelerator mass spectrometry
CEAG	Comisión Estatal del Agua de Guanajuato
CEASG	Comisión Estatal de Agua y Saneamiento de Guanajuato
CFC	chlorofluorocarbon
CMB	chloride mass balance
CNA	Comision Nacional del Agua
COREMI	Consejo De Recursos Minerales
DEM	Digital Elevation Model
DIC	dissolved inorganic carbon
DOC	dissolved organic carbon
EM	exponential model
GC	gas chromatography
IAEA	International Atomic Energy Agency
IC	ionchromatography
ICP	inductive coupled plasma
LMWL	local meteoric water line
Ma	million years
MRT	mean residence time
MS	mass spectrometry
MWL	meteoric water line
PFM	piston flow model
pmC	percent modern carbon
pptv	parts per trillion by volume
SRTM	Shuttle Radar Topography Mission
TU	tritium units
UNAM	Universidad Nacional Autónoma de México
VPDB	Vienna Pee Dee Formation (*Belemnitella Americana*)
VSMOW	Vienna standard mean ocean water

11 LIST OF FIGURES

12 LIST OF TABLES

APPENDIX

Appendix1: Precipitation data from El Conejo, Comanjilla, Silao and Romita provided by CNA, Celaya. All values are in mm.

El Conejo	Jan	Feb	Mar	Apr	May	Jun	Jul	Aug	Sept	Oct	Nov	Dec		prec. per year
1978	0	16	5	0	30	104	164	107	217	166	0	17		825
1979	0	25	0	0	4	49	114	83	90	0	2	50		418
1980	97	5	0	4	8	13	77	222	135	31	18	5		614
1981	58	11	2	56	15	107	133	165	57	143	0	27		773
1982	0	9	0	19	42	9	174	64	30	74	26	49		496
1983	17	3	2	0	31	23	265	141	92	29	44	1		647
1984	14	10	0	0	19	112	166	105	43	14	0	3		487
1985	0	1	3	49	16	120	135	129	131	29	11	2		625
1986	0	2	0	11	10	244	156	62	162	31	21	0		698
1987	3	0	0	10	25	119	173	64	92	21	44	0		551
1988	14	0	29	0	1	82	154	287	29	1	5	0		602
1989	0	1	0	5	2	40	119	191	76	2	4	13		453
1990	12	8	3	3	84	41	199	207	105	128	0	0		791
1991	2	2	0	0	18	185	403	82	124	27	6	20		869
1992	130	18	3	2	106	2	190	82	111	102	26	5		775
1993	8	4	0	20	2	138	147	143	219	21	17	0		718
1994	1	0	0	29	11	154	75	96	88	15	0	0		468
1995	0	13	0	2	72	95	176	191	88	1	19	21		676
1996	0	0	0	6	23	78	137	283	219	64	1	0		810
Mean	19	7	2	11	27	90	166	142	111	47	13	11		**647**

Comanjilla	Jan	Feb	Mar	Apr	May	Jun	Jul	Aug	Sept	Oct	Nov	Dec		prec. per year
1982	15	3	1	4	43	36	107	74	44	24	43	28		420
1983	22	1	0	0	85	81	128	73	106	24	53	2		574
1984	21	11	0	0	48	137	196	102	24	11	0	3		552
1985	1	0	7	14	54	155	153	122	96	40	7	4		649
1986	0	0	0	0	34	246	114	123	108	63	48	1		737
1987	1	5	1	35	16	71	319	76	95	0	2	0		620
1988	4	7	41	0	2	118	156	285	59	1	0	0		671
1989	0	0	0	0	0	40	107	203	59	0	3	6		417
1990	4	0	0	1	39	86	160	188	132	155	2	0		768
1991	0	2	0	0	0	101	336	73	93	6	1	16		627
1992	144	14	1	19	109	39	262	72	51	83	19	19		830
1993	9	2	0	21	3	97	136	81	87	33	0	0		467
1994	0	0	0	11	6	199	105	130	56	11	0	0		517
1995	0	0	4	0	55	68	131	127	80	0	6	0		471
1996	0	0	0	0	11	53	145	120	78	32	13	6		457
Mean	15	3	4	7	34	102	170	123	78	32	13	6		**585**

Silao	Jan	Feb	Mar	Apr	May	Jun	Jul	Aug	Sept	Oct	Nov	Dec		prec. per year
1981	53	26	5	55	10	87	78	166	74	81	0	12		648
1982	0	3	0	6	22	0	200	77	21	67	33	33		461
1983	13	3	1	0	47	79	242	88	92	6	49	4		623
1984	13	9	0	0	31	172	245	93	70	4	0	11		645
1985	0	2	0	13	57	153	129	115	76	21	2	1		569
1986	5	5	0	0	28	206	138	103	192	59	32	0		766
1987	6	4	0	7	13	46	252	171	147	0	2	0		647
1988	11	0	37	8	0	116	208	266	50	2	4	1		702
1989	0	0	0	7	68	130	191	139	95	28	16	9		682
1990	0	13	9	0	51	116	191	139	127	67	0	9		721
1991	2	23	0	0	2	113	238	83	96	19	0	10		583
1992	151	6	0	0	10	58	274	114	38	28	22	0		701
1994	18	0	0	0	36	212	175	139	134	42	16	0		770
1995	0	0	0	0	26	92	191	183	0	0	63	45		599
1996	0	0	0	0	21	162	111	211	214	0	0	0		719
Mean	18	6	3	6	28	116	191	139	95	28	16	9		**656**

Romita	Jan	Feb	Mar	Apr	May	Jun	Jul	Aug	Sept	Oct	Nov	Dec		prec. per year
1981	50	22	2	40	4	115	73	121	92	86	0	13		618
1982	0	10	0	3	38	17	227	30	19	66	32	11		452
1983	10	1	0	0	25	92	240	131	128	6	54	1		689
1984	11	12	0	0	38	210	197	99	68	8	0	1		646
1985	0	0	0	10	28	42	120	167	64	40	9	3		482
1986	0	3	0	9	17	220	139	70	148	38	23	2		668
1987	3	8	0	9	9	79	319	167	92	0	2	0		689
1988	20	0	34	15	0	39	114	223	39	3	0	0		486
1989	0	2	0	24	0	53	161	291	58	7	13	10		618
1990	7	13	9	1	41	128	244	159	132	130	0	0		863
1991	0	21	0	0	2	121	426	111	161	36	1	16		895
1992	127	12	3	5	53	43	254	85	47	121	27	10		785
1993	11	0	0	5	2	218	145	78	122	10	12	6		606
Mean	18	8	4	9	20	106	205	133	90	42	13	6		**654**

Appendix 2: Temperature data of Silao and Romita (provided by CNA, Celaya. All values are in °C.

Silao	Jan	Feb	Mar	Apr	May	Jun	Jul	Aug	Sept	Oct	Nov	Dec		annual mean
1981	13.5	16.9	18.7	21	22.8	23.2	22.4	22.2	20.9	20.1	16.8	15.8		19.5
1982	16.6	17.3	20.6	23.1	23.4	24.8	22.3	22.0	21.5	19.1	16.5	14.4		20.1
1983	13.8	14.2	17.2	20.4	24.3	24.2	21.8	21.9	21.3	19.7	17.8	16.2		19.4
1984	15.4	16.3	19.8	21.8	22.2	22.7	21.1	21.4	20.4	20.7	17.3	16.3		19.6
1985	15.0	16.8	19.3	20.3	22.9	21.4	20.6	21	20.4	19.7	17.1	15.6		19.2
1986	14.2	16.4	16.7	21.9	23.2	22.3	21.1	21.4	21.2	18.7	17.9	15.3		19.2
1987	14.7	15.7	17.5	19.9	21.7	22.6	21.9	22.1	21.8	18.0	16.5	16.2		19.1
1988	14.0	17.3	17.4	20.6	23.1	22.9	21.8	21.6	20.5	18.7	17.8	15.6		19.3
1989	16.4	16.8	17.3	20.3	23	22.8	21.6	21.1	20.4	19.1	17.1	15.4		19.3
1990	15.7	15.2	20.0	22.1	23.7	22.6	21.2	21.1	20.2	19.6	16.2	15.3		19.4
1991	15.9	16.2	19.9	20.1	20.6	19.6	18.3	20.8	18.0	17.3	17.0	15.9		18.3
1992	14.3	16.7	18.5	18.8	23.0	22.6	21.8	19.2	19.2	19.1	16.7	14.4		18.7
1995	18.0	20.3	21.0	20.8	24.8	21.7	21.2	18.7	19.1	18.6	17.3	14.3		19.7
1996	18.3	17.7	15.3	20.9	23.7	23.0	20.1	21.2	20.4	19.1	17.1	15.4		19.4
monthly mean	15.4	16.7	18.5	20.9	23.0	22.6	21.2	21.1	20.4	19.1	17.1	15.4		**19.3**

Romita	Jan	Feb	Mar	Apr	May	Jun	Jul	Aug	Sept	Oct	Nov	Dec		annual mean
1981	11.4	15.0	17.4	19.6	21.3	22.1	20.9	20.8	19.5	18.8	15.7	14.0		18.0
1982	14.9	16.2	19.6	22.2	22.6	24.0	20.8	20.9	19.9	17.9	14.9	14.8		19.1
1983	12.0	12.8	15.9	19.4	23.0	23.1	20.1	20.1	19.9	18.1	16.3	14.8		18.0
1984	13.6	14.7	17.8	20.1	20.3	20.4	18.3	19.0	18.1	18.6	15.4	14.2		17.5
1985	12.9	15.0	18.2	18.9	21.6	19.7	18.8	19.3	19.0	18.4	15.6	14.1		17.6
1986	12.8	14.9	15.6	20.8	22.0	20.4	18.5	19.8	19.7	17.4	16.6	14.0		17.7
1987	13.3	15.7	16.2	18.7	20.4	21.6	20.1	20.3	20.2	16.7	15.2	14.9		17.8
1988	12.7	16.1	16.1	19.7	22.1	21.6	20.1	20.0	20.0	18.9	17.8	15.7		18.4
1989	16.8	16.8	17.6	20.5	23.0	23.3	21.0	19.6	19.0	18.5	16.6	13.9		18.9
1990	15.7	16.1	18.6	21.2	23.0	22.7	20.5	20.7	20.1	18.9	17.1	15.7		19.2
1991	15.7	17.4	20	22.0	23.9	22.9	19.5	20.7	19.2	18.5	16.7	15.3		19.3
1992	13.9	14.5	19	19.2	20.8	22.2	21.2	20.5	20.7	18.4	17.7	16.7		18.7
1993	17.8	18.7	20.3	21.6	23.0	24.1	22.1	22.3	20.7	21.1	20.3	14.8		20.6
monthly mean	14.1	15.7	17.9	20.3	22.1	22.2	20.1	20.3	19.7	18.5	16.6	14.8		**18.5**

Appendix3: Monthly and annual means of potential evapotranspiration. All values are in mm.

	El conejo	**Comanjilla**	**Romita**	**Silao**
	1978-1996	1991-1996	1973-1993	1981-1991
Jan	119	95	109	113
Feb	144	120	138	134
Mar	213	187	206	190
Apr	241	189	234	232
May	235	194	246	262
Jun	207	175	215	217

Jul	172	135	178	176
Aug	161	135	167	168
Sept	142	117	146	157
Oct	139	116	135	152
Nov	120	94	112	133
Dec	110	93	99	119
annual mean	**2004**	**1651**	**1984**	**2053**

Appendix 4: Piezometric data of some wells in the study area (taken from COREMI et al., 2004; provided by CEAG)

Well	x	y	z	Oct. 1998 [m]	Oct. 2004[m]	Groundwater table 2004 [m]	Depression 98-04 [m]
L-55	221923	2304029	1761	65.42	80.09	1681.35	-14.67
L-76	220956	2302239	1752	64.42	73.15	1679.28	-8.73
L-115	228000	2303150	1748	58.45	60.52	1687.48	-2.07
L-151	225024	2304453	1762	67.36	81.90	1680.28	-14.54
L-160	226366	2309431	1765	76.52	88.30	1676.28	-11.78
L-196	230339	2304400	1737	50.75	55.22	1681.78	-4.47
L-247	236421	2300751	1737	44.46	40.11	1696.89	4.35
L-326	237030	2308031	1746	70.45	72.16	1673.58	-1.71
L-398B	238780	2314510	1785	98.71	102.40	1682.60	-3.69
L-412	237784	2312015	1758	88.46	94.82	1663.18	-6.36
L-473	234003	2309180	1751	77.50	85.29	1665.52	-7.79
L-631	245710	2318850	1785	31.32	36.28	1748.72	-4.96
L-651	242224	2321208	1793	117.47	122.93	1670.07	-5.46
L-764	240624	2308792	1746	83.11	90.05	1655.95	-6.94
L-942	241173	2299804	1736	49.56	57.52	1678.89	-7.96
L-1074	247907	2312375	1757	81.67	81.74	1675.26	-0.07
L-1104	246552	2305444	1739	99.42	103.92	1635.08	-4.50
L-1191	250647	2299327	1731	57.43	70.96	1660.04	-13.53
L-1195	247695	2301237	1738	59.63	66.20	1671.80	-6.57
L-1316	254705	2317486	1850	56.40	52.39	1797.61	4.01
L-1407	265500	2315920	1875	175.80	185.00	1690.00	-9.20
L-1546	249808	2296010	1732	49.24	48.10	1683.90	1.14
L-1555	245958	2292965	1736	81.48	89.30	1646.70	-7.82
L-1563	255860	2293380	1752	74.09	75.36	1676.64	-1.27
L-1576	257960	2296025	1760	69.53	69.97	1690.03	-0.44
L-1583	256921	2297830	1799	116.45	135.50	1663.50	-19.05
L-1629	254006	2302605	1752	26.99	36.87	1715.13	-9.88
L-1824	254720	2309350	1769	71.64	81.91	1687.09	-10.27
L-1850	254186	2309905	1768	98.60	109.50	1658.50	-10.90
L-1868	250880	2312814	1765	52.26	55.11	1709.89	-2.85
L-1922	248535	2317437	1775	143.13	146.77	1628.23	-3.64
L-1942	244590	2321722	1794	32.10	27.69	1765.86	4.41
L-1967	246956	2321756	1804	32.00	30.40	1773.60	1.60
L-1972	247148	2323688	1820	103.89	103.20	1716.80	0.69
L-1999B	253350	2317660	1800	10.85	26.39	1773.61	-15.54
L-2002	250061	2317252	1777	67.38	81.97	1695.03	-14.59
L-2075	253105	2319709	1835	56.65	64.98	1770.02	-8.33

Appendix 5: Sampling points

Sample	Location	Date	Type	Waterlevel [m]	Tot. depth [m]
MIS 1	Sangre de Cristo	14.10.2005	spring	0.0	0
MIS 2	Hotel Comanjilla	14.10.2005	therm.spring	0.0	0
MIS 3	Rancho Bustamante	14.10.2005	well	225.2	300
MIS 4	Zangarro	15.10.2005	well	135.1	300
MIS 5	San Ramon	15.10.2005	well	69.0	180
MIS 6	Ojos De Rana	15.10.2005	well	69.3	135
MIS 7	Prondencia	15.10.2005	well	69.2	150
MIS 8	Fracción El Sillero	15.10.2005	well	105.1	150
MIS 9	San Clemente	15.10.2005	well	52.7	100
MIS 10	Granja Lupita	16.10.2005	well	96.2	150
MIS 11	R. Sagrado Corazon de Jesús	16.10.2005	well	100.9	350
MIS 12	Vista Hermosa	16.10.2005	well	45.6	70
MIS 13	Ejico Tejamanil	16.10.2005	well	53.8	100
MIS 14	L-1036	17.10.2005	well	69.0	100
MIS 15	El renadito	17.10.2005	well	80.0	200
MIS 16	Las Trojas	17.10.2005	well	105.7	300
MIS 17	Trejo Ej. Benavente	17.10.2005	well	93.0	117
MIS 18	Rancho Gpe Paso Blanco	17.10.2005	well	56.3	150
MIS 19	Rancho Granja los Cedros	17.10.2005	well	78.2	200
MIS 20	La Purisma de los Torres	18.10.2005	well	125.4	300
MIS 21	San Vicente	18.10.2005	well	68.0	250
MIS 22	Code Juarez	18.10.2005	well	105.2	160
MIS 23	Los Rodriguez	18.10.2005	well	85.0	300
MIS 24	Rancho San Agustin	18.10.2005	well	255.7	500
MIS 25	Ej. San José de los Romeros	19.10.2005	well	150.0	150
MIS 26	Ej. Playas de Gotelo	19.10.2005	well	98.3	180
MIS 27	Ej. Guadalupe Ramales	19.10.2005	well	107.3	?
MIS 28	Rancho la Joga	19.10.2005	well	112.8	190
MIS 29	Balneano Tres Villas	19.10.2005	well	100.0	170
MIS 30	Agua Potable San Ignacio	19.10.2005	well	200.0	350

Appendix 6: Water chemical parameters (determined in-situ)

Sample	x_UTM	y_UTM	z_UTM	pH	Conduc-tivity [µS/cm]	Oxygen [mg/l]	Temper-ature [°C]	HCO_3 (Titration) [mg/l]
MIS 1	257052	2329131	2351	7.82	1370	5.8	16.3	413
MIS 2	243109	2333241	1937	8.74	619		96.3	265
MIS 3	244552	2319506	1787	7.08	879	6.4	22.8	467
MIS 4	263635	2307894	1873	7.36	614	5.1	27.2	375
MIS 5	219072	2302104	1768	7.38	601		24.4	361
MIS 6	224889	2300590	1759	7.39	508		29.6	289
MIS 7	229961	2305940	1746	7.34	2740	5.6	24.0	362
MIS 8	237379	2308165	1752	7.43	624	3.9	27.3	325
MIS 9	235644	2302994	1729	7.32	971	4.5	23.8	443
MIS 10	239792	2310667	1758	7.41	625	5.0	26.2	350
MIS 11	242601	2306134	1756	7.38	1209	4.3	23.0	390
MIS 12	237277	2297721	1747	7.31	575		25.5	333
MIS 13	240169	2299617	1748	7.40	572	2.8	24.0	321
MIS 14	247344	2315809	1784	7.17	1205	7.1	22.7	506
MIS 15	247166	2310101	1782	7.34	827	5.5	24.0	428
MIS 16	245969	2306155	1754	7.27	594	3.6	27.6	300
MIS 17	246569	2302785	1760	7.64	517	6.1	25.0	281
MIS 18	249041	2296768	1754	7.64	1318	3.4	29.0	400
MIS 19	251370	2299144	1740	7.32	914	3.1	27.8	336
MIS 20	252514	2307521	1762	7.15	724	4.0	22.8	407
MIS 21	256746	2305304		7.70	437	5.0	27.7	235
MIS 22	256436	2297796	1792	7.35	566	4.3	26.3	232
MIS 23	253762	2317318	1823	7.34	604	6.2	24.0	352
MIS 24	246253	2324281	1821	7.37	638	5.1	27.3	359
MIS 25	241217	2328032	1822	7.30	520	5.5	28.3	382
MIS 26	238427	2320178	1826	7.56	592	5.7	28.4	302
MIS 27	241480	2315326	1777	7.55	544	5.4	27.1	324
MIS 28	228031	2310860	1787	7.70	2450	4.7	29.0	77
MIS 29	215279	2306066	1810	7.40	633	4.0	34.7	226
MIS 30	254069	2313921	1800	7.70	782	4.7	30.2	340

Appendix 7: Trace elements (first analysis: performed in Monterrey)

Sample	As [mg/l]	Ba [mg/l]	Be [mg/l]	Cd [mg/l]	Cr [mg/l]	Fe [mg/l]	Mn [mg/l]	Se [mg/l]	Sr [mg/l]
MIS 1	<0.003	0.008	<0.0004	<0.0002	<0.002	0.033	0.0020	0.037	0.30
MIS 2	<0.003	0.003	<0.0004	0.0007	<0.002	0.015	0.0030	<0.003	0.05
MIS 3	<0.003	0.01	<0.0004	<0.0002	<0.002	0.011	0.0010	<0.003	0.27
MIS 4	<0.003	0.085	<0.0004	<0.0002	<0.002	<0.008	0.0003	<0.003	0.29
MIS 5	<0.003	0.087	<0.0004	<0.0002	<0.002	0.011	0.0010	<0.003	0.56
MIS 6	<0.003	0.026	<0.0004	<0.0002	0.003	0.010	0.0006	<0.003	0.27
MIS 7	<0.003	0.019	<0.0004	<0.0002	<0.002	0.028	0.0070	<0.003	0.99
MIS 8	<0.003	0.082	<0.0004	<0.0002	0.003	<0.008	0.0006	<0.003	0.46
MIS 9	<0.003	0.036	<0.0004	<0.0002	<0.002	0.033	0.0010	<0.003	0.97
MIS 10	<0.003	0.108	<0.0004	<0.0002	<0.002	<0.008	0.0004	<0.003	0.30
MIS 11	<0.003	0.073	<0.0004	<0.0002	<0.002	0.050	0.0009	<0.003	0.78
MIS 12	0.006	0.04	<0.0004	<0.0002	<0.002	0.010	0.0005	<0.003	0.40
MIS 13	<0.003	0.064	<0.0004	<0.0002	<0.002	0.028	0.0050	<0.003	0.42
MIS 14	<0.003	0.154	<0.0004	<0.0002	<0.002	0.008	0.0005	<0.003	0.07
MIS 15	0.01	0.094	<0.0004	<0.0002	<0.002	0.013	0.0008	<0.003	0.43
MIS 16	<0.003	0.053	<0.0004	<0.0002	<0.002	0.013	0.0007	<0.003	0.44
MIS 17	0.011	0.047	<0.0004	<0.0002	<0.002	0.328	0.0070	<0.003	0.24
MIS 18	0.059	0.023	<0.0004	<0.0002	<0.002	0.012	0.0008	<0.003	0.23
MIS 19	0.031	0.091	<0.0004	0.001	<0.002	0.010	0.0010	<0.003	0.47
MIS 20	<0.003	0.125	<0.0004	<0.0002	<0.002	<0.008	0.0010	<0.003	0.43
MIS 21	0.005	0.033	<0.0004	<0.0002	<0.002	<0.008	0.0020	<0.003	0.18
MIS 22	<0.003	0.059	<0.0004	<0.0002	<0.002	0.010	0.0150	<0.003	0.26
MIS 23	<0.003	0.039	<0.0004	<0.0002	<0.002	0.014	0.0005	<0.003	0.20
MIS 24	<0.003	0.015	<0.0004	<0.0002	<0.002	0.036	0.0246	<0.003	0.11
MIS 25	0.007	0.115	<0.0004	<0.0002	<0.002	<0.008	0.0002	<0.003	0.51
MIS 26	0.006	0.112	<0.0004	<0.0002	0.005	<0.008	0.0004	<0.003	0.24
MIS 27	0.005	0.081	<0.0004	<0.0002	<0.002	<0.008	0.0004	<0.003	0.29
MIS 28	0.011	0.009	<0.0004	<0.0002	<0.002	0.027	0.0054	<0.003	0.16
MIS 29	0.013	0.014	<0.0004	<0.0002	<0.002	<0.008	0.0003	<0.003	0.31
MIS 30	<0.003	0.039	<0.0004	<0.0002	<0.002	<0.008	0.0006	<0.003	0.11

Appendix 8: Cations and Anions (first analysis: performed in Monterrey)

Sample	Li [mg/l]	K [mg/l]	Na [mg/l]	Ca [mg/l]	Mg [mg/l]	SO_4 [mg/l]	Cl [mg/l]	NO_3 [mg/l]	F [mg/l]	PO_4 [mg/l]	Si [mg/l]
MIS 1	0.01	0.8	61.7	152.0	92.8	281.0	68.8	175.0	<0.045	<0.9	9.9
MIS 2	0.42	7.5	150.0	1.8	0.2	31.2	14.9	<0.074	12.2	<0.9	65.8
MIS 3	0.11	7.5	80.4	52.4	8.1	43.1	13.8	23.8	<0.045	<0.9	25.1
MIS 4	0.04	7.8	82.7	47.8	5.8	31.8	1.8	12.4	<0.045	<0.9	37.3
MIS 5	0.03	6.1	30.8	123.0	48.7	23.1	2.2	11.8	0.4	<0.9	6.4
MIS 6	0.11	7.0	62.0	48.0	7.2	34.4	3.1	9.2	0.4	<0.9	24.8
MIS 7	0.24	16.5	413.0	82.9	53.5	1181.0	8.1	16.9	0.8	<0.9	27.1
MIS 8	0.08	6.9	47.9	55.5	21.9	28.4	3.8	28.9	0.2	<0.9	30.5
MIS 9	0.10	17.5	107.0	82.2	29.8	103.0	9.5	37.6	0.6	<0.9	32.6
MIS 10	0.05	5.9	53.9	75.5	26.5	25.0	4.8	39.8	0.1	<0.9	31.7
MIS 11	0.05	6.1	79.1	102.0	42.9	295.0	5.5	43.3	<0.045	<0.9	0.9
MIS 12	0.07	8.8	60.5	38.9	17.2	33.6	2.3	9.6	0.3	<0.9	30.5
MIS 13	0.05	4.9	42.9	52.7	21.0	34.3	3.7	17.4	<0.045	<0.9	22.7

MIS 14	0.02	5.9	45.2	131.0	58.0	68.0	69.5	106.0	<0.045	<0.9	0.5
MIS 15	0.02	4.1	34.3	91.4	36.8	62.7	13.8	48.0	<0.045	<0.9	0.6
MIS 16	0.05	4.7	50.0	48.6	18.7	39.0	11.2	21.1	<0.045	<0.9	23.2
MIS 17	0.09	4.0	61.4	23.5	9.4	33.4	10.4	4.4	1.2	<0.9	19.5
MIS 18	0.20	4.4	185.0	25.8	8.2	241.0	38.1	8.7	2.0	<0.9	3.3
MIS 19	0.14	9.8	107.0	56.2	21.6	133.0	47.2	11.8	1.0	<0.9	25.9
MIS 20	0.01	11.4	54.2	87.4	10.7	35.7	7.6	42.8	<0.045	<0.9	15.8
MIS 21	0.03	6.1	38.5	35.9	8.4	16.3	9.6	6.0	<0.045	<0.9	0.5
MIS 22	0.01	4.3	12.9	56.6	4.6	51.2	25.8	29.6	<0.045	<0.9	16.4
MIS 23	0.01	2.5	41.6	53.3	26.1	46.2	3.0	4.1	<0.045	<0.9	12.2
MIS 24	0.00	1.7	11.8	20.1	9.9	36.2	5.1	27.3	<0.045	<0.9	1.0
MIS 25	0.04	13.6	66.4	46.1	14.5	9.9	5.2	18.0	0.6	<0.9	1.1
MIS 26	0.02	21.0	62.7	39.8	7.1	26.9	1.5	8.9	0.8	<0.9	37.4
MIS 27	0.05	7.4	45.1	55.4	17.9	24.6	4.4	12.7	0.2	<0.9	23.8
MIS 28	0.28	10.1	148.0	252.0	9.1	1459.0	5.6	1.6	1.9	<0.9	16.7
MIS 29	0.11	4.1	88.7	45.6	4.9	126.0	7.7	6.9	0.9	<0.9	19.2
MIS 30	0.03	3.8	71.6	20.1	4.4	111.0	9.6	4.7	0.1	<0.9	11.8

Appendix 9: Second analysis of major cations (performed in Monterrey)

Sample	Ca [mg/l]	Fe [mg/l]	K [mg/l]	Li [mg/l]	Mg [mg/l]	Mn [mg/l]	Na [mg/l]	Sr [mg/l]
MIS 1	140.0	<0.08	0.7	<0.011	89.5	<0.002	54.5	0.38
MIS 2	2.0	<0.08	8.6	0.50	0.2	<0.002	160.0	0.06
MIS 3	107.0	<0.08	6.1	0.03	44.7	0.002	28.8	0.57
MIS 4	52.7	<0.08	9.6	0.05	8.0	<0.002	94.5	0.39
MIS 5	54.0	<0.08	8.4	0.13	10.6	<0.002	85.5	0.33
MIS 6	49.9	<0.08	8.0	0.12	8.8	<0.002	68.1	0.33
MIS 7	253.0	<0.08	18.4	0.32	55.5	0.008	462.0	2.06
MIS 8	58.9	<0.08	8.4	0.09	24.1	0.006	52.6	0.57
MIS 9	82.2	<0.08	18.4	0.18	31.2	<0.002	118.0	1.37
MIS 10	69.6	<0.08	7.3	0.05	25.9	<0.002	52.4	0.42
MIS 11	160.0	<0.08	8.5	0.08	56.5	<0.002	113.0	0.98
MIS 12	46.8	<0.08	11.5	0.08	21.2	<0.002	75.6	0.56
MIS 13	60.8	<0.08	6.5	0.04	25.2	0.005	52.9	0.58
MIS 14	183.0	<0.08	6.8	0.01	65.4	<0.002	53.4	0.91
MIS 15	129.0	<0.08	5.1	0.02	44.9	<0.002	42.9	0.62
MIS 16	58.9	<0.08	6.1	0.06	23.4	<0.002	62.3	0.61
MIS 17	32.0	0.5	5.4	0.11	14.7	0.010	84.0	0.36
MIS 18	36.3	<0.08	6.1	0.29	14.4	<0.002	289.0	0.41
MIS 19	67.1	<0.08	10.8	0.14	26.0	<0.002	134.0	0.60
MIS 20	83.1	<0.08	14.8	0.00	16.8	<0.002	66.8	0.63
MIS 21	41.6	<0.08	7.2	0.03	12.1	<0.002	45.8	0.24
MIS 22	89.6	<0.08	8.1	0.01	9.7	<0.002	22.1	0.51
MIS 23	58.5	<0.08	2.7	<0.011	30.6	<0.002	48.3	0.26
MIS 24	62.1	<0.08	5.9	<0.011	37.2	<0.002	39.4	0.42
MIS 25	48.8	<0.08	14.1	0.03	16.8	<0.002	71.8	0.63
MIS 26	38.7	<0.08	20.6	0.02	9.0	<0.002	65.5	0.29
MIS 27	55.8	<0.08	8.5	0.04	19.4	<0.002	47.2	0.36
MIS 28	424.0	<0.08	11.1	0.35	13.3	0.003	173.0	2.48
MIS 29	41.9	<0.08	4.5	0.33	5.9	<0.002	88.9	0.36
MIS 30	32.8	<0.08	7.1	0.26	9.9	<0.002	132	0.20

Appendix 10: Third analysis of major cations and anions (made in Freiberg)

Sample	Li^+ [mg/l]	Na^+ [mg/l]	K^+ [mg/l]	Ca^{2+} [mg/l]	Mg^{2+} [mg/l]	NO_3^- [mg/l]	F^- [mg/l]	Cl^- [mg/l]	SO_4^{2-} [mg/l]	TIC [mg/l]	HCO [mg/l]
MIS 1	< 0,05	66.7	0.50	94.6	89.5	154.0	0.28	68.4	307.0	41.2	194
MIS 2	< 0,05	26.0	4.67	56.1	40.7	27.6	0.27	17.9	47.6	59.3	222
MIS 3	0.05	25.8	4.62	32.1	36.0	26.7	0.24	16.6	46.6	42.1	179
MIS 4	0.07	87.3	7.01	20.8	9.0	15.6	0.67	2.8	34.2	52.0	240
MIS 5	0.10	76.9	5.50	22.4	7.2	13.1	0.96	3.1	24.0	47.5	220
MIS 6	0.37	62.1	4.82	20.8	9.0	10.6	0.93	4.0	35.2	36.7	171
MIS 7	0.59	137.0	10.7	176.0	29.6	8.3	0.66	5.1	689.0	55.1	249
MIS 8	< 0.05	50.9	6.48	67.3	23.6	41.8	0.78	6.0	37.5	67.6	312
MIS 9	0.33	104.0	16.2	25.7	10.0	38.9	1.13	11.0	113.0	52.3	239
MIS 10	< 0.05	48.4	5.74	70.5	21.8	44.6	0.59	6.3	26.8	69.3	319
MIS 11	< 0.05	106.0	< 0.5	144.0	39.3	55.4	0.31	7.0	330.0	90.0	408
MIS 12	0.14	68.7	10.2	54.5	17.6	11.9	0.90	3.8	35.4	67.3	305
MIS 13	0.17	47.8	6.13	64.1	19.8	20.8	0.43	5.3	36.1	65.0	299
MIS 14	< 0.05	47.8	19.4	91.4	63.4	129.0	0.33	77.8	80.1	101.0	398
MIS 15	0.11	39.7	4.65	103.0	37.7	58.9	0.23	17.6	66.4	84.6	381
MIS 16	0.14	55.5	3.70	52.9	22.2	24.6	0.40	14.5	42.1	63.1	284
MIS 17	0.11	81.1	5.42	28.9	15.6	3.8	1.98	13.9	35.6	54.9	262
MIS 18	0.21	255.0	58.3	32.1	12.7	9.4	2.72	74.5	285.0	75.1	360
MIS 19	0.10	126.0	9.28	65.7	22.9	11.4	1.42	46.3	147.0	62.6	285
MIS 20	< 0.05	62.1	11.9	94.6	12.7	58.2	0.15	9.8	37.5	83.7	363
MIS 21	< 0.05	43.8	4.99	36.9	11.3	7.7	0.36	13.5	19.5	39.2	188
MIS 22	< 0.05	22.0	9.09	67.3	8.3	32.8	0.20	25.6	51.2	28.5	130
MIS 23	< 0.05	51.1	4.12	57.7	30.6	4.2	0.37	4.6	52.5	69.5	316
MIS 24	< 0.05	39.0	4.62	57.7	34.2	32.1	0.15	7.0	38.1	67.4	308
MIS 25	0.11	72.1	11.2	40.1	15.1	19.8	1.24	6.8	11.2	59.4	270
MIS 26	< 0.05	68.2	19.0	49.7	5.8	10.6	1.44	2.6	29.4	71.4	338
MIS 27	0.12	53.3	7.47	54.5	18.7	15.3	0.75	6.4	27.4	63.5	299
MIS 28	< 0.05	173.0	14.5	501.0	10.6	13.6	2.39	3.0	1832	13.8	63
MIS 29	0.17	98.9	4.72	38.5	5.5	7.0	1.60	9.0	133.0	42.8	200
MIS 30	0.16	142.0	4.79	40.1	6.4	5.2	0.78	14.8	144.0	70.1	337

Appendix 11: Ion balance errors calculated with PHREEQC

	First analysis + titrated HCO_3 values [%]	First analysis + calculated HCO_3 values [%]		Second analysis + titrated HCO3 values [%]	Second analysis + calculated HCO_3 values [%]		Third analysis + titrated HCO_3 values [%]	Third analysis + titrated HCO_3 values [%]
MIS 1	2.4	14.0		-2.1	10.2		-8.3	3.2
MIS 2	6.7	-6.9		10.3	-3.5		11.4	-14.1
MIS 3	-14.3	20.6		5.9	39.9		-24.9	9.2
MIS 4	-2.2	15.6		4.2	22.4		-10.7	6.6
MIS 5	29.3	46.7		6.2	26.7		-12.2	7.6
MIS 6	2.5	22.0		5.9	26.1		-10.3	9.1
MIS 7	-7.8	-4.9		11.9	15.3		-9.1	-4.4
MIS 8	3.9	3.2		7.1	7.5		6.1	5.4
MIS 9	7.3	26.4		9.5	29.0		-19.7	-1.5
MIS 10	13.7	12.1		7.2	9.8		6.7	5.1
MIS 11	-5.0	-7.4		16.2	13.7		2.8	0.5
MIS 12	-0.2	1.5		9.5	12.3		7.7	9.4
MIS 13	1.1	2.0		9.2	11.1		5.5	6.3
MIS 14	0.6	6.5		12.7	18.8		-7.1	-1.6
MIS 15	-1.1	1.4		13.1	16.0		1.9	4.3
MIS 16	-0.8	0.3		10.0	11.2		3.1	4.1
MIS 17	-6.6	-7.7		7.5	9.4		7.2	6.2
MIS 18	-12.0	-10.2		10.5	12.7		1.7	3.2
MIS 19	-0.6	2.2		8.8	12.7		5.2	7.8
MIS 20	-2.4	1.0		3.1	6.7		0.9	4.2
MIS 21	-1.7	5.6		7.3	15.6		1.4	8.4
MIS 22	-21.1	-7.2		3.1	19.1		-6.1	7.8
MIS 23	-0.1	2.1		5.3	8.8		6.0	8.1
MIS 24	-50.2	-47.8		5.6	10.7		3.0	5.8
MIS 25	1.5	13.3		2.8	17.3		0.0	11.6
MIS 26	2.6	-5.2		2.8	-3.3		6.1	-1.5
MIS 27	4.4	4.3		4.1	6.4		5.8	5.7
MIS 28	-28.9	-28.7		-3.8	-3.6		-11.4	-11.2
MIS 29	1.0	2.7		-0.7	2.2		0.5	2.1
MIS 30	-24.0	-29.9		1.1	0.6		3.8	-2.0

Appendix 12: Saturation indices (si) of some mineral phases

Sample	Calcite	Aragonite	Dolomite	Gypsum	Anhydrite	Chalcedony	Quartz	Strontianite
MIS 1	0.4	0.2	0.9	-1.2	-1.4	-0.1	0.3	-1.6
MIS 2	1.9	1.8	4.1	-2.2	-1.8	-0.2	0.0	-0.7
MIS 3	-0.6	-0.8	-0.9	-2.3	-2.5	0.2	0.6	-2.3
MIS 4	-0.4	-0.5	-0.7	-2.5	-2.7	0.3	0.7	-1.8
MIS 5	-0.4	-0.5	-0.9	-2.6	-2.8	-0.4	0.0	-1.5
MIS 6	-0.4	-0.6	-0.8	-2.5	-2.7	0.1	0.5	-1.9
MIS 7	0.3	0.1	0.1	-0.7	-0.9	0.2	0.7	-1.5
MIS 8	0.3	0.2	0.5	-2.1	-2.3	0.2	0.7	-1.4
MIS 9	-0.4	-0.6	-0.9	-2.0	-2.2	0.3	0.7	-1.4
MIS 10	0.3	0.2	0.4	-2.2	-2.4	0.3	0.7	-1.6
MIS 11	0.5	0.4	0.8	-1.0	-1.2	-1.3	-0.8	-1.3
MIS 12	0.1	-0.1	0.0	-2.2	-2.4	0.3	0.7	-1.6
MIS 13	0.2	0.0	0.2	-2.1	-2.3	0.1	0.6	-1.5
MIS 14	0.2	0.0	0.5	-1.7	-2.0	-1.5	-1.1	-2.5
MIS 15	0.4	0.3	0.7	-1.7	-2.0	-1.5	-1.0	-1.5
MIS 16	0.0	-0.1	0.0	-2.1	-2.3	0.1	0.5	-1.6
MIS 17	0.1	-0.1	0.2	-2.4	-2.6	0.1	0.5	-1.6
MIS 18	0.1	0.0	0.3	-1.6	-1.8	-0.8	-0.3	-1.6
MIS 19	0.1	0.0	0.1	-1.6	-1.8	0.2	0.6	-1.6
MIS 20	0.2	0.0	-0.2	-1.9	-2.2	0.0	0.4	-1.7
MIS 21	0.1	0.0	0.2	-2.5	-2.7	-1.6	-1.2	-1.7
MIS 22	-0.1	-0.3	-0.8	-1.9	-2.1	0.0	0.4	-2.1
MIS 23	0.1	0.0	0.3	-2.0	-2.2	-0.1	0.3	-1.9
MIS 24	0.2	0.0	0.5	-2.1	-2.4	-1.3	-0.8	-2.1
MIS 25	-0.1	-0.2	-0.2	-2.8	-3.0	-1.2	-0.8	-1.5
MIS 26	0.4	0.2	0.2	-2.3	-2.5	0.3	0.7	-1.5
MIS 27	0.3	0.2	0.6	-2.3	-2.5	0.1	0.5	-1.5
MIS 28	0.4	0.3	-0.4	-0.1	-0.3	0.0	0.4	-2.6
MIS 29	-0.1	-0.2	-0.6	-1.7	-1.9	-0.1	0.3	-1.8
MIS 30	0.4	0.2	0.3	-1.7	-1.9	-0.2	0.2	-1.8

Appendix 13: Dendrogram of Cluster analysis

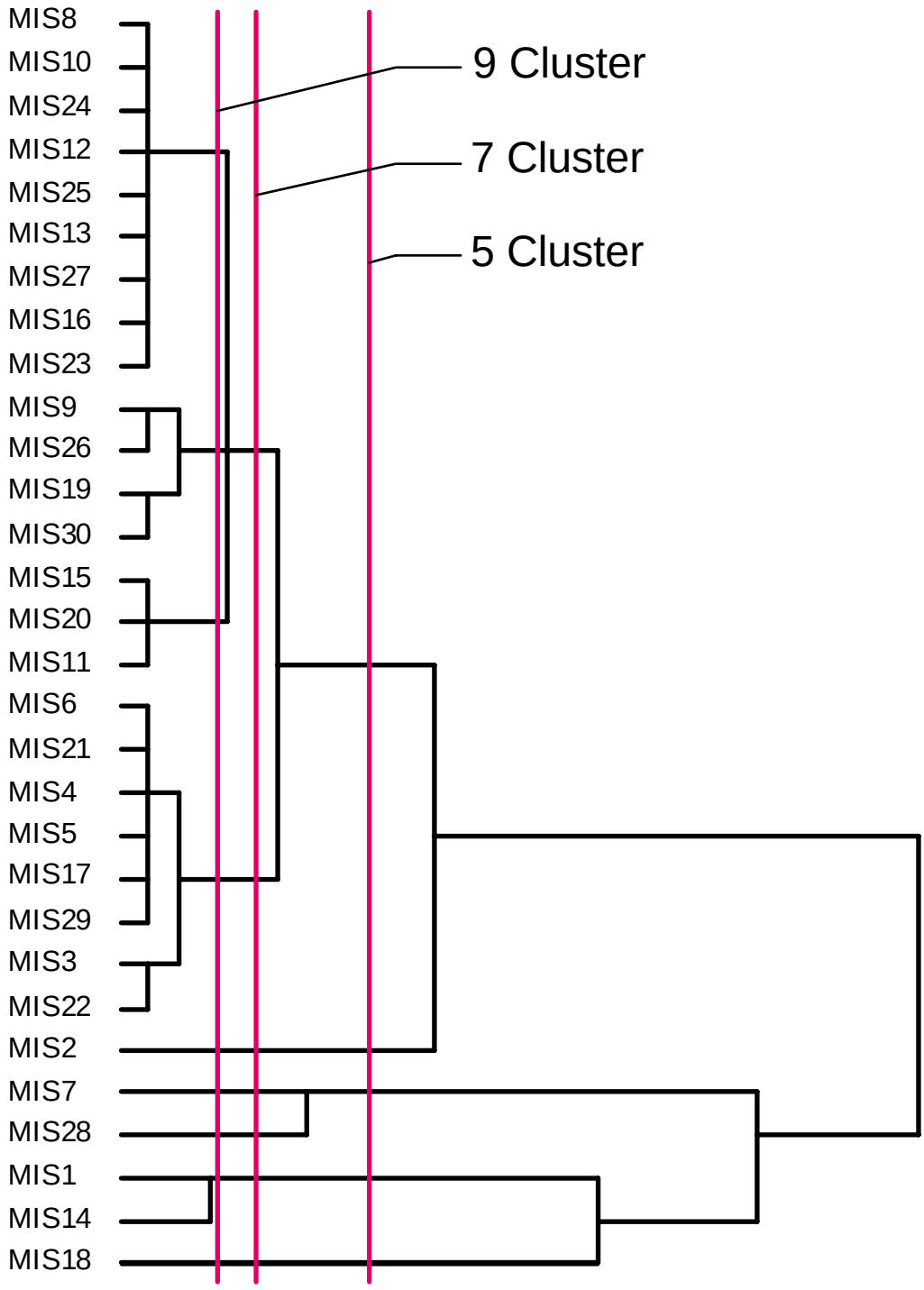

Appendix 14: Chloride in precipitation

CEASG (1999)

Station	Cl^- mg/l	Elevation m (asl)	Precipitation volume litres
Barretos	0.6	1794	20
La Gavia	0.76	1749	17
Jesús de Monte	0.8	1807	27
La Muralla	0.8	2000	23
J. Cánovas	0.84	1744	28
Presa Reventada	0.9	1826	27
Pañuelas	1.3	1725	27

SAPAL (2000)

	Precipitation [mm]	Cl [mg/l]
max	596.3	2.6
min	380	<0,3 n.d.
med	612	0.85

COREMI et al. (2004)

Station	Cl^- [mg/l]	Elevation [m]	Precipitation volume [litres]
Sardinas	1.06	1722	35
Irapuato	1.06	1723	30
Huanimario	1.37	1721	28
Presa la Purisma	1.1	1845	27
Silao	1.37	1779	25
Los Mexicanos	1.15	2424	25
Poblado De Comanjilla	1.23	1919	25
Guanajuato	1.22	1977	30

Appendix 15: Variogram of chloride-distribution-plot

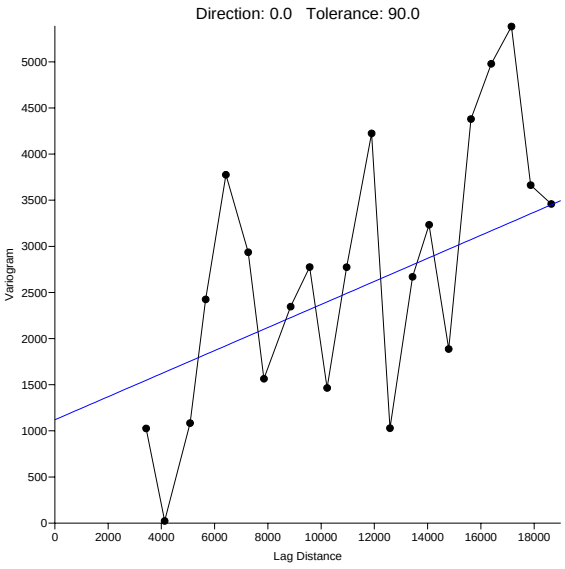

Appendix 16: Atmospheric tritium input data for Veracruz taken from IAEA-GNIP webside

Date	TU	Date	TU	Date	TU	Date	TU	Date	TU
15.04.1962	69.1	15.11.1971	12.5	15.12.1975	10.1	15.01.1980	4.5	15.06.1984	2.7
15.07.1962	35.5	15.12.1971	15.9	15.01.1976	11.6	15.05.1980	8.4	15.07.1984	4.3
15.09.1962	42.9	15.02.1972	17.5	15.02.1976	11.9	15.06.1980	5.7	15.08.1984	5.0
15.11.1962	46.3	15.03.1972	24.2	15.04.1976	11.6	15.07.1980	3.5	15.09.1984	3.7
15.01.1963	65.1	15.04.1972	11.7	15.05.1976	11.3	15.08.1980	5.9	15.10.1984	3.6
15.09.1963	310	15.05.1972	14.9	15.06.1976	6.5	15.09.1980	4.3	15.11.1984	5.0
15.10.1966	33.6	15.07.1972	19.5	15.07.1976	7.6	15.10.1980	5.2	15.12.1984	3.0
15.04.1967	34.5	15.08.1972	16.3	15.08.1976	6.4	15.11.1980	7.2	15.02.1985	3.4
15.06.1967	37.5	15.09.1972	12.2	15.09.1976	7.1	15.12.1980	5.1	15.04.1985	5.6
15.07.1967	36.5	15.10.1972	11.7	15.10.1976	6.2	15.01.1981	14.6	15.05.1985	4.9
15.08.1967	34.4	15.11.1972	11.5	15.11.1976	8.4	15.02.1981	5.2	15.06.1985	4.4
15.09.1967	20.6	15.12.1972	17.4	15.02.1977	5.6	15.03.1981	12.6	15.07.1985	8.9
15.10.1967	24.5	15.01.1973	11.5	15.03.1977	9.8	15.04.1981	7.2	15.08.1985	2.9
15.11.1967	25.1	15.02.1973	13.0	15.04.1977	7.9	15.06.1981	5.3	15.10.1985	10
15.12.1967	18.6	15.05.1973	10.5	15.05.1977	10.6	15.07.1981	5.7	15.11.1985	3.0
15.01.1968	17.6	15.06.1973	12.3	15.06.1977	8.5	15.08.1981	4.5	15.12.1985	3.9
15.03.1968	33.6	15.07.1973	11.5	15.07.1977	11.5	15.09.1981	4.7	15.01.1986	7.2
15.05.1968	31.4	15.08.1973	10.5	15.08.1977	7.6	15.10.1981	4.5	15.02.1986	7.2
15.06.1968	23.0	15.09.1973	8.7	15.09.1977	7.1	15.12.1981	5.9	15.05.1986	2.8
15.07.1968	29.0	15.10.1973	7.5	15.10.1977	8.0	15.02.1982	5.4	15.10.1986	3.1
15.08.1968	20.2	15.11.1973	8.8	15.11.1977	6.6	15.04.1982	6.0	15.11.1986	3.7
15.09.1968	19.0	15.12.1973	27.9	15.12.1977	11.3	15.05.1982	5.3	15.03.1987	5.5
15.10.1968	17.6	15.01.1974	9.9	15.01.1978	14.6	15.06.1982	4.0	15.04.1987	6.0
15.11.1968	21.1	15.02.1974	24.1	15.02.1978	16.1	15.07.1982	3.9	15.05.1987	3.7
15.10.1969	15.9	15.05.1974	11.7	15.03.1978	20	15.08.1982	5.0	15.06.1987	3.2
15.12.1969	19.2	15.06.1974	10.5	15.05.1978	8.5	15.09.1982	2.9	15.09.1988	3.4
15.01.1970	21.6	15.07.1974	14.5	15.06.1978	9.6	15.10.1982	4.0	15.12.1988	2.8
15.03.1970	44.4	15.08.1974	14.7	15.07.1978	8.5	15.11.1982	6.1		
15.06.1970	26.0	15.09.1974	10.7	15.08.1978	7.6	15.12.1982	2.6		
15.07.1970	32.7	15.10.1974	10.0	15.09.1978	7.5	15.01.1983	6.1		
15.09.1970	17.6	15.11.1974	10.9	15.10.1978	10.2	15.02.1983	7.6		
15.12.1970	15.5	15.01.1975	10.0	15.04.1979	12.7	15.03.1983	2.5		
15.01.1971	10.3	15.02.1975	14.8	15.05.1979	6.6	15.07.1983	4.1		
15.04.1971	40.9	15.05.1975	22.0	15.06.1979	6.8	15.08.1983	4.4		
15.05.1971	32.1	15.06.1975	9.7	15.07.1979	6.4	15.10.1983	4.3		
15.06.1971	26.8	15.07.1975	12.6	15.08.1979	6.5	15.11.1983	4.0		
15.07.1971	20.7	15.08.1975	7.5	15.09.1979	8.3	15.12.1983	2.8		
15.08.1971	19.6	15.09.1975	7.0	15.10.1979	5.6	15.01.1984	3.3		
15.09.1971	12.5	15.10.1975	8.9	15.11.1979	9.6	15.03.1984	5.0		
15.10.1971	18.3	15.11.1975	13.0	15.12.1979	5.7	15.05.1984	3.4		

Appendix 17: Atmospheric tritium input data for Chihuahua taken from IAEA-GNIP webside

Date	TU	Date	TU	Date	TU
15.07.1964	727.2	15.09.1975	13.1	15.08.1985	10.1
15.08.1964	641.2	15.12.1975	4.7	15.09.1985	8.4
15.01.1965	141.0	15.05.1976	34.9	15.05.1986	12.7
15.06.1965	402.0	15.06.1976	25.4	15.06.1986	15.1
15.07.1965	325.0	15.07.1976	20.9	15.07.1986	4.9
15.08.1965	175.0	15.08.1976	18.7	15.08.1986	7.6
15.09.1965	237.0	15.09.1976	12.3	15.09.1986	5.2
15.04.1966	296.0	15.10.1976	19.7	15.10.1986	8.7
15.06.1966	81.1	15.11.1976	29.2	15.12.1986	6.5
15.08.1966	124.0	15.12.1976	18.2	15.04.1987	11.9
15.09.1966	123.0	15.06.1977	52.1	15.05.1987	13.9
15.10.1966	31.5	15.07.1977	57.1	15.06.1987	13.8
15.03.1967	175.0	15.08.1977	42.5	15.07.1987	11.7
15.06.1967	400.0	15.09.1977	20.5	15.08.1987	7.0
15.07.1967	167.5	15.10.1977	20.0	15.06.1988	14.4
15.08.1967	45.0	15.06.1978	25.0		
15.09.1967	37.3	15.07.1978	11.8		
15.04.1968	298.6	15.08.1978	21.6		
15.07.1968	78.4	15.09.1978	7.5		
15.08.1968	96.6	15.10.1978	23.4		
15.08.1972	40.6	15.12.1978	16.6		
15.09.1972	29.8	15.05.1979	48.8		
15.10.1972	25.9	15.06.1979	3.5		
15.11.1972	9.4	15.07.1979	23.9		
15.02.1973	30.6	15.08.1979	13.2		
15.04.1973	15.8	15.05.1981	2.0		
15.05.1973	69.2	15.01.1984	9.0		
15.07.1973	60.1	15.05.1984	9.8		
15.08.1973	21.7	15.06.1984	6.8		
15.09.1973	26.4	15.07.1984	5.3		
15.04.1974	11.4	15.08.1984	16.0		
15.07.1974	34.8	15.09.1984	11.8		
15.08.1974	32.1	15.10.1984	6.0		
15.09.1974	27.8	15.11.1984	17.5		
15.10.1974	17.4	15.12.1984	7.2		
15.11.1974	15.2	15.01.1985	11.5		
15.12.1974	17.9	15.03.1985	12.1		
15.01.1975	43.8	15.04.1985	16.2		
15.06.1975	19.0	15.06.1985	16.5		
15.08.1975	27.2	15.07.1985	8.9		

Appendix 18: Averaged yearly input for tritium of Veracruz and Chihuahua and estimated input for Guanajuato

	Chihuahua	Veracruz		Guanajuato (estimated)				
year	TU	TU		year	TU		year	TU
1962		48.5		1945	3.0		1977	23.5
1963		187.6		1946	3.0		1976	15.6
1964	684.2	140.0		1947	3.0		1977	23.5
1965	256.0	80.0		1948	3.0		1978	14.5
1966		33.6		1949	3.0		1979	15.0
1967	165.0	29.0		1950	3.0		1980	13.4
1968	157.9	23.6		1951	3.0		1981	11.7
1969		17.6		1952	4.0		1982	10.1
1970		26.3		1953	4.7		1983	8.5
1971		21.0		1954	6.1		1984	6.9
1972	26.4	15.7		1955	8.4		1985	8.6
1973	37.3	12.2		1956	12.4		1986	6.7
1974	22.4	13.0		1957	19.4		1987	8.1
1975	21.6	11.6		1958	31.6		1988	8.8
1976	22.4	8.9		1959	53.1		1989	8.4
1977	38.4	8.6		1960	90.6		1990	8.1
1978	17.7	11.4		1961	156.3		1991	7.8
1979	22.4	7.6		1962	272.1		1992	7.5
1980		5.5		1963	450.0		1993	7.2
1981		7.0		1964	272.1		1994	6.9
1982		4.5		1965	168.0		1995	6.6
1983		4.5		1966	111.8		1996	6.3
1984	9.9	3.9		1967	97.0		1997	6.0
1985	12.0	5.2		1968	90.7		1998	5.7
1986	8.7	4.8		1969	73.3		1999	5.4
1987	11.7	4.6		1970	55.9		2000	5.1
1988	14.4	3.1		1971	38.5		2001	4.8
				1972	21.1		2002	4.5
				1973	24.8		2003	4.2
				1974	17.7		2004	3.9
				1975	16.6		2005	3.6
				1976	15.6			

Appendix 19: Tritium values (analysed by TRICAR laboratory, Freiberg) and corresponding residence times for piston flow and exponential model

	Activity			Residence time, Piston flow model		Mean residence time, Exponential model
Sample	TU	2-σ		years		years
MIS1	3.5	0.6		0, 14, 27, 28, 30, 32, 34, 47		50
MIS2	0.5	0.4		> 50		>300
MIS3	0.2	0.4		> 50		>300
MIS4	2.9	0.5		19, 21, 24, 48		73
MIS5	0.7	0.4		> 50		>300
MIS6	0.4	0.4		> 50		>300
MIS7	0.9	0.4		> 50		>300
MIS8	0.8	0.4		> 50		>300
MIS9	1.0	0.4		50		300
MIS10	0.6	0.4		> 50		>300
MIS11	0.9	0.4		> 50		>300
MIS12	0.0	0.3		> 50		>300
MIS13	0.6	0.4		> 50		>300
MIS14	1.3	0.4		49		220
MIS15	0.9	0.4		> 50		>300
MIS16	0.1	0.4		> 50		>300
MIS17	0.0	0.3		> 50		>300
MIS18	1.4	0.4		49		200
MIS19	0.6	0.4		> 50		>300
MIS20	0.2	0.4		> 50		>300
MIS21	0.0	0.3		> 50		>300
MIS22	2.0	0.5		21, 48		128
MIS23	1.6	0.5		49		170
MIS24	0.1	0.4		> 50		>300
MIS25	0.1	0.4		> 50		>300
MIS26	0.0	0.3		> 50		>300
MIS27	0.1	0.3		> 50		>300
MIS28	0.0	0.3		> 50		>300
MIS29	0.0	0.3		> 50		>300
MIS30	0.1	0.4		> 50		>300

Appendix 20: Atmospheric input data of CFCs from Nivot Ridge, Colorado. Bold values are estimated.

	CFC				CFC				CFC		
year	11	12	113	year	11	12	113	year	11	12	113
1940.0	0.01	0.34	0.00	1964.0	21.8	59.2	2.47	1988.0	248.6	459.5	61.2
1940.5	0.01	0.40	0.00	1964.5	23.9	63.3	2.66	1988.5	254.0	469.1	64.9
1941.0	0.02	0.48	0.00	1965.0	26.3	67.9	2.85	1989.0	257.4	476.7	68.5
1941.5	0.02	0.56	0.00	1965.5	28.6	72.5	3.06	1989.5	262.0	484.0	71.5
1942.0	0.02	0.66	0.00	1966.0	31.2	77.6	3.28	1990.0	265.8	493.5	74.5
1942.5	0.02	0.76	0.00	1966.5	33.8	82.8	3.53	1990.5	266.9	497.1	76.6
1943.0	0.03	0.88	0.00	1967.0	36.7	88.5	3.77	1991.0	269.2	503.4	78.8
1943.5	0.03	1.01	0.01	1967.5	39.7	94.3	4.06	1991.5	270.1	508.8	80.3
1944.0	0.04	1.18	0.01	1968.0	43.0	100.7	4.33	1992.0	271.5	517.7	81.5
1944.5	0.04	1.34	0.03	1968.5	46.4	107.2	4.66	1992.5	272.2	520.5	82.3
1945.0	0.05	1.56	0.04	1969.0	50.2	114.4	4.98	1993.0	272.3	523.0	82.7
1945.5	0.05	1.77	0.06	1969.5	54.1	121.5	5.35	1993.5	272.4	526.0	83.0
1946.0	0.07	2.15	0.07	1970.0	58.5	129.3	5.73	1994.0	272.8	528.2	83.2
1946.5	0.08	2.53	0.09	1970.5	62.9	137.2	6.15	1994.5	272.2	533.3	83.5
1947.0	0.11	3.11	0.11	1971.0	67.7	145.5	6.57	1995.0	272.0	534.7	83.6
1947.5	0.14	3.70	0.13	1971.5	72.5	153.9	7.05	1995.5	271.3	534.8	83.7
1948.0	0.20	4.37	0.15	1972.0	77.8	162.9	7.54	1996.0	271.0	535.7	83.6
1948.5	0.25	5.04	0.17	1972.5	83.2	172.0	8.10	1996.5	269.5	537.4	83.5
1949.0	0.34	5.76	0.20	1973.0	89.4	182.0	8.65	1997.0	269.0	539.3	83.4
1949.5	0.43	6.48	0.22	1973.5	95.5	192.1	9.29	1997.5	268.0	540.9	83.3
1950.0	0.56	7.28	0.25	1974.0	102.2	202.9	9.93	1998.0	267.3	542.1	83.2
1950.5	0.68	8.07	0.27	1974.5	108.9	213.7	10.67	1998.5	266.3	543.7	83.0
1951.0	0.85	8.93	0.30	1975.0	114.6	224.0	11.39	1999.0	265.6	544.0	82.8
1951.5	1.02	9.80	0.33	1975.5	122.1	234.3	12.23	1999.5	264.2	544.6	82.6
1952.0	1.28	10.7	0.37	1976.0	128.9	244.2	13.07	2000.0	263.8	545.1	82.3
1952.5	1.53	11.6	0.41	1976.5	135.1	254.0	14.02	2000.5	263.2	546.3	82.1
1953.0	1.88	12.6	0.44	1977.0	142.1	263.3	14.99	2001.0	261.8	546.5	81.7
1953.5	2.22	13.6	0.49	1977.5	146.7	272.5	16.09	2001.5	260.8	546.1	81.3
1954.0	2.64	14.7	0.53	1978.0	150.0	282.4	17.19	2002.0	260.1	545.3	81.0
1954.5	3.06	15.9	0.58	1978.5	156.5	292.9	18.44	2002.5	258.6	544.7	80.6
1955.0	3.58	17.1	0.63	1979.0	159.8	298.1	19.70	2003.0	258.1	543.3	80.3
1955.5	4.09	18.4	0.69	1979.5	162.6	301.2	21.14	2003.5	**256.1**	**542.8**	**79.9**
1956.0	4.74	19.9	0.75	1980.0	168.6	311.2	22.59	2004.0	**255.1**	**542.1**	**79.6**
1956.5	5.38	21.4	0.81	1980.5	172.8	317.4	24.15	2004.5	**253.5**	**541.2**	**79.1**
1957.0	6.09	23.1	0.87	1981.0	176.0	322.7	25.72	2005.0	**252.4**	**540.3**	**78.8**
1957.5	6.81	24.7	0.94	1981.5	179.7	333.8	27.34	2005.5	**251.0**	**539.7**	**78.4**
1958.0	7.46	26.5	1.02	1982.0	183.8	343.6	28.96	2006.0	**249.6**	**538.7**	**78.1**
1958.5	8.11	28.3	1.11	1982.5	188.3	352.7	30.76				
1959.0	8.76	30.2	1.19	1983.0	193.3	361.6	32.55				
1959.5	9.42	32.2	1.29	1983.5	198.0	372.2	34.80				
1960.0	10.3	34.5	1.38	1984.0	201.9	378.6	37.03				
1960.5	11.2	36.9	1.49	1984.5	206.0	386.2	39.70				
1961.0	12.3	39.5	1.60	1985.0	211.2	395.4	42.3				
1961.5	13.4	42.1	1.73	1985.5	217.3	403.3	45.2				
1962.0	14.9	45.1	1.86	1986.0	223.0	414.6	48.0				
1962.5	16.3	48.1	1.99	1986.5	227.9	423.5	51.1				
1963.0	18.0	51.6	2.14	1987.0	233.5	433.6	54.2				
1963.5	19.8	55.1	2.31	1987.5	241.0	449.3	57.7				

Appendix 21: CFC data, corresponding air mixing ratios and residence times for piston flow and exponential model

	CFC11	Stand. dev.	Air mixing ratios		Recharge date	Residence time (PFM)		Mean res. time (EM)
Sample	pmol/l	1-σ	pptv	1-σ		years	1-σ	years
MIS 3	2.30	0.30	204	27	1984.5	21.5	2.5	19.0
MIS 4	0.06	0.05	5	4	1956.0	50	3	1570.0
MIS 5	0.60	0.10	53	9	1969.0	37	1	127.0
MIS 7	1.20	0.20	108	18	1974.0	32	1	56.0
MIS 8	1.20	0.20	107	18	1974.0	32	1.5	56.0
MIS 9	1.20	0.20	107	18	1974.0	32	1.5	56.0
MIS 10	0.90	0.10	80	9	1972.0	34	1	82.0
MIS 11	1.90	0.20	169	18	1980.0	26	2.5	27.7
MIS 12	0.53	0.10	47	9	1968.5	37.5	1	148.0
MIS 13	0.49	0.05	44	4	1968.0	38	0.5	164.0
MIS 14	2.20	0.30	196	27	1983.0	23	2.5	20.6
MIS 15	1.00	0.10	89	9	1972.5	33.5	0.5	71.0
MIS 16	0.54	0.10	48	9	1968.5	37.5	1	145.0
MIS 17	1.70	0.20	151	18	1978.0	28	2	33.6
MIS 18	0.61	0.10	54	9	1969.5	36.5	1	127.5
MIS 19	0.63	0.10	56	9	1969.5	36.5	1	122.4
MIS 20	1.20	0.20	107	18	1974.0	32	1.5	56.0
MIS 21	0.18	0.05	16	4	1962.0	44	1.5	478.0
MIS 22	1.50	0.20	133	18	1976.0	30	2	40.9
MIS 23	1.80	0.20	160	18	1979.0	27	2	30.2
MIS 24	12.00	3.00	1065	270	cont.	cont.		cont.
MIS 25	0.43	0.05	38	4	1967.0	39	1	500.0
MIS 27	0.70	0.10	62	9	1970.0	36	0.5	109.0
MIS 28	1.10	0.20	99	18	1973.5	32.5	1.5	62.0
MIS 29	0.12	0.05	11	4	1960.0	46	2	700.0
MIS 30	0.10	0.05	9	4	1959.0	47	2.5	850.0

Sample	CFC12	Stand. dev.	Air mixing ratios		Recharge date	Residence time (PFM)		Mean res. time (EM)
	pmol/l	1-σ	pptv	1-σ		years	1-σ	years
MIS 3	1.60	0.10	525	33	1993.0	13.0	5.0	7.0
MIS 4	0.03	0.05	10	17	1951.5	54.5	6.0	1500.0
MIS 5	0.55	0.05	180	17	1972.5	33.5	0.5	69.7
MIS 7	0.90	0.10	298	33	1979.0	27.0	2.5	35.0
MIS 8	1.00	0.10	328	33	1981.0	25.0	2.0	29.4
MIS 9	1.00	0.10	328	33	1981.0	25.0	2.0	29.4
MIS 10	0.58	0.05	190	17	1973.0	33.0	0.5	65.1
MIS 11	1.70	0.10	559	-	recent	0.0		0.0
MIS 12	0.41	0.05	134	17	1970.0	36.0	1.0	99.5
MIS 13	0.48	0.05	157	17	1971.5	34.5	1.0	82.5
MIS 14	1.50	0.10	493	33	1989.5	16.5	4.0	10.3
MIS 15	0.80	0.10	262	33	1976.5	29.5	1.5	41.9
MIS 16	0.35	0.05	115	17	1969.0	37.0	1.0	119.5
MIS 17	1.40	0.10	459	33	1987.5	18.5	2.0	13.6
MIS 18	0.55	0.05	181	17	1972.5	33.5	0.5	69.7
MIS 19	0.51	0.05	167	17	1972.0	34.0	1.0	76.5

MIS 20	0.84	0.10	276	33	1977.5	28.5	2.0	39.0
MIS 21	0.17	0.05	56	17	1963.5	42.5	12.0	266.0
MIS 22	1.00	0.10	328	33	1981.0	25.0	2.0	29.4
MIS 23	1.20	0.10	393	33	1984.5	21.5	1.0	20.6
MIS 24	0.27	0.05	88	17	1966.5	39.5	1.0	161.2
MIS 25	0.41	0.05	134	17	1970.0	36.0	1.0	270.0
MIS 27	0.43	0.05	141	17	1970.5	35.5	1.0	94.5
MIS 28	0.71	0.10	235	33	1975.5	30.5	1.5	49.8
MIS 29	0.07	0.05	23	17	1956.5	49.5	4.0	670.0
MIS 30	0.11	0.05	36	17	1960.0	46.0	2.5	435.0

Sample	**CFC113**	**Stand. dev.**	**Air mixing ratios**		**Recharge date**	**Residence time (PFM)**		**Mean res. time (EM)**
	pmol/l	**1-σ**	**pptv**	**1-σ**		**years**	**1-σ**	**pmol/l**
MIS 3	0.23	0.05	69	15	1989.0	17	6.5	11
MIS 4	<0.01		3	-	<1965	> 40	-	>1500
MIS 5	0.08	0.05	24	15	1980.0	26	3.5	67
MIS 7	0.14	0.05	42	15	1985.0	21	2	31.8
MIS 8	0.15	0.05	45	15	1985.0	21	2	28.7
MIS 9	0.12	0.05	36	15	1983.5	22.5	3	39.7
MIS 10	0.08	0.05	24	15	1980.0	26	3.5	67.0
MIS 11	0.15	0.05	45	15	1985.0	21	2	28.7
MIS 12	0.07	0.05	21	15	1979.0	27	4	78.5
MIS 13	0.07	0.05	21	15	1979.0	27	4	78.5
MIS 14	0.11	0.05	33	15	1983.0	23	3	44.7
MIS 15	0.11	0.05	33	15	1983.0	23	3	44.7
MIS 16	0.05	0.05	15	15	1977.0	29	5	115.0
MIS 17	0.21	0.05	63	15	1988.0	18	17	14.6
MIS 18	0.06	0.05	18	15	1978.0	28	5	94.0
MIS 19	0.07	0.05	21	15	1979.0	27	4	78.5
MIS 20	0.10	0.05	30	15	1982.0	24	3	50.7
MIS 21	0.03	0.05	9	15	1973.0	33	7.5	200.0
MIS 22	0.15	0.05	45	15	1985.0	21	2	28.7
MIS 23	0.19	0.05	57	15	1987.0	19	2.5	18.9
MIS 24	0.04	0.05	12	15	1975.0	31	6	148.0
MIS 25	0.06	0.05	18	15	1978.0	28	5	200
MIS 27	0.07	0.05	21	15	1979.0	27	4	78.5
MIS 28	0.11	0.05	33	15	1983.0	23	3	44.7
MIS 29	0.02	0.05	6	15	1970.0	36	9.5	310.0
MIS 30	0.02	0.05	6	15	1970.0	36	9.5	310.0

Appendix 22: Time lags of CFCs (bold water level depths are corrected to measurements made in 2003)

H	CFC11				CFC12				CFC113	
	Time lag [years]		Residence time corrected [years]		Time lag [years]		Residence time corrected [years]		Time lag [years]	Residence time corrected [years]
m	exp.	linear	exp.	linear	exp.	linear	exp.	linear	exp.	exp.
57.0	20	25	1	-3	16	22	-3	-9	24	-7
135.1	55	139	-5	-89	44	126	10	-72	70	
69.0	26	36	11	1	20	33	13	1	31	-5
69.2	26	36	6	-4	20	33	7	-6	31	-10
78.0	30	46	2	-14	24	42	1	-17	36	-15
52.7	18	21	14	11	14	19	11	6	22	1
96.2	38	70	-4	-36	30	64	3	-31	47	-21
51.0	18	20	8	6	14	18			21	0
45.6	15	16	22	22	12	14	24	22	18	9
53.8	19	22	19	16	15	20	20	14	23	4
69.0	26	36	-3	-13	20	33	-4	-16	31	-8
80.0	31	49	3	-15	24	44	5	-15	38	-15
105.7	42	85	-5	-47	34	77	3	-40	52	-23
93.0	36	66	-8	-38	29	60	-11	-41	45	-27
56.3	20	24	17	12	16	22	18	12	24	4
78.2	30	46	7	-10	24	42	10	-8	37	-10
125.4	51	119	-19	-87	41	109	-12	-80	64	-40
68.0	25	35	19	9	20	32	22	11	31	2
105.2	42	84	-12	-54	33	77	-8	-52	52	-31
48.0	16	17	11	10	13	16	9	6	19	0
86.0	33	56		-56	27	51	13	-12	41	-10
133.2	54	135	-15	-96	44	123	-8	-87	68	-40
107.3	43	87	-7	-51	34	80	1	-44	53	-26
112.7	45	96	-13	-64	36	88	-6	-57	57	-34
100.0	40	76	6	-30	32	69	18	-20	49	-13
93.0	36	66	11	-19	29	60	17	-14	45	-9

Appendix 23: Deuterium and ^{18}O ratios (analyses performed by the EIL-laboratory at the University of Waterloo, Canada)

Sample	^{18}O	Result	Repeat	^{2}H	Result	Repeat
δx‰ VSMOW						
MIS 1	X	-9.71		X	-73.38	-72.78
MIS 2	X	-9.64	-9.73	X	-75.18	-75.07
MIS 3	X	-9.81		X	-75.79	-76.19
MIS 4	X	-9.14		X	-74.68	-73.20
MIS 5	X	-9.22		X	-73.03	-71.73
MIS 6	X	-9.71		X	-75.10	-76.25
MIS 7	X	-8.79		X	-70.01	-70.60
MIS 8	X	-9.98		X	-76.19	-76.48
MIS 9	X	-8.80	-8.71	X	-70.24	-69.64
MIS 10	X	-10.20		X	-76.12	-77.30
MIS 11	X	-9.13		X	-72.41	-70.68
MIS 12	X	-9.74		X	-77.67	-77.42
MIS 13	X	-9.76		X	-75.10	-75.51
MIS 14	X	-9.93		X	-76.32	-76.67
MIS 15	X	-10.20		X	-77.86	-78.16
MIS 16	X	-9.43	-9.39	X	-71.36	-71.80
MIS 17	X	-9.58		X	-74.84	-73.70
MIS 18	X	-9.38		X	-73.12	-73.10
MIS 19	X	-9.43	-9.39	X	-73.22	
MIS 20	X	-9.39		X	-73.14	
MIS 21	X	-9.69	-9.56	X	-75.88	-74.33
MIS 22	X	-9.35		X	-71.34	-71.87
MIS 23	X	-9.13		X	-69.94	-71.04
MIS 24	X	-9.82	-10.01	X	-76.38	-75.76
MIS 25	X	-9.92		X	-75.16	-76.01
MIS 26	X	-9.48		X	-76.30	-75.34
MIS 27	X	-10.20		X	-80.14	-78.48
MIS 28	X	-9.40		X	-73.72	-74.59
MIS 29	X	-9.79		X	-73.69	-73.87
MIS 30	X	-9.48		X	-74.46	-74.28

Appendix 24: Precipitation data of Deuterium and 18-O

COREMI et al. (2004)

Station	$\delta^{18}O$ ‰	δ D ‰
Sardinas	-10.2	-70
Irapuato	-9.4	-64
Huanimario	-9.9	-68
Presa la Purisma	-9.8	-68
Cerro del Cubilete	-10.5	-74
Silao	-9.3	-65
Los Mexicanos	-10.5	-72
Poblado de Coman-jilla	-9.6	-67
Guanajuato	-10.7	-74

CEASG (1999)

Station	$\delta^{18}O$ ‰	δ D ‰
Gavia de Rionda	-9.6	67
La Muralla	-7.5	53
Hacienda Peñuelas	-8.7	56
Presa Reventada	-10.2	67
Jesús del Monte	-8.4	58
Barretos	-10.4	73

Appendix 25: ^{14}C data (analysis performed by the IsoTrace laboratory, University of Waterloo, Canada)

Sample	δ ^{13}C [‰]	CO_2 [mg/l]	$^{14}C/^{12}C$ uncorrected [pmC]	1 σ	$^{14}C/^{12}C$ corrected [pmC]	1 σ
MIS 1	-10.46	5.8	104.27	0.63	101.2	0.62
MIS 2	-9.28	5.5	6.53	0.12	6.3	0.11
MIS 3	-11.91	4.7	111.9	0.62	109.0	0.6
MIS 4	-7.88	5	70.4	0.43	68.0	0.42
MIS 5	-7.51	5.4	80.41	1.14	77.6	1.1
MIS 6	-8.10	6.3	54.32	0.94	52.5	0.91
MIS 7	-10.38	5.9	83.11	0.53	80.7	0.51
MIS 8	-9.35	5.8	89.57	0.54	86.8	0.52
MIS 9	-8.80	5.2	99.65	0.56	96.4	0.55
MIS 10	-9.00	6.2	95.85	0.57	92.8	0.56
MIS 11	-10.13	5.8	100.78	0.57	97.8	0.55
MIS 12	-8.55	5.5	77.98	0.5	75.4	0.49
MIS 13	-9.56	5.6	71.88	0.45	69.7	0.44
MIS 14	-9.71	5	109.54	0.64	106.1	0.62
MIS 15	-9.45	5.9	108.33	0.61	105.0	0.59
MIS 16	-8.96	6.4	71.84	0.46	69.5	0.44
MIS 17	-8.38	5.6	47.45	0.44	45.9	0.42
MIS 18	-9.74	5.2	64.67	0.54	62.7	0.52
MIS 19	-9.45	6.1	51.82	0.55	50.2	0.53
MIS 20	-9.42	4.7	95.44	0.82	92.5	0.8
MIS 21	-7.60	4.6	78.42	0.69	75.7	0.66
MIS 22	-8.61	6.2	85.46	0.76	82.7	0.73
MIS 23	-9.61	6	90.76	0.79	88.0	0.77
MIS 24	-9.13	6.2	86.59	0.81	83.8	0.79
MIS 25	-6.87	5.2	64.04	0.6	61.7	0.58
MIS 26	-8.47	5.4	89.53	0.57	86.6	0.55
MIS 27	-8.63	5.7	77.08	0.73	74.6	0.71
MIS 28	-10.62	3.9	65.82	0.44	63.9	0.43
MIS 29	-8.05	5.6	60.28	0.4	58.2	0.39
MIS 30	-7.18	5.4	27.38	0.25	26.4	0.24

Appendix 26: Calculated residence times (^{14}C) with the help of different carbonate correction models

	Assumed initial activity	Measured activity	Residence time uncorr.	Residence time Vogel correction		Initial activity Gonfiantini correcti-on	Residence time ^{13}C correction model		
	pmC	pmC	years	q=0,75	q=0,9	pmC	$^{13}C_{rech}$	q	years
MIS 1	105	101.23	302	-2076	-569	30.2	-11.4	0.91	-433
MIS 2	105	6.32	23232	20854	22361	34.9	-18.2	0.51	17667
MIS 3	120	108.95	799	-1580	-72	35.4	-13.2	0.90	-56
MIS 4	120	67.99	4697	2318	3826	23.8	-13.0	0.61	554
MIS 5	105	77.6	2500	1226	2733	22.5	-12.7	0.59	-756
MIS 6	105	52.49	5732	3354	4861	24.7	-13.2	0.61	1705
MIS 7	105	80.67	2179	905	2412	31.0	-12.7	0.82	1612
MIS 8	105	86.76	1577	303	1810	28.3	-12.9	0.72	16
MIS 9	120	96.42	1809	-570	938	26.2	-12.8	0.69	-1262
MIS 10	105	92.78	1023	-251	1256	27.1	-12.8	0.70	-807
MIS 11	105	97.77	590	-685	823	30.1	-12.6	0.81	-85
MIS 12	105	75.42	2735	357	1864	25.7	-12.9	0.66	-681
MIS 13	105	69.66	3392	2118	3625	28.5	-12.6	0.76	2182
MIS 14	120	106.14	1015	-1364	144	28.8	-12.9	0.75	-1356
MIS 15	120	104.95	1108	-1270	237	28.2	-12.7	0.74	-1354
MIS 16	105	69.53	3408	1029	2537	27.1	-13.2	0.68	219
MIS 17	105	45.88	6845	4466	5973	25.1	-12.5	0.67	3559
MIS 18	120	62.69	5368	2989	4497	29.7	-12.8	0.76	3081
MIS 19	105	50.2	6101	4826	6333	28.7	-13.1	0.72	4505
MIS 20	105	92.46	1051	-1327	180	28.0	-13.0	0.72	-1619
MIS 21	105	75.7	2705	327	1834	23.0	-12.7	0.60	-1533
MIS 22	120	82.66	3082	703	2211	25.9	-12.9	0.67	-285
MIS 23	120	87.96	2568	190	1697	28.7	-12.7	0.75	237
MIS 24	105	83.84	1860	-518	989	27.6	-13.0	0.70	-1054
MIS 25	105	61.72	4393	2014	3522	20.9	-13.2	0.52	-1002
MIS 26	105	86.57	1596	-783	725	25.7	-12.9	0.66	-1863
MIS 27	105	74.55	2831	453	1960	26.1	-12.8	0.68	-399
MIS 28	105	63.92	4103	1725	3232	32.4	-12.8	0.83	2569
MIS 29	105	58.24	4872	2494	4001	25.1	-13.6	0.59	525
MIS 30	105	26.41	11410	9032	10539	22.0	-12.9	0.56	6551

Appendix 27: Strontium data (measurements done by the isotope laboratory of the TUBA Freiberg, Germany)

Water samples				Rock samples		
Sample	**$^{87}Sr/^{86}Sr$ ratio**	**1δ**		**Sample**	**$^{87}Sr/^{86}Sr$ ratio**	**1δ**
MIS 1	0.704297	0.000068		MIS1G (carb)	0.707325	0.000051
MIS 2	0.706214	0.000043		M4G (carb)	0.704065	0.000102
MIS 3	0.704920	0.000083		M5G (carb)	0.704869	0.000112
MIS 4	0.705329	0.000097		MIS29 I G (carb)	0.704898	0.000064
MIS 5	0.704664	0.000065		MIS29 II G (carb)	0.704918	0.000147
MIS 6	0.704762	0.000091				
MIS7(1)	0.704617	0.000111		MIS1G (residue)	0.708191	0.000111
MIS7(2)	0.704513	0.000117		M4G (residue)	0.704706	0.000064
MIS 8	0.704681	0.000085		M5G (residue)	0.704832	0.000086
MIS10	0.704809	0.000123		MIS29 I G (residue)	0.705430	0.000075
MIS11	0.704688	0.000127		MIS29 II G (residue)	0.704550	0.000113
MIS12	0.704581	0.000107				
MIS13	0.704619	0.000119				
MIS14	0.704701	0.000146				
MIS15	0.704721	0.000097				
MIS16	0.704734	0.000052				
MIS17	0.704743	0.000076				
MIS18	0.704759	0.000107				
MIS 19	0.704669	0.000141				
MIS 20	0.704669	0.000141				
MIS 21	0.705009	0.000078				
MIS 22	0.704663	0.000096				
MIS 23	0.704450	0.000071				
MIS 24	0.704657	0.000094				
MIS 25	0.704245	0.000169				
MIS 26	0.704879	0.000063				
MIS 27	0.704885	0.000128				
MIS 28	0.704840	0.000102				
MIS 29	0.704774	0.000119				
MIS 30	0.704660	0.000148				